

**Application of Materials Science Approach to the
Structural Properties of Whey Protein Based
Composite Gels Influenced by Change in pH**

A thesis submitted in fulfillment of the requirements for the degree of
Master of Applied Science

Lita Katopo
Bachelor of Science

School of Applied Sciences
College of Science, Engineering and Health (SEH)
RMIT University
July 2011

CONTENTS

DECLARATION	iii
ACKNOWLEDGEMENTS	iv
PUBLICATION AND PRESENTATION	vi
SUMMARY	vii
TABLE OF CONTENTS	ix
LIST OF FIGURES	xi
LIST OF TABLES	xvi
LIST OF ABBREVIATIONS	xvii
LIST OF SYMBOLS	xix

DECLARATION

I hereby declare that except where due acknowledgement has been made, the work is that of the author alone; the work has not been submitted previously, in a whole or in part, to qualify for any other academic award. The content of the thesis is the result of work, which has been carried out at School of Applied Science, RMIT University, since the official commencement date of the approved research program. Furthermore, any editorial work, paid or unpaid, carried out by a third party is acknowledged; and, ethics procedures and guidelines have been followed.

Lita Katopo

17 July 2011

ACKNOWLEDGEMENTS

I owe my deepest gratitude to my supervisor, Prof. Stefan Kasapis, for his guidance, support and encouragement during my study at RMIT. His supervision from the preliminary to the concluding level enabled me to develop an understanding of the subject. It would have been next to impossible to write this thesis without his help and guidance.

I would also like to show my gratitude to my co-supervisor, Dr. Yacine Hemar, for his invaluable assistance in giving practical approaches to solving any difficulties occurred during the research program.

I thank God for the wisdom and perseverance that He has been bestowed upon me during this research project, and indeed, throughout my life.

I also like to extend my sincere gratitude to the staff at Food Science Lab of RMIT, Michael Kakoullis, Lillian Chuang, and Mary Pecar for their invaluable support and patience in providing information and training for the instruments.

I am indebted to my many of my colleagues to support me, Paul George, Vinita Chaudhary, Omar Almrhag, Diep Duong, Anastasia Devi, and Lillian Chuang. Many thanks for your support, assistance and insight in time of need and special thanks for making my time at RMIT a wonderful and memorable one. I wish you the best with your studies as well. Particular thank and gratitude go to Philip Button for providing helpful feedback and suggestion in revising my thesis.

I thank Phil Francis at RMIT Microscopy and Microanalysis Facility for providing training and technical assistance with environmental scanning electron microscopy throughout my study. Furthermore, many thanks to Peter Rummel, and duty

microscopists for their continual support and patience particularly when difficulties encountered in using the instrument.

I also wish to thank Prof. Robert Shanks for giving me the opportunity to use the extruder at his laboratory at RMIT. His extensive knowledge and guidance regarding extruder and polymer have been very helpful in my research.

Last but certainly not the least, I am very grateful to my parents and siblings for their continual love, unconditional support both financially and emotionally during my study. Without their encouragement it would have been impossible to finish this research.

PUBLICATION AND PRESENTATIONS

Publication

The result from this work has been submitted for publication in *Langmuir*.

Katopo, L., Kasapis, S., and Hemar, Y. Segregative phase separation in agarose/whey protein systems induced by sequence-dependent trapping and change in pH.

Poster Presentations

Katopo, L., Kasapis, S., and Hemar, Y. (2010). Structural properties of whey protein gels influenced by pH. Poster presented at the 43rd Annual AIFST Convention that was held from 24th-27th July in Melbourne, Victoria, Australia.

Katopo, L., Kasapis, S., and Hemar, Y. (2010). Application of the materials science approach to the structural properties of whey protein based composite gels influenced by pH. Poster presented at the RMIT University 2010 HDR Conference that was held on 20th October in Melbourne, Victoria, Australia.

SUMMARY

Despite the increasing appreciation that whey is a valuable resource of dairy industry, as opposed to a waste product of the cheese and casein industries, there have been drawbacks in its utilization as a functional ingredient in processed food products. Potential benefits include improvement in nutritional quality, imparting flavor and color due to the presence of lactose that takes part in Maillard reactions with the protein, as fat replacer in low-fat dairy products when co-gelled with polysaccharide, and as an ingredient in starch-based formulations (e.g. snacks and cereals). Therefore, the aim of this research is to apply the technique and concepts of the material science approach for the determination of the composition of individual phases in biphasic gels of whey protein in the presence of other polysaccharide such as agarose.

The structural properties and morphology of mixed gels made of aqueous preparations of agarose and whey protein were modified by changing thermal treatment and pH. The conformationally dissimilar polymers phase separated and this process was followed by small-deformation dynamic oscillation in shear, differential scanning calorimetry and scanning electron microscopy.

Experimental protocol encourages formation of a range of two-phase systems from continuous agarose matrices perforated by liquid-like whey protein inclusions to phase inverted preparations where a soft protein matrix suspends hard agarose-filler particles. These distinct morphologies have widely different mechanical moduli, which were followed by adapting a theoretical analysis (isostress-isostrain and Lewis-Nielsen blending laws) from the literature in synthetic block polymers and polyblends. Based on this framework of thought, reasonable predictions of the elastic moduli in the composite gels were made that led to patterns of solvent partition between the two polymeric

networks. It was shown that proteins, in mixture with polysaccharide, exhibit favorable relative affinity (*P*-factor) for water molecules at a pH above their isoelectric point. This is an unexpected outcome that adds to the central finding of a single *P* value for the distribution of solvent between the continuous matrix and discontinuous inclusions of binary gels. It was thus proposed that phase continuity and solvent distribution in agarose/whey protein systems are under kinetic control that can be heavily governed by pH changes in the aqueous environment.

TABLE OF CONTENTS

CHAPTER 1	INTRODUCTION	1
1.1	AGAROSE	1
1.2	WHEY PROTEIN	3
1.3	BIOPOLYMER MIXTURES	15
1.4	PHASE SEPARATION	18
1.5	POLYMER BLENDING LAWS	19
CHAPTER 2	MATERIALS AND METHODS	30
2.1	DIFFERENTIAL SCANNING CALORIMETRY	30
2.2	RHEOLOGY	34
2.3	SCANNING ELECTRON MICROSCOPY	39
2.4	MATERIALS	42
2.5	INSTRUMENTS	44
2.6	SAMPLE PREPARATION	48
2.6.1	Agarose preparation	48
2.6.2	Whey protein preparation	48
2.6.3	Binary mixtures preparation	48
2.7	METHODS	49
CHAPTER 3	SEGREGATIVE PHASE SEPARATION IN AGAROSE/WHEY PROTEIN SYSTEMS INDUCED BY SEQUENCE-DEPENDENT TRAPPING AND CHANGE IN pH	52
3.1	ABSTRACT	52
3.2	INTRODUCTION	53
3.3	EXPERIMENT PROTOCOL	56
3.3.1	Materials	56
3.3.2	Sample Preparation	57
3.3.3	Methods	57
3.4	RESULTS AND DISCUSSION	59

3.4.1	Network Formation in Single Gels of Agarose Polysaccharide and Whey Protein Isolate	59
3.4.2	Thermomechanical and Microscopy Observations on the Structural Characteristics of Agarose/Whey Protein Mixtures	67
3.4.3	Theoretical Modeling of the Phase Behavior in Agarose/Whey protein Mixtures	79
3.5	CONCLUSIONS	89
CHAPTER 4	EPILOGUE AND FUTURE RESEARCH	92
	REFERENCES	96
	APPENDICES	108

LIST OF FIGURES

- Figure 1.1 Basic disaccharide moieties of agars (agarobiose)
- Figure 1.2 Composition of whey proteins
- Figure 1.3 Tertiary structure of β -Lactoglobulin
- Figure 1.4 Model for β -lactoglobulin showing the range of structures in solution, denatured state and aggregated state
- Figure 1.5 Model for protein folding, unfolding, and aggregation proposed by Chiti and Dobson
- Figure 1.6 Three different types of polymer network
- Figure 1.7 Phase diagram of a protein-polysaccharide-water system
- Figure 1.8 Variation of calculated moduli as a function of X , the proportion of solvent in phase X , illustrated for $n=2$ ($M_Y = 4M_X$). G_X and G_Y are the moduli of the individual phases. G_U and G_L are upper and lower bound moduli respectively from isostrain and isostress blending laws, with the continuous phase indicated in parentheses
- Figure 1.9 Modulus ratio of composites containing rubber and a rigid polymer
- Figure 2.1 Heat flux DSC schematic
- Figure 2.2 MDSC thermogram of PET/PC bilayer film
- Figure 2.3 Basic shear diagram of shear rate versus shear stress of Newtonian, shear-thinning, and shear-thickening. The diagram also includes

Bingham and Herschel-Bulkley (H-B) with a yield stress that must be exceeded for flow to occur

Figure 2.4 The principle of oscillation viscometry. Applied strain versus time (a) and resultant stress versus time that is measured in an elastic solid (b), Newtonian liquid (c) and viscoelastic liquid (d)

Figure 2.5 Schematic diagram of a SEM

Figure 2.6 Modulated Differential Scanning Calorimeter Q2000

Figure 2.7 Advanced Rheometer Generation 2 (ARG-2)

Figure 2.8 FEI Quanta™ 200 at RMIT

Figure 2.9 Experimental designs of binary mixtures (agarose and whey protein isolate) preparation and analysis

Figure 3.1a Cooling profiles of G' for 1.0 (●), 1.25 (▲), 1.5 (■) and 2.0% (◆) agarose at pH of 4.0 and 7.0 for each polymer concentration (scan rate of 1°C/min)

Figure 3.1b Cooling profiles of G' for 1.0% agarose at varying pH values (pH 4 [◆], pH 5 [▲], pH 6 [○], pH 7 [◇], and pH 8 [□]) at a scan rate of 1°C/min

Figure 3.1c Calibration curves of G' at 5°C as a function of agarose concentration at pH values of 4.0 (◆), 4.5 (■), 5.0 (▲), 5.5 (+), 6.0 (○), 6.5 (●), 7.0 (◇), 7.5 (X) and 8.0 (□)

Figure 3.2a G' variation for 15.0% whey protein at pH 4.5 (heating, ◆; cooling, ◇), pH 5.0 (heating, ■; cooling, □) and pH 7.0 (heating, ●; cooling, ○) at a scan rate of 1°C/min

Figure 3.2b Calibration curves of G' at 5°C as a function of whey protein

concentration at pH values of 4.0 (◆), 4.5 (■), 5.0 (▲), 5.5 (+), 6.0 (○), 6.5 (●), 7.0 (◇), 7.5 (X) and 8.0 (□)

Figure 3.3a Heating (closed symbols) and cooling (open symbols) profiles of G' for mixtures of 1.0% agarose with 15.0% whey protein at pH 5.0 (◆,◇), pH 7.0 (▲,Δ) and pH 8.0 (●,○) at a scan rate 1°C/min

Figure 3.3b Cooling profiles only of G' for mixtures of 1.0% agarose with 15.0% whey protein at pH 4.0 (□), pH 7.5 (■), and pH 8.0 (+) at the same scan rate

Figure 3.4a DSC endotherms for the heating profiles of 15.0% whey protein at pH of 4.0, 4.5, 5.0, 5.5, 6.0, 6.5, 7.0, 7.5 and 8.0 shown in the graph from top to bottom

Figure 3.4b DSC exotherms for the cooling profiles of 2.0% agarose at pH of 4.0, 4.5, 5.0, 5.5, 6.0, 6.5, 7.0, 7.5 and 8.0 shown in the graph from top to bottom

Figure 3.4c DSC endotherms for the heating profiles of 2.0% agarose with 15.0% whey protein mixture at pH of 4.0, 4.5, 5.0, 5.5, 6.0, 6.5, 7.0, 7.5 and 8.0 shown in the graph from top to bottom

Figure 3.4d DSC exotherms for the cooling profiles of 2.0% agarose with 15.0% whey protein mixtures at pH of 4.0, 4.5, 5.0, 5.5, 6.0, 6.5, 7.0, 7.5 and 8.0 shown in the graph from top to bottom (scan rate in both cases is 1°C/min)

Figure 3.5 ESEM images of 15.0% whey protein (a) at pH 4.0, (b) at pH 5.0, (c) at pH 6.0 and (d) at pH 7.5, with all samples being thermally treated (heating followed by cooling); magnification is 200 μm

Figure 3.6 ESEM images of (a) 15.0% whey protein at pH 4.0, (b) 15.0% whey protein at pH 7.0, (c) 2.0% agarose with 15.0% whey protein at pH 4.0

and (d) 2.0% agarose with 15.0% protein at pH 7.0, with all samples being thermally treated (heating followed by cooling); magnification is 100 μm

Figure 3.7 SEM images of 2.0% agarose with 15% whey protein (a) at pH 4.0 and (b) at pH 7.5, without thermal treatment (cooling only)

Figure 3.8a Computerized modeling of the phase topology of 1.0% agarose with 15.0% whey protein mixture, which was exposed to heating and cooling, at pH 4.5 using the isostrain and isostress blending laws. Storage modulus values of agarose (G'_{ag}) and whey protein (G'_{wp}) are represented by dashed lines while the upper ($G'_{U(ag)}$; $G'_{U(wp)}$) and lower ($G'_{L(ag)}$; $G'_{L(wp)}$) bounds are illustrated as solid lines. Experimental composite modulus (G'_{exp}) taken at 5°C is also shown to intersect the calculated lower bound at a specific value of S_{wp}

Figure 3.8b Computerized modeling of the phase topology of 1.0% agarose with 15.0% whey protein mixture, which was exposed to heating and cooling, at pH 7.5 using the isostrain and isostress blending laws. Storage modulus values of agarose (G'_{ag}) and whey protein (G'_{wp}) are represented by dashed lines while the upper ($G'_{U(ag)}$; $G'_{U(wp)}$) and lower ($G'_{L(ag)}$; $G'_{L(wp)}$) bounds are illustrated as solid lines. Experimental composite modulus (G'_{exp}) taken at 5°C is also shown to intersect the calculated lower bound at a specific value of S_{wp}

Figure 3.9a Computerized modeling of the phase topology of 1.0% agarose plus 15.0% whey protein, which was exposed to a cooling routine only, at pH 4.5 using the Lewis-Nielsen and isostrain blending laws. Storage modulus values of agarose (G'_{ag}) are represented by a dashed line while the calculated composite moduli according to Lewis-Nielsen ($G'_{c(LN)}$) and blending ($G'_{c(BL)}$) laws are illustrated as solid lines. Experimental composite modulus (G'_{exp}) taken at 5°C is also shown to intersect the Lewis-Nielsen predictions at a specific value of S_{wp}

Figure 3.9b Computerized modeling of the phase topology of 1.0% agarose plus 15.0% whey protein, which was exposed to a cooling routine only, at pH 7.5 using the Lewis-Nielsen and isostrain blending laws. Storage modulus values of agarose (G'_{ag}) are represented by a dashed line while the calculated composite moduli according to Lewis-Nielsen ($G'_{c(LN)}$) and blending ($G'_{c(BL)}$) laws are illustrated as solid lines. Experimental composite modulus (G'_{exp}) taken at 5°C is also shown to intersect the Lewis-Nielsen predictions at a specific value of S_{wp}

Figure 3.10 Data for the relative solvent partition (P -factor) plotted against adjusted pH for the mixed systems of 1.0% agarose plus 15.0% whey protein, which were subjected to both heating and cooling (●) or a cooling only treatment (○)

LIST OF TABLES

Table 1.1	Food applications of agars
Table 1.2	Applications of whey proteins
Table 1.3	Characteristics of major whey proteins
Table 1.4	Intermolecular forces stabilizing protein and polysaccharide structures
Table 1.5	Maximum packing fractions ϕ_m values
Table 1.6	<i>Einstein</i> coefficients for composites
Table 2.1	Rheological parameter
Table 2.2	Basic information of SEM
Table 2.3	List of materials
Table 2.4	List of instruments

LIST OF ABBREVIATIONS

μm	micrometer
ARG-2	Advanced Rheometer Generation-2
Asn	Asparagine
BSA	Bovine Serum Albumin
BSE	Backscattered Electrons
Ca^{2+}	Calcium ions
cP	centipoise
CRTs	Cathode Ray Tubes
CWMS	Cross-linked Waxy Maize Starch
DSC	Differential Scanning Calorimeter
ESEM	Environmental Scanning Electron Microscope
Gln	Glutamine
GSED	Gaseous Secondary Electron Detector
HCl	Hydrochloric acid
Ig	Immunoglobulins
kDa	Kilo Dalton
keV	Kilo electron volt
LVR	Linear Viscoelastic Region
M	Molar
MDSC	Modulated Differential Scanning Calorimeter
MF	micro-filtration
mg	milligram
mM	milli Molar
NaOH	Sodium hydroxide
nm	nanometer
Pa	Pascal
PC	Polycarbonate
PET	Polyethylene terephthalate
pI	Isoelectric point
rad	radian

RMIT	Royal Melbourne Institute of Technology
SC	Specimen, absorbed, induced currents
SE	Secondary Electrons
SEM	Scanning Electron Microscopy
Ser	Serine
Thr	Threonine
Tyr	Tyrosine
UF	ultra-filtration
VPSEM	Variable-Pressure Scanning Electron Microscope
w/w	Weight by weight
WPC	Whey Protein Concentrate
WPI	Whey Protein Isolate
α -Lac	α -Lactalbumin
β -Lg	β -Lactoglobulin

LIST OF SYMBOLS

$\dot{\gamma}$	Shear rate
σ	Shear stress
γ	Shear strain
η	Viscosity
ω	Frequency
η'	Dynamic viscosity
σ_0	Yield stress
η^*	Complex viscosity
ϕ_2	Volume fraction in dispersed phase
ϕ_m	Maximum packing fraction
ϕ_X	Phase volume of component X
ϕ_Y	Phase volume of component Y
c_x	Effective concentrations (% w/w) of polymers X in the two phases
c_y	Effective concentrations (% w/w) of polymers Y in the two phases
D	Relative density
D_X	Relative density of phase X
D_Y	Relative density of phase Y
G''	Loss modulus
G'	Storage modulus
G_{ag}	Storage modulus of agarose
G_C	Modulus of composite gels
G'_{exp}	Experimental storage modulus
G_L	Lower bound moduli
$G'_{L(wp)}$	Lower bound moduli which correspond to agarose
G_U	Upper bound moduli
$G'_{U(ag)}$	Upper bound moduli which correspond to agarose
G'_{wp}	Storage modulus of whey protein
G_X	Modulus of phase X

G_y	Modulus of phase Y
k	Einstein coefficient
M_x	Moduli of polymer X
M_y	Moduli of polymer Y
n	Square root of R
p	Solvent partition
R	Ratio of the two moduli, M_y/M_x
S_{wp}	Solvent content of the whey-protein phase
S_x	Fraction of solvent in the polymer X phase
$\tan \delta$	Phase angle
T_{max}	Maximum heat flow temperature
tw_x	Total weights of phase X
tw_y	Total weights of phase Y
V_x	Relative volume of region X
V_y	Relative volume of region Y
w	Total weight of water in system
w_x	Weight of water in phase X
w_y	Weight of water in phase Y
τ	Characteristic time of the material
T	Time over which the deformation is observed
R (equation [1.10])	Concentration coefficient particular to the experimental system
D (Equation [2.2])	Deborah number

CHAPTER 1

INTRODUCTION

1.1 AGAROSE

Agar is one of biopolymers that have been used extensively in many applications such as clinical diagnostic testing, molecular biology, biomedical research and food. In food products, agar is used for its ability to bind water and to form thermoreversible gels (Table 1.1). In addition to gelling properties, agar is also known for a high dietary fiber content.

Table 1.1 Food applications of agars (Padua, 1993)

Products	Application
Bakery	Baked goods, icing, and glazes
Confectionary and desserts	Jelly confections, particularly in Japan
Meat, fish, and poultry	Canned products
Dairy	Stabilizer for sherbets and ice cream
	Improves texture in cheese
Beverage	Fining and flocculating agent in wine and fruits
	juice preparations

Agar is a complex mixture of polysaccharides extracted from species of the red algae known as the agarophytes (Duckworth, Hong, & Yaphe, 1970). Agar is composed of alternating $\beta(1,3)$ - and $\alpha(1,4)$ -linked galactose residues and is lightly sulfated. Early investigation by Araki (1937) on the agar from *Gelidium amansii* showed that agar

consists of two major fractions: agarose, a neutral polymer, and agarpectin, a sulphated polymer. However, later work has shown that agar is actually composed of a complex mixture of polysaccharides instead of one neutral and one anionic polysaccharide. Stanley (2006) stated that the complex mixture of polysaccharides range from a virtually uncharged molecule (the unsubstituted polymer of agarobiose, which is shown in Figure 1.1) to various charged galactans, some rich in ester sulfate, others in pyruvate, which occur as the ketal across positions 4- and 6- in the (1,3)-linked galactose residues [4,6-*O*-(1'-carboxyethylidene)-D-galactose].

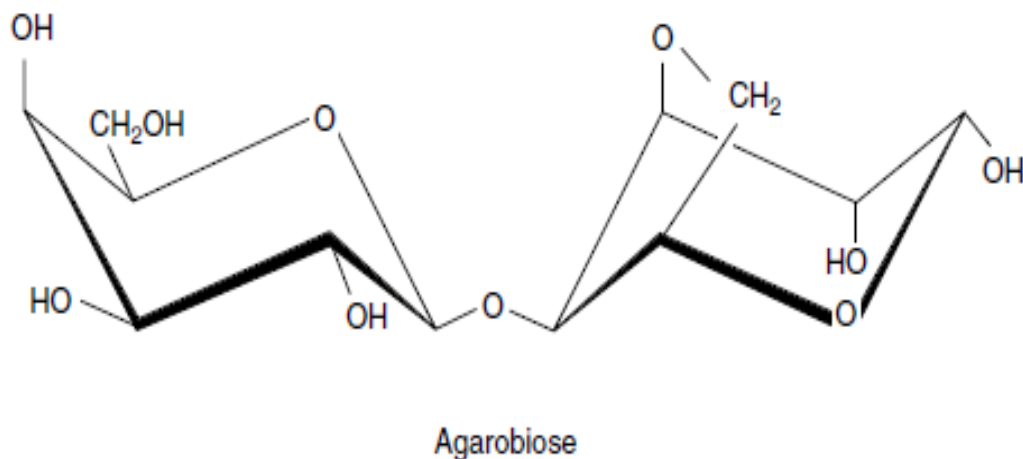


Figure 1.1 Basic disaccharide moieties of agar (agarobiose) (Stanley, 2006).

Agarose gels, which consist of thick bundles of agarose chains and large pores of water, exhibit strong elasticity and high turbidity (Aymard et al., 2001). Braudo et al. (1991a; 1991b) considered hydrogen bonding to be the primary mechanism involved in agarose gelation. Agarose in solution exists as random coils and when the solution is cooled the coils become ordered, thus, the agarose gels are formed. As cooling progresses, double helices are formed for gel network (Arnott et al., 1974). Arnott et al. (1974) further suggested that the helices are aggregated due to the turbidity of gels and

the behavior of short, helix-forming chains in precipitating from solution as soon as they begin to undergo the transition to double helices (Dea, McKinnon, & Rees, 1972).

Agars form sols if they are heated above their gel melting point (85°C or higher). The sols then can be cooled to much lower temperatures before setting to gels. In order to melt the gels, reheating to a higher temperature is required. This phenomenon is known as “gelation hysteresis phenomenon” (i.e. difference between melting and gelling temperature) (Stanley, 2006). Another phenomenon that can be observed in agarose gels is syneresis or a spontaneous loss of water on standing (Arnott et al., 1974).

Barrangou, Daubert, and Foegeding (2006) reported that agarose gels with higher concentration exhibit stronger gel network with decreasing deformability. According to Ross-Murphy and Shatwell (1993) aqueous gels can be classified as strong and weak. Both exhibit similar mechanical spectra when applied with a small strain with storage modulus (G') greater than the loss modulus (G'') – both moduli are independent of frequency. Strong gels show linear viscoelasticity at high strains (>0.25), whereas weak gels do so only for strains at <0.05 . Applying a large strain on strong gels causes the gels to rupture and fail and they do not heal without melting and resetting. On the contrary, weak gels will recover and flow without fracture.

1.2 WHEY PROTEIN

Whey is a by-product from cheese making. It is a source of high quality protein that contains rich amino acid profile. Despite the increasing appreciation that whey is a valuable resource of dairy industry, as opposed to a waste product of the cheese and casein industries, there have been drawbacks in its utilization as a functional ingredient in processed food products. In Australia, only 20% of whey production finds its way into

domestic manufacture, with the remainder being “off-loaded” abroad as a cost-effectively managed waste stream of cheese processing.

Table 1.2 Applications of whey proteins (Cayot & Lorient, 1997)

Applications	Functional properties	Proteins used
Bread making	Waterholding	WPC or WPC + caseinates
Biscuit manufacturing	Fat dispersibility	WPI
Cereals	Emulsion stability	WPI, coprecipitates
	Overrun of foam	Whey
	Gelling properties	
	Browning	
Pasta	Binding and texturing effect	Coprecipitates
	Browning	
Confectionary	Emulsion manufacturing	WPC + hydrolyzed caseinates
Chocolate	Overrun of foam	WPC
confectionary	Browning, aroma	Whey
	Antioxidizing effect	Coprecipitates
Ice cream	Emulsion stability	WPC + caseinates and total
	Overrun of foams	milk proteins
	Gelling properties	
Meat products	Emulsion making	WPC, WPI alone or in
Delicatessen	Waterholding (creamy and	mixture with caseinate

Meat	smooth texture) Adhesive or binding properties	
Sauces	Emulsion stability	WPC + caseinates + egg yolk
Soups	Waterholding	WPC + caseinates + whole
Ready-to-eat food		egg
Milk products (cheese, yoghurts, “light” butter)	Emulsion stability Waterholding Gelling properties	Caseinates WPC + caseinates WPI
Alcoholic beverages	Cream stabilization Cloudy aspect	WPC + caseinates WPC or WPI
Nutritional uses	Protein intake Enteral nutrition	Whey, WPC, or WPI WPC hydrolysates
Cosmetics	Skin protection Antimicrobial properties	Lactoferrin, WPC hydrolysates Lactoferrin, lactoperoxidase

Whey protein is popular in sports nutrition and infant foods, but could be used further in breakfast cereals, snacks, and energy/nutrition bars (Table 1.2). Whey protein has many potential benefits such as:

- improvement in nutritional quality
- imparting flavor and color due to the presence of lactose that takes part in Maillard reactions with the protein
- as fat replacer in low-fat dairy products when co-gelled with polysaccharides
- as an ingredient in starch-based formulations (e.g. snacks and cereals)

Structure of whey proteins

Whey proteins are globular proteins with a limited number of disulfide bonds (Fox & Mulvihill, 1982; Swaisgood, 1982) that confer a certain degree of structural constraint and impart stability. β -Lactoglobulin (β -Lg) is the major protein (Figure 1.2) of whey with one thiol group and two disulfide bonds. The functionalities of whey proteins mainly reflect those of β -Lg because β -Lg represents approximately 50% of the total whey proteins. The native state of β -Lg is dimer with two disulfide bonds (Figure 1.3) and a free thiol group in the pH range of 5.0–8.0. β -Lg exists as an octomer in the pH range of 3.0–5.0, and as monomer above pH 8.0 or below pH 2.0, and the monomeric units of these complexes are identical (Cayot & Lorient, 1997).

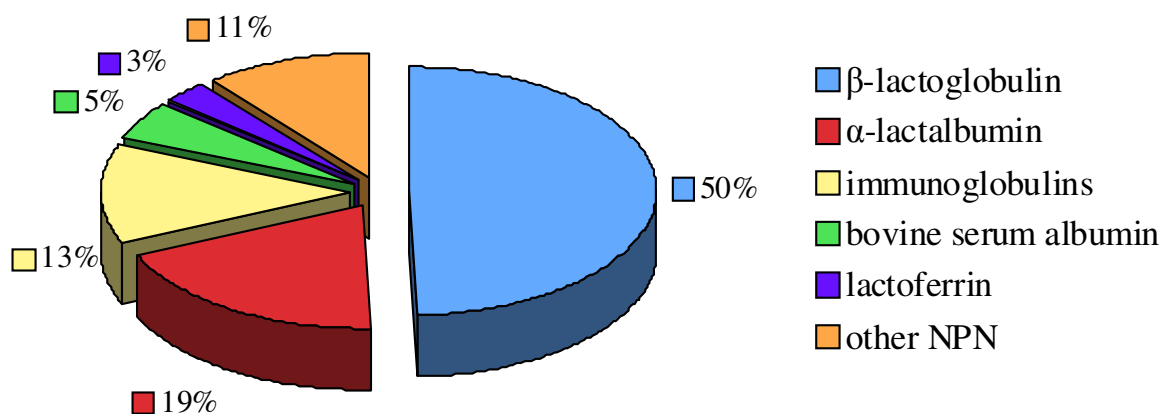


Figure 1.2 Composition of whey proteins (adapted from Cayot & Lorient, 1997)

α -Lactalbumin (α -Lac) is the second major protein in whey after β -Lg with four disulfide bonds (Table 1.3) and rich in essential amino acid such as lysine, leucine, threonine, tryptophan, and cystine (Kinsellaa & Whitehead, 1989). α -Lac binds calcium,

which may stabilize the molecule against irreversible thermal denaturation (Hiraoka & Sugai, 1984). The other two major whey proteins are bovine serum albumin (BSA) and the immunoglobulins (Ig). Their characteristics are summarized in Table 1.3.

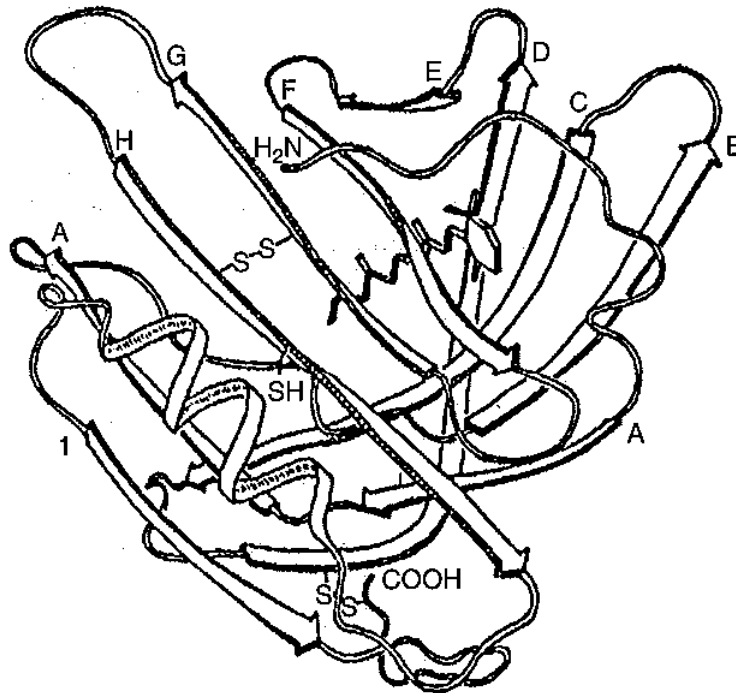


Figure 1.3 Tertiary structure of β -Lactoglobulin (Papiz et al, 1986)

Protein hydration

Protein interaction with water influences various functional characteristics of proteins, such as dispersibility, solubility, viscosity, gelation, coagulation, emulsification, and foaming. Water molecules bind to several groups in proteins that include charged groups (ion-dipole interactions); backbone peptide groups; the amide groups of Asn and Gln; hydroxyl groups of Ser, Thr, and Tyr residues (all dipole-dipole interactions); and nonpolar residues (dipole-induced dipole interaction and hydrophobic hydration).

Table 1.3 Characteristics of major whey proteins (Cayot & Lorient, 1997)

Characteristics	β- Lactoglobulin	α- Lactalbumin	Bovine serum albumin	Immunoglobulin
Molar mass (g/mol)	18,362	14,714	69,000	150,000 – 1,000,000
Isoelectric point (pI)	5.2	4.5 – 4.8	4.7 – 4.9	5.5 – 8.3
Cysteyl residue/mol	5	8	35	—
Amino acid residues/mol	162	123	582	>1000
Disulfide bonds/mol	2	4	17	4.x
Thiol function/mol	1	0	1	—
Lysyl residues/mol	15	12	59	—
Arginyl residues/mol	3	1	23	—
Histidyl residues/mol	2	3	18	—
Glutamyl residues/mol	16	8	59	—
Aspartyl residues/mol	10	9	39	—
Average hydrophobicity (kJ/residue)	508	468	468	458

Hydration of whey proteins can be influenced by several factors such as pH of the dispersing medium and ionic strength. Proteins with a strong net negative or positive charge tend to bind more water and are more soluble than if the net charge is minimal (at isoelectric point), where enhanced protein-protein interactions result in minimal interaction with water. Most proteins tend to bind more water at pH between 9 and 10 than at any other pH due to ionization of sulfhydryl and tyrosine residues. Above pH 10, the loss of positively charged ϵ -amino groups of lysyl residues results in reduced water binding (Damodaran, 2008).

Ionic strength affects protein solubility according to ion species and valency; salt concentrations up to 0.1M enhance solubility because hydrated salt ions, especially the anions, bind (weakly) to charged groups on proteins, but above 0.15M can reduce the solubility (Damodaran & Kinsella, 1981a). Salt at high concentrations can cause protein dehydration by competing with the protein for water, thus, reducing the amount of available water for hydration (Smith & Culbertson, 2000). Ions in solution exert their influence by affecting the net charge of proteins, hydration and electrostatic interactions (Kinsellaa & Whitehead, 1989). At low concentration, binding of salt ions to protein does not affect the hydration shell of the charged groups on protein, and the increase in water binding essentially comes from water associated with bound ions.

Protein denaturation

Whey proteins denature at temperature above 65°C and their denaturation can be affected by various factors such as pH, ionic strength, time, temperature, and protein concentration. The denaturation of whey proteins is pH sensitive and the isoelectric point of approximately 4.6 is used to recover heat-denatured whey proteins. The pH affects the rate of denaturation and coagulation by affecting the net charge of the proteins

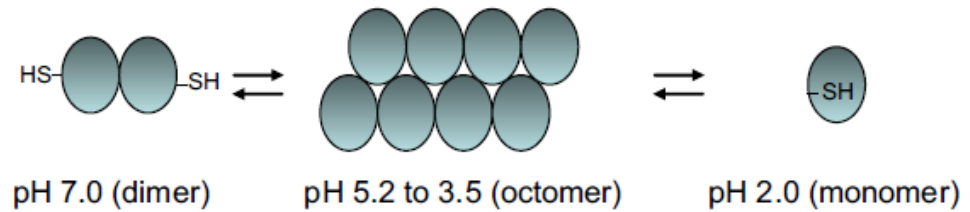
(Harwalkar, 1986). Thus, minimal coagulation occurs above pH 6.5 (deWit, 1981) or below the critical pH range of 3.7 to 3.9 (Bernal & Jelen, 1985).

Using differential scanning calorimeter (DSC), deWit and Klarenbeek (1984) showed that α -lactalbumin has a thermal denaturation range from 62°C to 68°C whereas β -lactoglobulin denatures between 78°C and 83°C. Heating β -lactoglobulin solution between 50°C and 80°C (at pH 6.85) increases the reactivity of thiol group due to dissociation of the binary units (Ross-Murphy & Shatwell, 1993). Figure 1.4 illustrates the solution properties and denaturation of β -lactoglobulin.

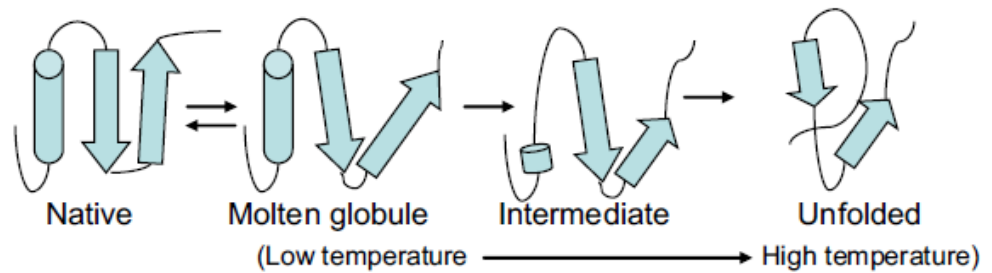
The denaturation temperature increases as the pH value decreases from pH 9 to pH 3 (Paulsson, Hegg, & Castberg, 1985). In an acidic environment (pH < 4), α -Lac is more sensitive to heat or enzyme-induced denaturation due to the loss of Ca^{2+} (Miranda, Haxe, Scanff, & Pelissier, 1989). The Ca^{2+} ion is an important factor in preventing the unfolding when one or two of the four disulfide bonds are reduced (Ewbank & Creighton, 1993a; 1993b).

Proteins are more stable against denaturation at their isoelectric point than at any other pH due to low electrostatic repulsive energy. At neutral pH, most proteins are negatively charged although a few are positively charged. On the contrary, the intramolecular electrostatic repulsion is strong at extreme pH value (either acid or alkaline) due to high net charge. The swelling and unfolding of the protein molecule is a result of this strong electrostatic repulsion, with a higher degree of protein unfolding at extreme alkaline pH values than it is at extreme acidic pH values. This higher degree of unfolding is attributed to ionization of partially buried carboxyl, phenolic, and sulfhydryl groups that cause unravelling of the polypeptic chain as they attempt to expose themselves to the aqueous environment (Damodaran, 2008).

I. pH-dependent solution properties



II. Heat-induced unfolding



III. Primary aggregate structure



Figure 1.4 Model for β -lactoglobulin showing the range of structures in solution, denatured state and aggregated state (van der Linden & Foegeding, 2009).

Calcium ions often induce aggregation of proteins. This is attributable to formation of ionic bridges involving Ca^{2+} ions and carboxyl groups. Addition of calcium in whey protein isolate leads to a formation of a stable colloidal aggregate. However, in the case of other proteins such as caseins and soy proteins, calcium aggregation leads to precipitation. The concentration of calcium ions influences the extent of aggregation. Most proteins show maximum aggregation at 40-50 mM Ca^{2+} ion concentration (Damodaran, 2008).

Protein gelation

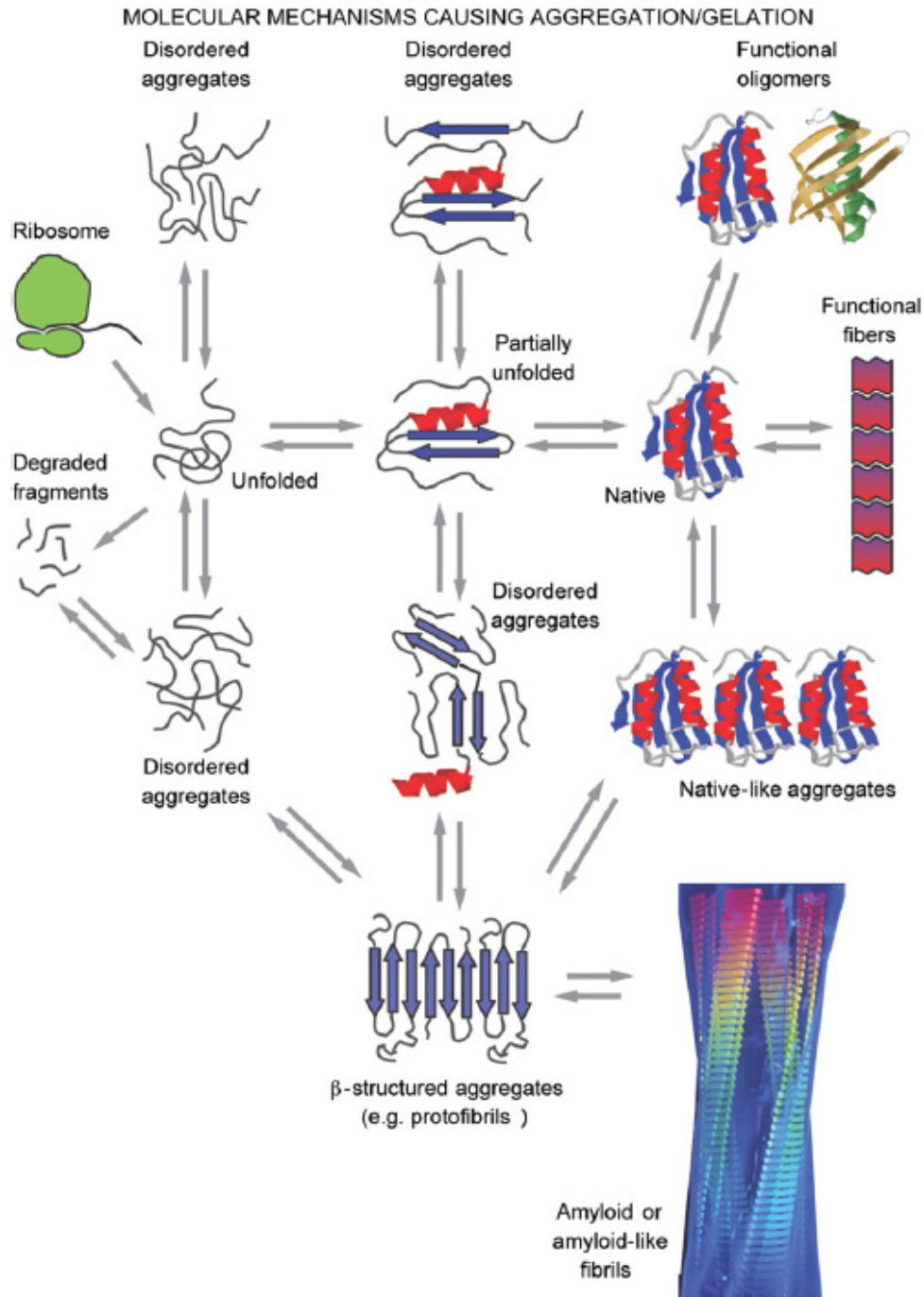
Gel is a form of matter intermediate between a solid and a liquid. The formation of gel can be attributed to polymers cross-linked together through either covalent or noncovalent bonds (Table 1.4) to form a network that can entrap water and other low molecular-weight molecules. Protein gelation refers to transformation of a protein from the “sol” state to a “gel-like” state. In the progel state, some degree of protein denaturation and polymerization has already occurred. Furthermore, in this state, several previously hidden functional groups, such as hydrogen bonding and hydrophobic groups that are responsible for intermolecular noncovalent bonds, become exposed, thus, promotes the formation of protein network (Oakenfull, Pearce, & Burley, 1997; Damodaran, 2008). Hydrogen bonds, hydrophobic interactions, and electrostatic interactions are involved in network formation (Smith & Culbertson, 2000). The disulfide bonds of cystine residues are the main bonds that connect protein chains and these bonds stabilize the structure of proteins (Oakenfull, Pearce, & Burley, 1997).

The gelation of protein can be induced by several factors such as heat, extreme pH, and addition of salts or enzymes to a concentrated protein solution. In the case of whey protein, the heat-induced gelation is a two-step process. The first step is initial unfolding of the hydrogen-bonding groups that bind water. The second step is aggregation of molecules. The basic model for protein folding, unfolding, and aggregation proposed by Chiti and Dobson (2006) is shown in Figure 1.4 in which the native molecules can have quaternary structures of functional fibers or oligomers. The model illustrates that the native monomer can interact to form native-like aggregates, which eventually formed β -structured aggregates (Figure 1.5).

Table 1.4 Intermolecular forces stabilizing protein and polysaccharide structures (Oakenfull, Pearce, & Burley, 1997)

Bond type	Example
Noncovalent	
Hydrogen bonds	-H...O...H- -H...N...H-
Hydrophobic interactions	-CH ₃ ...CH ₃ -
Electrostatic — salt links	-COO ⁻ ... ⁺ H ₃ N-
Electrostatic — metal ion bridges	-COO ⁻ ...Ca ²⁺ ... ⁻ COO-
Covalent	
Disulfide	-S-S-
Gamma glutamyl	-CH ₂ -CH ₂ -CO...NH-CH ₂ -CH ₂ -

Whey protein heat-induced gelation is affected by protein concentration, salt concentration (e.g., Ca²⁺) and pH. The gels which are formed at acid and alkaline environment are strong, viscoelastic and translucent (except at pH < 3–4 where weak gels are formed). On the other hand, weak and coagulum-type opaque gels are formed at the pI (Cayot & Lorient, 1997). Langton and Hermansson (1992) conducted a study to investigate the effect of varying pH on β-Lg and whey protein gels. They concluded that the microstructure of whey protein gels at different pH is similar to the microstructure of β-Lg gels at comparable pH. According to the authors, β-Lg forms two types of gels: white particulate (between pH 4 and pH 6) and transparent fine-stranded (below pH 4 and above pH 6).




 Chiti F, Dobson CM. 2006. Annu. Rev. Biochem. 75:333–66

Figure 1.5 Model for protein folding, unfolding, and aggregation proposed by Chiti and Dobson (2006).

1.3 BIOPOLYMER MIXTURES

According to Clark and Ross-Murphy (2009) polymer networks depend upon covalent or non-covalent interactions between macromolecules. These interactions include cross-links, junction zone and particulate-type interactions. Gel can be defined as a swollen polymer network. Flory (1974) suggested four types of gels based on the following:

- Type 1: Well-ordered lamellar structure, including gel mesophases.
- Type 2: Covalent polymeric networks; completely disordered.
- Type 3: Polymer networks formed through physical aggregation, mainly disordered, but with regions of local order.
- Type 4: Particular, disordered structures.

Figure 1.6 illustrates type 2, 3, and 4 gels. Examples of type 2, 3, and 4 gels respectively are the rubber-like arterial protein elastin, carrageenans, and the globular protein gels formed by heating and/or changing pH, without substantial unfolding. Nonetheless, Figure 1.6 is highly idealized; for example if the solvent is 'poor', gel collapse is seen.

When mixing two biopolymers, two possible interactions may occur: associative and segregative interactions (Morris, 2009). An associative interaction occurs in a limited number of systems and can be characterized by formation of ordered heterotypic junctions analogous to the homotypic junction zones in single-component polysaccharide gels. Gels produced from this type of network formation are often called 'synergistic gels'. Example of this system is the gel formed by locust bean gum, konjac glucomannan and related (1→4)-diequatorially linked plant polysaccharides in combination with xanthan. However, an electrostatic attraction between polyanions (e.g. negatively charged polysaccharides) and polycations (e.g. proteins below their isoelectric point) is

the more general type of associative interaction. In comparison to associative, segregative interactions are more common and occur in almost all biopolymer mixtures where there is no over-riding drive to heterotypic binding. In segregative, the individual molecules prefer to be surrounded by molecules of the same type. This characteristic is often called ‘thermodynamic incompatibility’ (Syrbe et al., 1995) which can be attributed to the differences in polarity, the specific structure and compositional features of biopolymers, and the molecular weight and conformation of the biopolymers (Schorsch, Jones, & Norton, 1999; Zeman & Patterson, 1972).

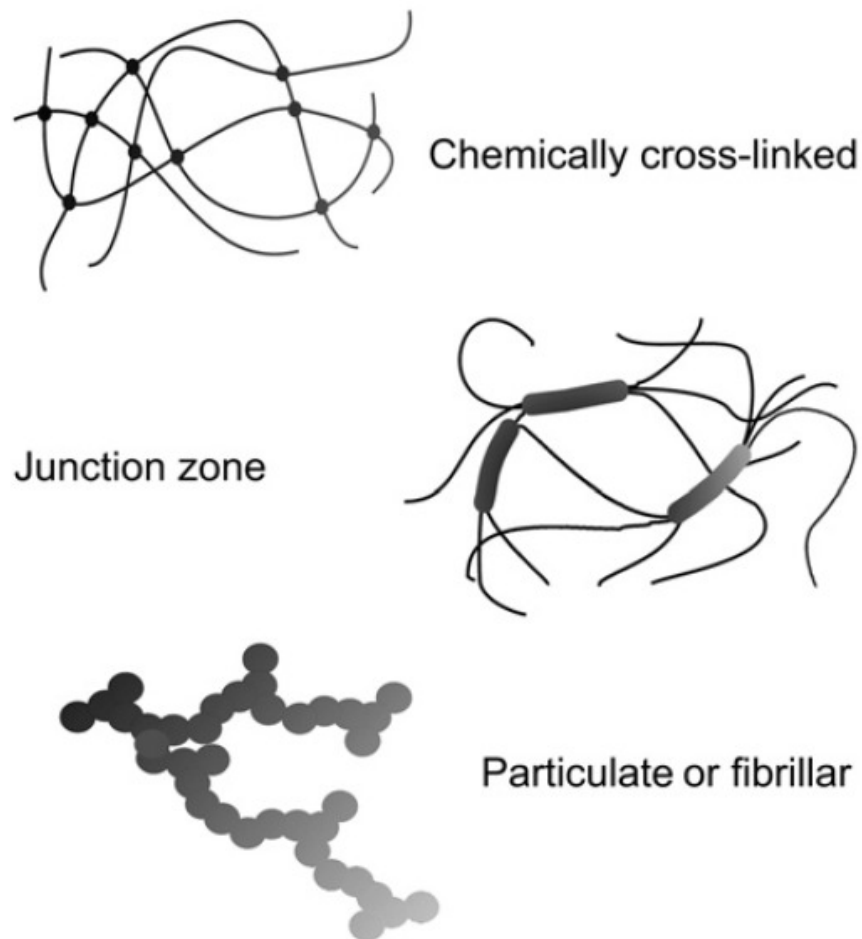


Figure 1.6 Three different types of polymer network (Clark & Ross-Murphy, 2009).

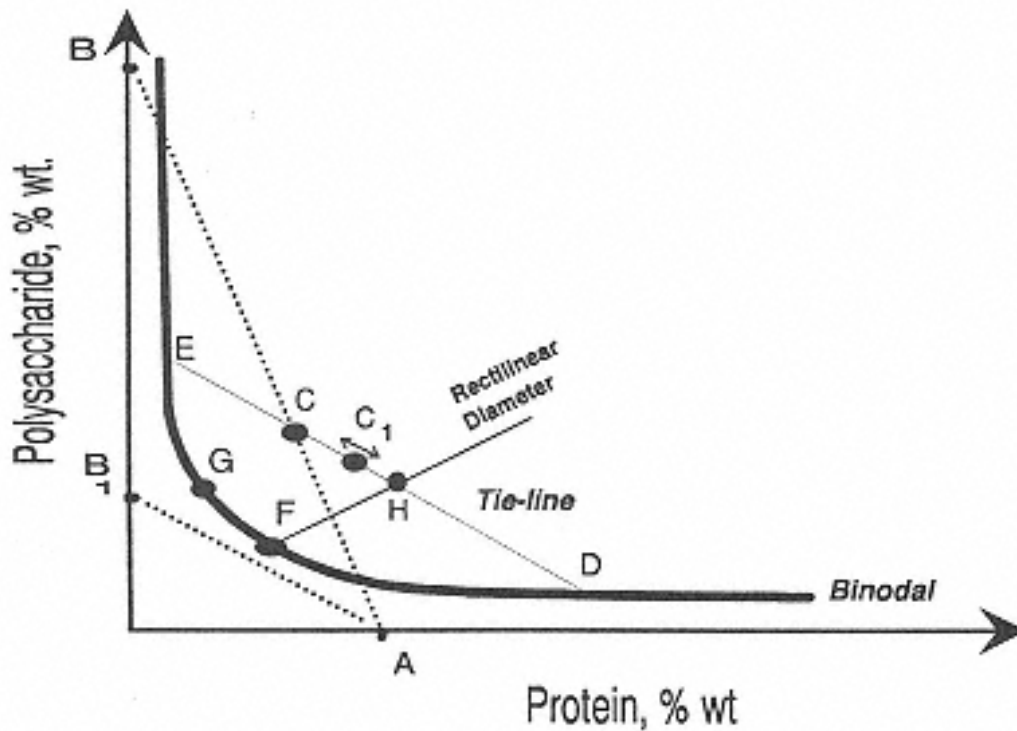


Figure 1.7 Phase diagram of a protein-polysaccharide-water system (Tolstoguzov, 1993; 1995; 1997).

The phenomenon of thermodynamic incompatibility of protein and polysaccharide is illustrated in Figure 1.7. The solid line (DFGE) in Figure 1.7 is a binodal curve that represents co-solubility profile of biopolymers in a given medium. The region under the binodal curve correlates to one-phase mixed solutions (AB_1) whereas the region above the curve corresponds to two-phase systems (AB). The point at which the two co-existing phases are of the same composition and volume is called the critical point, F. The compositional difference between coexisting phases usually increases with distance from the critical point (F). The phase separation threshold (G) is the minimal total concentration of biopolymers required for phase separation to occur. The tie line (ED) connects the binodal points (D and E) corresponding to the composition of the co-existing phases (Tolstoguzov, 1995). The diagram shows that a mixture C is obtained by mixing solutions A and B in the volume proportion BC/AC . The mixed solution C breaks down into two phases D and E (Tolstoguzov, 1997).

1.4 PHASE SEPARATION

Segregative interactions lead the separation of molecules in mixed systems into two co-existing phases. Phase separation in solution usually can be detected by development of turbidity on mixing that is caused by formation of a 'water-in-water emulsion', in which one phase exists as a continuous phase with the other dispersed through it as small liquid droplets (e.g. Grinberg and Tolstoguzov, 1972, 1997; Polyakov et al., 1997). Mixtures composed of non-gelling biopolymers usually exhibit gradual resolution into two clear layers after initial phase separation. However, that is not the case with gelling biopolymers; the water-in-water emulsion structure can be trapped by network formation, forming a biphasic co-gel with one phase as the continuous phase and the other as the dispersed phase (Morris, 2009). Several examples of phase separation in biopolymer mixtures are described in the following paragraphs.

In several studies (Piculell, Nilsson, & Muhrbeck, 1992; Gilsenan, Richardson, & Morris, 2003a, 2003b), there is evidence of a bicontinuous co-gel in which the first component gels and exists as continuous phase, and the second component forms a second continuous phase running through the interstices of the original network (like a jelly set in the pores of a sponge). Furthermore, Shrinivas et al. (2009) reported that observation of bicontinuous gels of agarose and gelatin with addition of lipid phase could be interpreted as a mixed system consist of non-interacting agarose and gelatin phases which support the lipid component in tertiary matrix.

In the case of maltodextrin-whey protein system, cooling of the mixed system, followed by heating displayed a transition from an isostrain condition to an isostress condition (Manoj, Kasapis, & Hember, 1997). Gelled maltodextrin matrix surrounded the liquid whey protein inclusions in isostrain condition whereas in isostress condition, heating denatured whey protein resulted in the protein inclusions being the strongest

phase. In another system that consists of cross-linked waxy maize starch (CWMS) and whey protein isolate (WPI), the continuous phase is the whey proteins with swollen starch granules dispersed within. According to the authors, “the WPI/CWMS system can be described as a suspension of swollen starch granules whose packing is disrupted by the insertion of protein aggregates formed upon heating” under the experiment conditions (Dang, Loisel, Desrumaux, & Doublier, 2009). The authors also suggested that the WPI/CWMS system might be described as a multiple suspension of a continuous water phase with different types of dispersed materials (starch granules, protein aggregates, and complex particles of starch granules with adsorbed protein on the surface).

Application of polymer blending laws (Section 1.5) in agarose-crosslinked waxy maize starch system resulted in calculated storage modulus values (G') that similar to the measured values (Z.H. Mohammed, M.W.N. Hember, R.K. Richardson, & E.R. Morris, 1998). The dispersed component influenced the overall moduli of the composite relative to that of the continuous phase by, at most, a factor of ~ 2 . The study reported that the measured values of G' were in close agreement with the values obtained by application of the polymer blending laws, using the isostress and isostrain model.

1.5 POLYMER BLENDING LAWS

A mixed system of biopolymers usually results in one polymer as the continuous phase and the other as the discontinuous phase (‘filler’). In one arrangement, the continuous phase could be the stronger component with the weaker component as the ‘filler’. This particular type of arrangement is called the isostrain condition (Equation [1.1]) according to the Takayanagi polymer blending laws due to both components are deformed to the same extent (parallel arrangement). On the contrary, in the isostress condition (Equation [1.2]), the weaker component, which is the continuous phase, limits

the force transmitted to stronger component, thus both components are subjected to the same stress (series arrangement).

$$G_c = \phi_x G_x + \phi_y G_y \quad (\text{isostrain}) \quad [1.1]$$

$$G_c = (\phi_x / G_x + \phi_y / G_y)^{-1} \quad (\text{isostress}) \quad [1.2]$$

The modulus of composite gels (G_c) can be related to the modulus of individual phases (G_x and G_y) using the equations mentioned above. ϕ_x and ϕ_y refers to the phase volume of component X and Y respectively ($\phi_x + \phi_y = 1$). In addition to Takayanagi polymer blending laws, Davies (1971) proposed an equation for phase-separated bicontinuous network:

$$(G_c)^{1/5} = \phi_x (G_x)^{1/5} + \phi_y (G_y)^{1/5} \quad (\text{bicontinuous}) \quad [1.3]$$

where in Equation [1.3] ϕ_x and ϕ_y are the volume-fractions ('phase volumes') of respective phases, X and Y with $\phi_x + \phi_y = 1$.

Morris (2009) summarized the rheology of biphasic co-gels as follows:

- The continuous phase determines the strength of composites.
- The dispersed phase has little direct influence on the moduli of biopolymer composites.
- However, it can contribute an indirect effect, by occupying part of the total volume, and hence increasing the polymer concentration in continuous phase.
- Overall moduli can be calculated using the Takayanagi blending laws.
- Melting of a strong dispersed gel phase is unlikely to reduce the overall moduli by more than about a factor of 4.
- Any larger change would indicate a bicontinuous network structure.

Clark and his colleagues suggested that phase volumes in phase-separated biopolymer gels are determined by the way in which the solvent (water) is partitioned between the two phases (Clark, 1987). In order to characterize the solvent partition, he introduced a parameter, p , defined as the ratio of water/polymer in one phase divided by corresponding ratio for the other phase:

$$p = \frac{(water_X / polymer X)}{(water_Y / polymer Y)} \quad [1.4]$$

In binary mixtures where weights of both polymers (X and Y) and water ($w = water_X + water_Y$) are known, the p factor (Equation [1.4]) defines phase volumes, thus, the effective concentrations and real moduli of each biopolymer within its own phase (Kasapis, 2009).

Solvent Partition

In the work by Morris (1992), the author suggested an approach to calculate values of storage modulus on shear for all possible distributions and find which ones matched the experimental values of the mixture. In this study, the effect of solvent partition for a biphasic gel composed of biopolymers X and Y would have shear moduli of M_X and M_Y , with $M_Y = n^2 M_X$. The ratio of the two moduli, M_Y/M_X , is expressed as R and parameter n equals to square root of R . The author also proposed application of isostrain and isostress blending laws to calculate ‘upper and lower bound’ moduli (G_U and G_L) of composite gels with one phase dispersed within the other phase:

$$G_U = G_X \phi_X + G_Y \phi_Y \quad (\text{upper bound}) \quad [1.5]$$

$$(1/G_L) = (\phi_X / G_X) + (\phi_Y / G_Y) \quad (\text{lower bound}) \quad [1.6]$$

The upper and lower bound (Equations [1.5] and [1.6]) curves pass at one point called ‘critical point’ where $G_X = G_Y = G_U = G_L = M_X (n+1)^2$, with the two bounds passing through minimum and maximum values respectively.

Kasapis et al (1993) proposed the following algorithm (Equations [1.7]-[1.12]) for each possible distribution of solvent between the component phases of mixed-gel combinations: the total weight of water in system (w) can be calculated by subtracting the combined weights of the two polymers from the total weight. In the following framework, S_X refers to the fraction of solvent in the polymer X phase and the weight of water in phases X and Y is:

$$\begin{aligned} w_X &= S_X w \\ w_Y &= (1 - S_X) w \end{aligned} \quad [1.7]$$

The total weights of the phases are then obtained by adding to the weight of the appropriate polymer:

$$\begin{aligned} tw_X &= x + w_X \\ tw_Y &= y + w_Y \end{aligned} \quad [1.8]$$

Thus, the effective concentrations (% w/w) of polymers X and Y in the two phases are:

$$\begin{aligned} c_X &= 100x / tw_X \\ c_Y &= 100y / tw_Y \end{aligned} \quad [1.9]$$

To a good first approximation the total weights of the two phases then define the phase volumes (ϕ_x and ϕ_y in Equations [1.1] and [1.2]). To obtain true phase volumes, the relative weights must be adjusted for density differences between the phases. The relationship between polymer concentration, c , and relative density, D , is described as follow:

$$\begin{aligned} D_X &= 1.0 + Rc_X \\ D_Y &= 1.0 + Rc_Y \end{aligned} \quad [1.10]$$

where R is the concentration coefficient particular to the experimental system. Then, the relative volumes of regions X and Y can be calculated from their total weights and individual densities:

$$\begin{aligned} V_X &= tw_X / D_X \\ V_Y &= tw_Y / D_Y \end{aligned} \quad [1.11]$$

Finally, the phase volumes in the composite can be written in terms of the relative volumes as:

$$\begin{aligned} \phi_X &= V_X / (V_X + V_Y) \\ \phi_Y &= V_Y / (V_X + V_Y) \end{aligned} \quad [1.12]$$

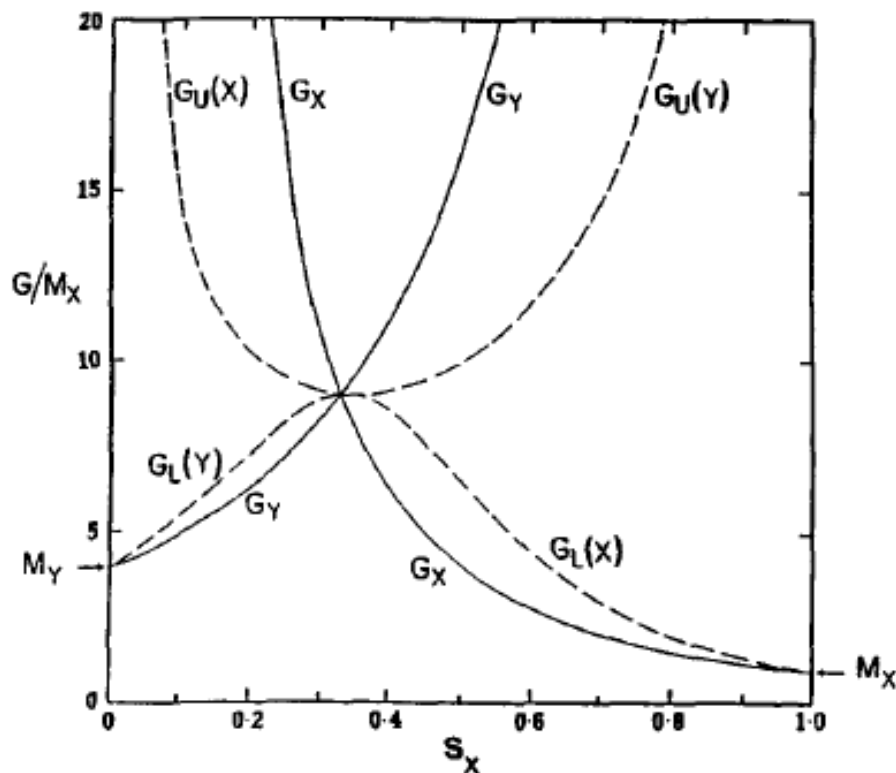


Figure 1.8 Variation of calculated moduli as a function of X , the proportion of solvent in phase X , illustrated for $n=2$ ($M_Y = 4M_X$). G_X and G_Y are the moduli of the individual phases. G_U and G_L are upper and lower bound moduli respectively from isostrain and isostress blending laws, with the continuous phase indicated in parentheses (Morris, 1992).

Figure 1.8 is an example of analysis of Morris's work (1992) showing the effect of solvent partition in a phase-separated mixed gel consists of two polymers X and Y with their respective moduli, M_X and M_Y . According to Figure 1.8, as the proportion of solvent in phase X (S_X) increases from 0 to 1, the calculated values of G_X decrease while the calculated values of G_Y increase. At one point, the two curves cross ($G_X = G_Y$), so that the rigidity of the phases is identical (Morris, 1992). At the same time, the upper bound (G_U) of X-continuous descends from top-left of the diagram, with the lower bound (G_L) of Y-continuous rising from bottom-left, meeting at the same 'critical point'. Beyond this point, the significance of the two blending laws interchanges, with the upper bound now corresponds to Y-continuous system and lower bound to X-continuous (Kasapis, 1993).

Phase Inversion

In two-phase systems, one phase is usually continuous phase and the other is the dispersed phase. Nevertheless, both phases can be continuous or the phases can become inverted, that is, the dispersed phase can become the continuous phase. Lewis and Nielsen (Nielsen, 1974b) developed *Halpin-Tsai* equations to cover a wide range of biphasic morphologies including phase inversion. The *Halpin-Tsai* equations are described as follows:

$$\frac{G'}{G_1'} = \frac{1 + AB\phi_2}{1 - B\phi_2} \quad [1.13]$$

$$B = \frac{\frac{G_2'}{G_1'} - 1}{\frac{G_2'}{G_1'} + A} \quad [1.14]$$

where in Equations [1.13] and [1.14] subscript 1 and 2 refer to the continuous phase and dispersed phase, respectively. The volume fraction in dispersed phase is denoted as ϕ_2 and the constant A is determined by the morphology of the system; for dispersed spheres in an elastomeric matrix $A = 1.5$, for example. Lewis and Nielsen (Nielsen, 1974b) further extended *Halpin-Tsai* equations as follows:

$$\frac{G'}{G_1'} = \frac{1 + AB\phi_2}{1 - B\psi\phi_2} \quad [1.15]$$

$$A = k - 1 \quad [1.16]$$

$$\psi = 1 + \frac{(1 - \phi_m)}{\phi_m^2} \phi_2 \quad [1.17]$$

Table 1.5 Maximum packing fractions ϕ_m values (Nielsen, 1974a)

Particles	Type of packing	ϕ_m
Spheres	Hexagonal close packing	0.7405
Spheres	Face centered cubic	0.7405
Spheres	Body centered cubic	0.60
Spheres	Simple cubic	0.5236
Spheres	Random close packing	0.637
Spheres	Random loose packing	0.601
Fibers	Parallel hexagonal packing	0.907
Fibers	Parallel cubic packing	0.785
Fibers	Parallel random packing	0.82
Fibers	Random orientation	0.52

These equations ([1.15]-[1.17]) also take into account the concept of maximum packing fraction (ϕ_m) of the filler phase. The maximum packing fraction (ϕ_m) varies with particle shape and state of agglomeration as listed in Table 1.5. In Equation [1.16], k is a generalized *Einstein* coefficient, which is very sensitive to the morphology of system (refer to Table 1.6 for list of *Einstein* coefficients for different morphology).

Equations [1.14]-[1.16] can be rewritten to produce Equations [1.18]-[1.20] that can be used for inverted systems in which the continuous phase is the more rigid one:

$$\frac{G_1'}{G'} = \frac{1 + A_i B_i \phi_2}{1 - B_i \psi \phi_2} \quad [1.18]$$

$$B_i = \frac{\frac{G_1'}{G_2'} - 1}{\frac{G_1'}{G_2'} + A_i} \quad [1.19]$$

$$A_i = \frac{1}{A} \quad [1.20]$$

where G' , G_1' , and G_2' are the shear moduli of the composite, continuous phase, and the filler (dispersed phase) respectively, and the ϕ_2 is the phase volume of the filler. In this inverted system, the *Einstein* coefficient is now given as A_i (Equation [1.20]).

Table 1.6 *Einstein* coefficients for composites (Nielsen, 1974b)

Filler Phase	Modulus	<i>Einstein</i> coefficient, k
Spheres	G	$1 + (7 - 5\nu_1)/(8 - 10\nu_1)$
Large aggregates of spheres	G	$2.50/\varphi_a$
Aggregates of two spheres	G	2.58
Rods-axial ratio 4	G	3.08

Rods-axial ratio 6	G	3.84
Rods-axial ratio 8	G	4.80
Rods-axial ratio 10	G	5.93
Rods-axial ratio 15	G	9.4
Uniaxial fiber-filled	E_L	$1 + 2 L/D$
Uniaxial fiber-filled	E_T	1.5
Uniaxial fiber-filled	G_{LT}	2.0
Uniaxial fiber-filled	G_T	1.5
Ribbon-filled ($w/t \rightarrow \infty$)	E_L	∞
Ribbon-filled	E_T	$1 + 2w/t$
Ribbon-filled	E_{TT}	1.0
Ribbon-filled	G_{LT}	$1 + (w/t) (13)$
Ribbon-filled ($w/t \rightarrow \infty$)	G_{LT}	1.0
Ribbon-filled ($w/t \rightarrow \infty$)	G_{TT}	1.0
$M = M_1 \varphi_1 + M_2 \varphi_2$	M	∞
$1/M = (\varphi_1/ M_1) + (\varphi_2/ M_2)$	M	1.0

Note: ν_1 Poissons ratio of matrix (for elastomer phase $\nu_1=0.5$ and for the rigid phase $\nu_1=0.35$)

φ_a Packing fraction of spheres in aggregate

L Length of rod

D Diameter of rod

w Width of rod

t Thickness of ribbon

T Transverse to fibers or ribbons

Subscript L Longitudinal direction

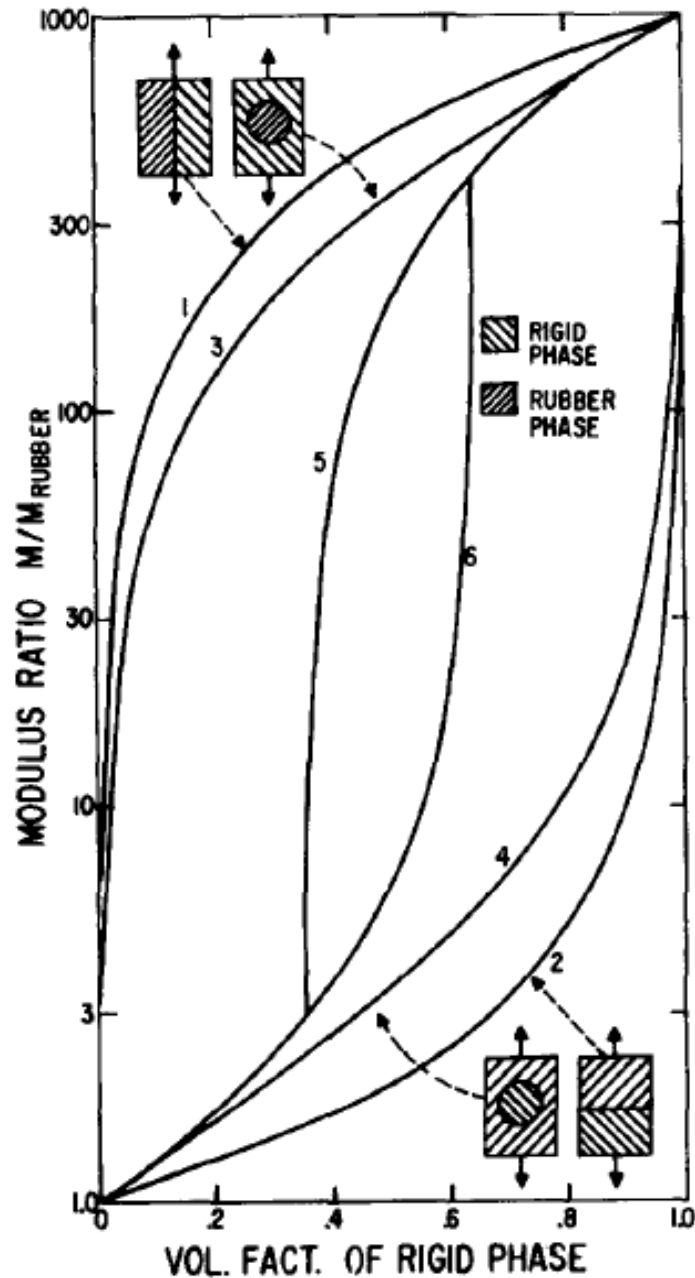


Figure 1.9 Modulus ratio of composites containing rubber and a rigid polymer (Nielsen, 1974b).

Curve 1: parallel element model

Curve 2: series model

Curve 3: *Halpin-Tsai* (or *Kerner*) shear modulus for elastomeric spheres dispersed in a rigid polymer

Curve 4: rigid spheres dispersed in elastomeric phase

Curve 5: elastomeric spheres in rigid matrix for $\phi'_m = 0.64$ (random packing)

Curve 6: rigid spheres dispersed in an elastomeric matrix for $\phi_m = 0.64$

Figure 1.9 illustrated dispersed and inverted systems of composites containing rubber and a rigid polymer. In this figure, the rigid polymer has a modulus 1000-fold higher than that of the rubber. Curves 1 and 2 of Figure 1.7 correspond to Equations [1.5] and [1.6] respectively in which Equation [1.5] models parallel arrangement and Equation [1.6] models series arrangement. Curves 3 and 4 of Figure 1.7 represent the *Halpin-Tsai* equations for dispersed spheres. Curves 5 and 6 of Figure 1.7 illustrate the Equations [1.15] – [1.20] for dispersed spheres with a *Poissons* ratio of 0.5 for the elastomer phase, and a *Poissons* ratio of 0.35 for the rigid phase. Phase inversion in which both phases are continuous occurs in the range of volume fractions between curves 5 and 6 of Figure 1.7 (Nielsen, 1974a).

CHAPTER 2

MATERIALS AND METHODS

2.1 DIFFERENTIAL SCANNING CALORIMETRY

Differential Scanning Calorimetry (DSC) is a thermal analytical technique commonly used in food science. It is a technique to study and measure temperatures and heat flows associated with thermal transitions in a material such as glass transition, melting, crystallization, and denaturation. This technique is able to differentiate two types of thermal processes: exothermic (release of heat) and endothermic (absorption of heat).

DSC measures any gain or loss of heat energy at a given temperature rise over a given temperature interval. The area of the thermogram is proportional to the heat energy absorbed or released by the sample during a given process (Rahman, Machado-Velasco, Sosa-Morales, & Velez-Ruiz, 2009). In this method, both sample and reference (empty) pans are heated and cooled at the same time under identical conditions. The heating or cooling takes place at a controlled rate. The schematic of typical DSC heat flux is shown in Figure 2.1.

This study used a modulated differential scanning calorimeter (MDSC) that not only it measures the difference in heat flow between a sample and a reference as a function of time and temperature; it also applies two simultaneous heating rates to the sample. A sinusoidal modulation (oscillation) is overlaid on the conventional linear heating ramp to yield a heating profile in which the average sample temperature still

continuously increases with time but not in a linear fashion. The benefits of MDSC over traditional DSC include (TA Instruments, n.d.-a):

- separation of complex transitions
- increased resolution without loss of sensitivity
- increased sensitivity for detection of weak transitions
- ability to measure of heat flow and heat capacity in one experiment

The effect of applying two heating rates is the same as if two experiments were run simultaneously on the material – one experiment at the traditional linear (average) heating rate and one at a sinusoidal (instantaneous) heating rate.

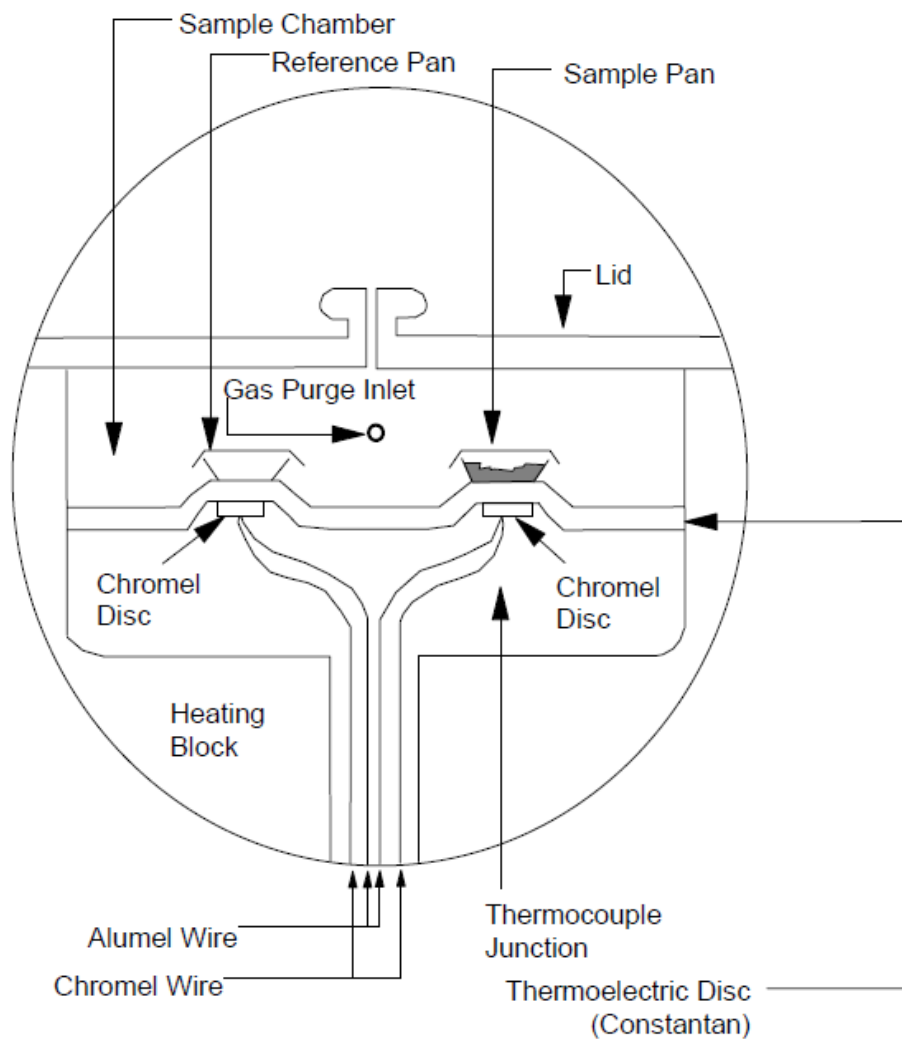


Figure 2.1 Heat flux DSC schematic (TA Instruments, n.d.-c).

The average heating rate provides total heat flow information and a sinusoidal heating rate provides heat capacity information from the heat flow that responds to the rate of temperature change. Total heat flow is the sum of all heat flow occurring at any point in time and temperature. Total heat flow has two individual components, which are the heat capacity component and the kinetic component as shown in Equation [2.1] below. The heat capacity component includes reversing heat flow, in-phase component and heating rate-related components whereas the kinetic component includes nonreversing heat flow, out-of-phase component, and time dependent component (TA Instruments, n.d.-c). Most material transitions exhibit either reversing characteristics (e.g., glass transition and melting) or nonreversing characteristics (e.g., evaporation, cold crystallization, and decomposition). However, several material transitions, such as polymer melting, may contain both reversing and nonreversing characteristics. MDSC is able to facilitate the separation of reversing and nonreversing transitions as shown in Figure 2.2. The figure shows thermogram of bilayer film containing polycarbonate (PC) and amorphous PET. The DSC curve (solid line) exhibits transitions between 130°C and 150°C, but it is difficult to interpret these transitions due to overlapping transitions. The MDSC can clearly separate these transitions; the PC glass transition is a reversing transition whereas the PET recrystallization is a nonreversing transition (Gill, Sauerbrunn, & Reading, 1993).

The equation that describes heat flow in either DSC or MDSC is (Thomas, 2005):

$$\frac{dH}{dt} = C_p \frac{dT}{dt} + f(T, t) \quad [2.1]$$

where: $\frac{dH}{dt}$ = total heat flow rate

C_p = heat capacity

$\frac{dT}{dt}$ = heating rate

$f(T,t)$ = heat flow which is a function of temperature and time

Total heat flow = the sum of all heat flow, dH/dt

Reversing heat flow = heat capacity component, $C_p \times dT/dt$

Nonreversing heat flow = kinetic component, $f(T,t)$

The total heat flow in MDSC is calculated as the average value of the raw modulated heat flow signal using a Fourier transformation analysis. The kinetic (nonreversing) component of the total heat flow is the difference between the total heat flow and the heat capacity (reversing) component.

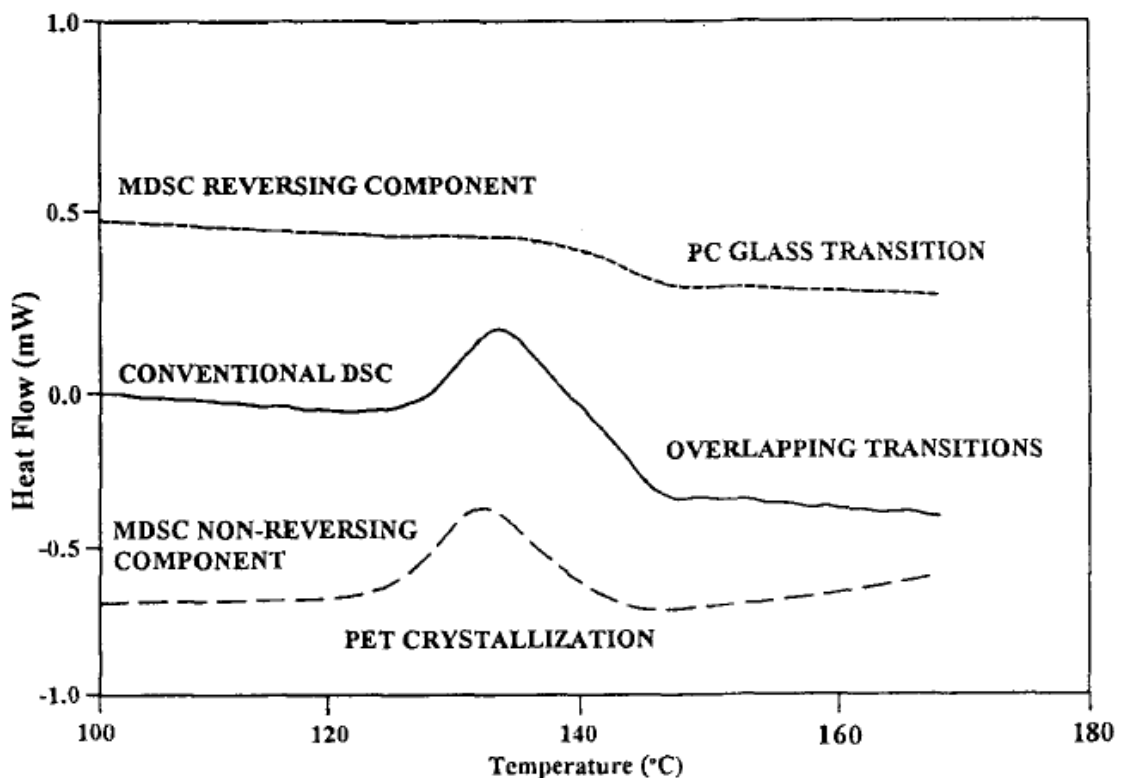


Figure 2.2 MDSC thermogram of PET/PC bilayer film (Gill, et al., 1993).

2.2 RHEOLOGY

Rheology is a study of deformation and flow of matter. Rheology was first developed for synthetic polymers due to the many uses of the polymers in day-to-day applications but it can be applied to any material such as food and soil. Nevertheless, food rheology is one of the critical factors in product development and quality control. Food rheology provides a direct measurement of process parameters, correlates with final product performance, and is used as a problem solver in quality control.

According to Bourne (2002) rheology influences three categories of food acceptability: appearance, flavor, and texture. The appearance of food can exhibit certain structural properties, for example how syrup flows from the bottle and covers a pancake. In regards to flavor, the breakdown of food in mouth can affect the release of flavor compounds. The quality of food by sense of touch depends mostly on rheological analysis. Table 2.1 shows rheological parameters that are commonly used in rheological analysis.

Fluid and semisolid foods exhibit a wide variety of rheological behavior such as Newtonian, shear-thinning, shear-thickening and time-dependent behavior (Figure 2.3). Newtonian behavior exhibits a linear relationship between shear rate and shear stress and the plot begins at origin. Examples of Newtonian materials include water, sugar syrups, most honeys, filtered juices and milk. Non-Newtonian material exhibits time-dependent rheological behavior as a result of structural changes, which indicates the shear stress-shear rate plot is not linear and/or the plot does not begin at the origin. With shear-thinning fluids, increasing shear rate gives less than proportional increase in shear stress.

Table 2.1 Rheological parameter

Parameter	Definition	Symbol	Units (SI)
Shear stress	Force per unit area	σ	Pa
Shear strain	Relative deformation in shear	γ	-
Shear rate	Change of shear strain per unit time	$\dot{\gamma}$	s ⁻¹
Viscosity	Resistance to flow	η	Pa.s
Shear storage modulus	Measure of elasticity of material	G'	Pa
Shear loss modulus	The ability of the material to dissipate energy	G''	Pa
Complex viscosity	Resistance to flow of the sample in the structured state, originating as viscous or elastic flow resistance to the oscillating movement	η^*	Pa.s
Dynamic viscosity	Internal friction of a liquid	η'	Pa.s
Phase angle	Degree of viscoelasticity	$\tan \delta$	-

Shear-thinning fluids also called pseudoplastic. Many salad dressings and some concentrated fruit juices exhibit shear-thinning behavior. Some materials may not commence to flow until a threshold of stress, the yield stress (σ_0), is exceeded. Examples of foods with this type of behavior include tomato ketchup, mustard, and mayonnaise. Bingham plastic materials exhibit linear relationship between shear rate and shear stress with yield stress. Shear-thickening behavior can be observed in partially gelatinized

starch dispersions where an increase in shear stress gives less than proportional increase in shear rate. Time-dependent behavior can be categorized into two types, time-dependent shear-thinning (thixotropic) and time-dependent shear-thickening (antithixotropic) behavior (Rao, 2007).

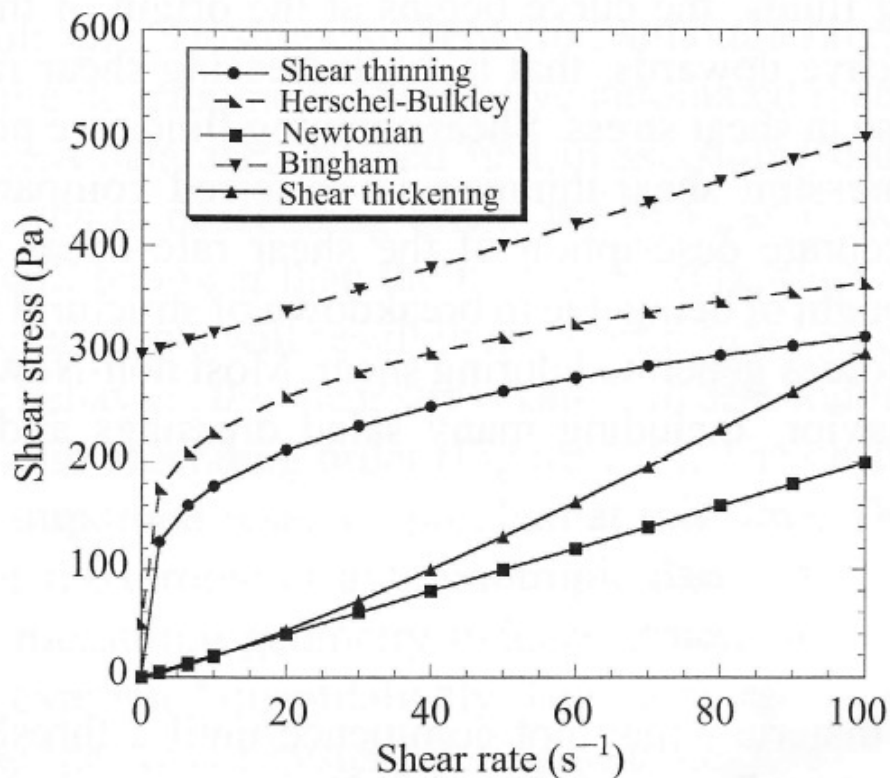


Figure 2.3 Basic shear diagram of shear rate versus shear stress of Newtonian, shear-thinning, and shear-thickening. The diagram also includes Bingham and Herschel-Bulkley (H-B) with a yield stress that must be exceeded for flow to occur (Rao, 2007).

Viscoelastic materials exhibit some of the elastic properties of an ideal solid and some of the flow properties of an ideal liquid simultaneously. Figure 2.4 shows the differences between ideal elastic solid, ideal liquid, and viscoelastic material. Bourne (2002) explained that when an experiment is performed over a short period of time on viscoelastic material, the material would appear to be mostly elastic. On the contrary, when an experiment is performed slowly or over a long period of time the material will appear to be more viscous. Dr. Marcus Reiner explained that everything will flow if

given enough time (Reiner, 1964). He proposed the equation below (equation 2.2) to describe this effect:

$$D = \frac{\tau}{T} \quad [2.2]$$

where D is the Deborah number, τ is the characteristic time of the material, and T is the time over which the deformation is observed. Liquid-like behavior is observed when $D < 1$, and solid-like behavior is observed when $D > 1$ (Borwankar, 1992). Dynamic or oscillatory tests are used to measure the viscoelastic properties of a material. These tests are nondestructive because they apply small amplitude. The sample is usually placed between a cone and a plate or between parallel plates mounted in a rheometer.

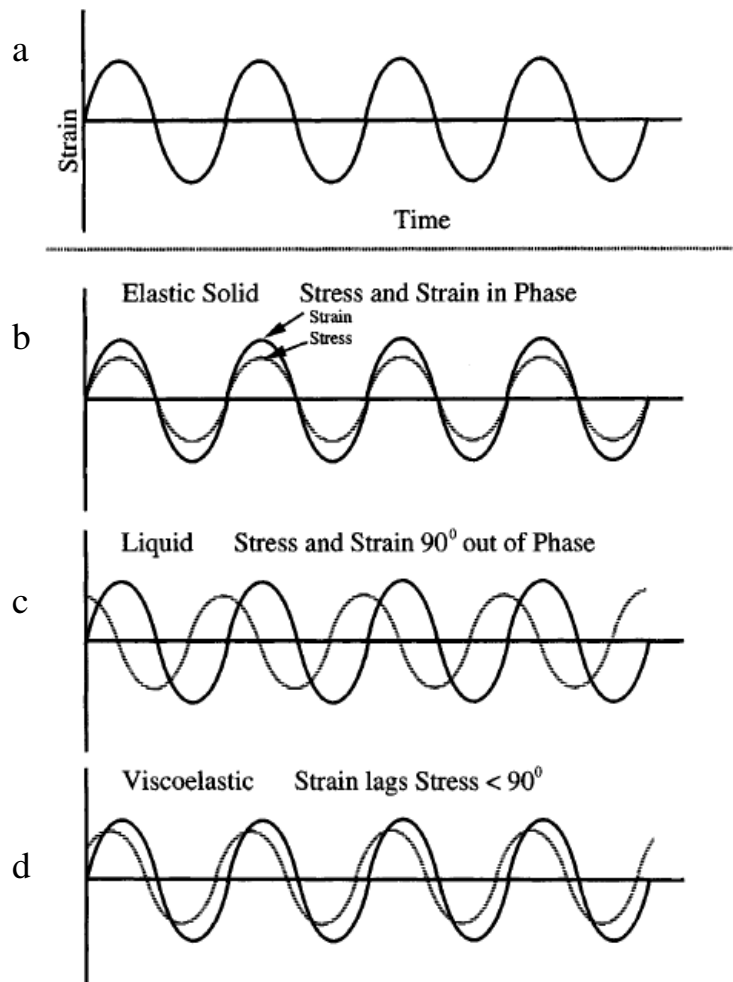


Figure 2.4 The principle of oscillation viscometry. Applied strain versus time (a) and resultant stress versus time that is measured in an elastic solid (b), Newtonian liquid (c) and viscoelastic liquid (d). (Bourne and Rao, 1990)

The viscoelastic behavior of materials can be categorized into two types, linear viscoelastic and nonlinear viscoelastic. In linear viscoelastic, the rheological properties are influenced by time only. On the other hand, the rheological properties in nonlinear viscoelastic are dependant on time, the magnitude of stress, and the rate of applied stress. Most foods that are compressed in mouth fall in nonlinear viscoelastic range (Bourne, 2002).

The linear viscoelastic (LVR) region of a material should be established before performing dynamic tests. The LVR region of a material can be determined by increasing the amplitude of oscillation and observed the magnitude of phase lag and amplitude ratio. The limit of the LVR region is shown by drastic changes in values of rheological properties (e.g., G' and G''). Rao (2007) explained that viscoelastic properties of foods such as gelation and melting of gels could be analyzed using three types of dynamic rheological tests described below:

- Frequency sweep

G' and G'' are determined as a function of frequency (ω) at a fixed temperature. Based on frequency sweep data, one can determine whether the material is true gels or weak gels. True gels are indicated when G' is higher than G'' throughout the frequency range and almost independent of frequency. On the contrary, weak gels are dependent on frequency and the differences between G' and G'' values in weak gels are smaller compared to true gels.

- Temperature sweep

G' and G'' are determined as a function of temperature at a fixed frequency (ω). This test is very useful to study the gel formation (e.g. protein) and gelatinization of starch dispersion.

- Time sweep

G' and G'' are determined as a function of time at a fixed frequency (ω) and temperature. Time sweep test provides information regarding structure development in physical gels. This type of test is often called a gel cure experiment.

2.3 SCANNING ELECTRON MICROSCOPY

Scanning electron microscopy (SEM) is a technique to examine and analyze the microstructure of a material. The SEM is capable of obtaining two-dimensional images of the surfaces of a wide range of materials and high-resolution micrographs (magnification range of 10 – 10,000x). In general, an SEM consists of lens system, electron gun, electron detector, visual and photorecording cathode ray tubes (CRTs), and the associated electronics as shown in Figure 2.5. The electron gun produces electrons and accelerates them to energy in the range of 0.1-30 keV (100-30,000 electron volts). The beam from the electron gun is passed through electron lenses in order to reduce spot size, thus, generating a sharper image. The deflection coils are used for controlling the magnification by causing the beam to move to a series of locations along several lines until a rectangular raster is generated on the specimen. Afterwards, the electron detector collects signals from the beam-specimen interaction from various locations, converts the signals to point-by-point intensity changes on the viewing screen, and produces an image. Secondary electrons (SE) and backscattered electrons (BSE) are the two signals most often used to produce SEM images (Goldstein, et al., 2003).

Secondary electrons (SE) are usually generated by interactions with the primary electrons of the beam. These electrons have low energy and as result they can escape only from a very shallow region at the sample surface. This characteristic contributes to better imaging resolution. Secondary image resembles the sample's visual image. In contrast, images from BSE have low resolution due to high energy therefore these images are not easy to interpret. However, they can provide useful information regarding sample composition (Kimseng & Meissel, 2001).

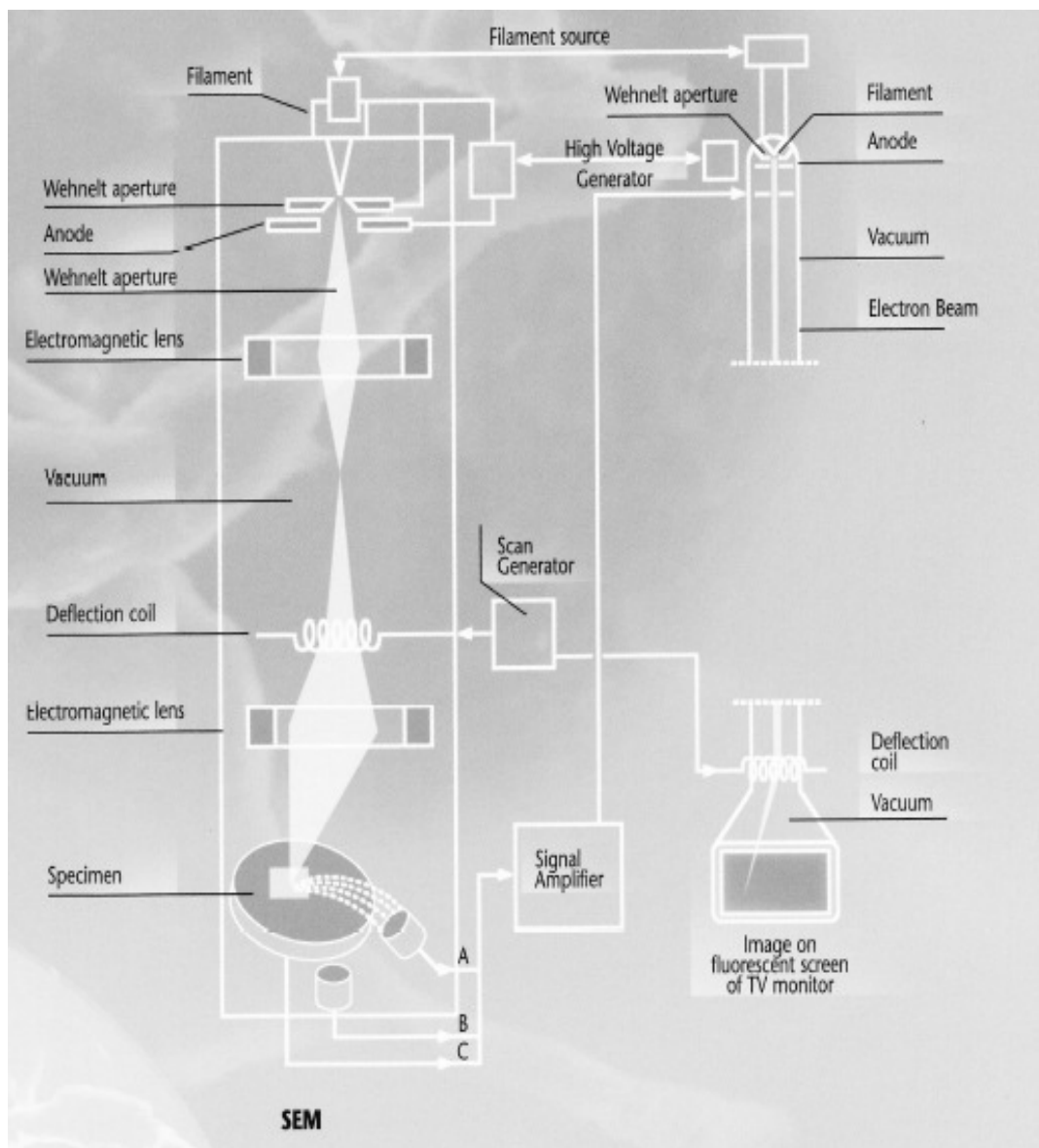


Figure 2.5 Schematic diagram of a SEM (FEI Company, 2008).

The most recent developments in SEM are variable-pressure scanning electron microscope (VPSEM) and environmental scanning electron microscope (ESEM). VPSEM can examine the surfaces of wet or dry specimen because it can operate while its specimen chamber contains a gas or a vapor at a pressure range from approximately 10 to 2500 Pa (0.1-20 torr). In general, ESEM is similar to VPSEM except that ESEM offers a proprietary secondary electron detector for use in gas. VPSEM generally relies only on BSE detection for imaging when there is gas in the chamber (Goldstein, et al., 2003).

Table 2.2 summarizes materials that can be analyzed with SEM and their respective settings, low vacuum, high vacuum, VPSEM or ESEM. Furthermore, it also lists types of images that can be generated by SEM.

Table 2.2 Basic information of SEM (Goldstein, et al., 2003)

	Description
Specimen types	General: thick, bulk (millimeter to centimeter dimensions), solid, low vapor pressure (no water); conductors (at least semiconducting) Special: microscopic particles; film(s)-on-substrate; fixed biological specimens; wet specimens (variable-pressure or environmental SEM); nonconductors with conductive coating (conventional high beam energy and high vacuum) or uncoated (low beam energy, high vacuum; or high beam energy, variable pressure or environmental SEM).
Signals detected	Backscattered electrons (BSE) Secondary electron (SE) Specimen, absorbed, induced currents (SC)

Resolution (Lateral)	Conventional electron source: 10-50 nm Field emission electron source: 1-5 nm
Resolution (Depth)	10-1000 nm (BSE) 1-10 nm (SE)
Depth of field	Selectable with final aperture: 0.1-1 unit of the image field width; high value enables stereomicroscopy for the three-dimensional recognition.
Types of image information	Topography (SE, BSE) Composition (BSE) Crystal orientation (BSE) Electrical field (SE) Magnetic field (SE, BSE) Beam-induced current (SC)

2.4 MATERIALS

The summary of materials used in this study is listed in Table 2.3 including supplier's information.

Table 2.3 List of materials

Materials	Supplier	Description
Agarose Type I-B	Sigma Aldrich (Gillingham, UK)	Product no. A0576 Lot no. 75K0077
Whey protein isolate Instantised 894	Fonterra (Auckland, New Zealand)	Batch no. GT20

Hydrochloric acid (HCl) reagent grade, 37%	Sigma-Aldrich (Wisconsin, USA)	Lot no. 435570-2.5L Batch no. 00659BH
Sodium hydroxide (NaOH) pellets	Merck (Darmstadt, Germany)	Lot no. 1064825000
Milli-Q water	Millipore (Molsheim, France)	Lot no. F7EN26803
Dimethylpolysiloxane	Sigma Aldrich (Missouri, USA)	Batch no. MKBC9787

Agarose has an off-white color and high gel strength. Using aqueous size exclusion chromatography, the supplier determined the number average molecular weight of this agarose sample ($M_n \sim 120$ kDa). Moisture, ash and sulfate contents were of less than 5.0%, 0.25% and 0.10% (w/w), respectively. Furthermore, the pH of 1.5% (w/w) agarose gel was 7.16.

The sample of whey protein was supplied in the form of a creamy white powder. It is a protein isolate commercially available as WPI Instantised 894. Based on the certificate of analysis provided by the supplier, Kjeldahl analysis produced a protein content ($N \times 6.38$) of 90.0% (w/w; dry basis), which consists of β -lactoglobulin (71.0%; ratio of monomer to dimer is 5:1), α -lactalbumin (18.0%) and 6.0% bovine serum albumin (BSA). Molecular weight of the proteins are 18.6 (monomer), 14.2 and 66.0 kD, respectively (Aguilera, 1995). The fat, ash and moisture contents are 0.93%, 3.3%, and 4.83% (w/w), respectively, with the pH being around 6.9. The isoelectric point (pI) ranges from 4.8 for α -La and 5.1 for BSA to 5.3 for β -Lg (Kinsella & Whitehead, 1989). The method of production involves cross flow micro-filtration (MF) and ultra-filtration (UF) through cellulose acetate membranes at ambient temperature, which leaves the final product in the

native form. This possesses good dispersibility/solubility for the water-holding modelling of the present work.

Sodium hydroxide (NaOH) pellets from lot number 1064825000 were supplied by Merck (Darmstadt, Germany). Hydrochloric acid (HCl) reagent grade, 37%, was supplied in liquid form with colorless appearance. The purity of hydrochloric acid is 37.1%, which was determined by supplier using titration with NaOH.

2.5 INSTRUMENTS

The summary of instruments used in this study including the manufacturer's information is listed in Table 2.4 below.

Table 2.4 List of instruments

Instrument	Type	Manufacturer	Serial Number
ARG-2	Rheometer	TA Instruments (New Castle, DE, USA)	Serial no: 8I3920
MDSC Q2000	Calorimeter	TA Instruments (New Castle, DE, USA)	Serial no: 2000-1251
Quanta™ 200	Microscope	FEI (Hillsboro, OR, USA)	Serial no: XTE25/D7531
labCHEM - pH	pH meter	TPS (Springwood, QLD, Australi	Serial no: V0927
FDB 5503	Freeze dryer	Operon (Gimpo City, South Korea)	Serial no: OPR - 20100611-E

Modulated Differential Scanning Calorimeter (MDSC) Q2000

MDSC Q2000 is a sophisticated DSC with high stability, sensitivity and resolution. Q2000 features Advanced Tzero™ and Modulated DSC™ technologies, 50-position autosampler, and Platinum™ software. The Platinum™ software enables the user to schedule tests automatically at off-work periods. (TA Instruments, n.d.-a). Figure 2.6 shown MDSC Q2000 instrument at RMIT that was used in this study.



Figure 2.6 Modulated Differential Scanning Calorimeter Q2000.

Advanced Rheometer Generation 2 (ARG-2)

ARG-2 is a rheometer with patented magnetic thrust bearing technology for ultra-low, nano-torque control. It is an advanced rheometer due to its sophisticated capabilities such as controlled stress, direct strain and controlled rate. Furthermore, it also features Smart Swap™ Geometries that detects and stores geometry information automatically (TA Instruments, n.d.-b). The ARG-2 (Figure 2.7) is also equipped with a peltier plate that can hold temperature between -20°C and 200°C.



Figure 2.7 Advanced Rheometer Generation 2 (ARG-2).

Quanta™ 200 Scanning Electron Microscope

The Quanta™ 200 from FEI (Figure 2.8) is a high performance instrument which features three imaging modes – high vacuum, low vacuum, and ESEM™, thus, it can accommodate a wide range of samples. Preparing samples suitable for conventional high-vacuum SEM is time consuming but analyzing in low-vacuum or ESEM mode in Quanta 200 can eliminate sample preparation and reduce time. Another benefit of using this instrument is it permits the user to analyze irregular specimens without requiring mechanical adjustments (FEI, 2009).

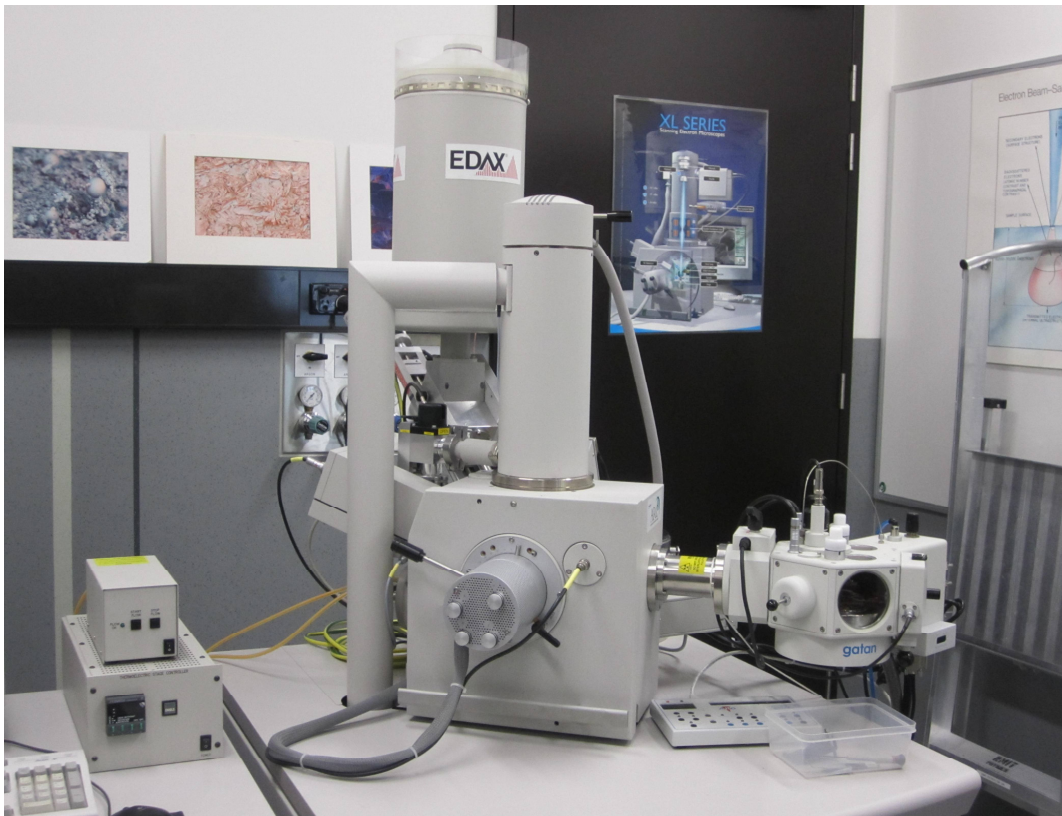


Figure 2.8 FEI Quanta™ 200 at RMIT.

2.6 SAMPLE PREPARATION

2.6.1 Agarose preparation

Agarose solutions (1.0, 1.25, 1.5 and 2.0% w/w) were prepared by dissolving the powder in mili-Q water at 80°C using vigorous agitation for 20 minutes. For each sample, the pH was then adjusted to specific values (from 4.0 to 8.0 with 0.5 increments) by adding either NaOH (0.01 M) or HCl (0.01 M). Agarose gels were prepared by cooling the agarose solutions to room temperature. Then, the gels were freeze dried (freeze dryer FDB 5503) at -55°C for 24 hours prior to microscopy observation.

2.6.2 Whey protein preparation

Whey protein solutions were readily prepared by dispersing the powder in mili-Q water at ambient temperature to produce concentrations of 15.0, 20.0, 25.0 and 30.0% (w/w). These were gently stirred for 30 minutes and then hydrated at 4°C for 24 hours. The following day, dispersions were stirred once more for 15 minutes at ambient temperature to re-suspend the precipitated protein. Values of pH were adjusted, similar to the agarose, to vary between 4.0 and 8.0.

Whey protein gels were prepared by heating the whey protein solutions, which were prepared in advance, in 80°C water bath for about 30 minutes. Afterwards, the gels were stored overnight at 4°C for microscopy observation on the following day.

2.6.3 Binary mixtures preparation

Binary mixtures of agarose and whey protein (total volume = 50 mL) were made by preparing initially solutions of the individual components, as outlined in the preceding sections. Appropriate amounts of these stock preparations (2.0% agarose and 15.0% whey protein isolate) were combined (w/w) at 45°C, a temperature at which both components

remain stable in solution. Addition of NaOH or HCl adjusted the pH of mixtures within the working range (from 4.0 to 8.0 with 0.5 increments).

Preparation for binary gels of agarose and whey protein was divided into two routines. The first routine implemented heating treatment of binary solutions in 80°C water bath for about 30 minutes after pH adjustment and then followed by cooling at 4°C for overnight. The second routine implemented only cooling treatment of binary solutions, after pH adjustment, at 4°C for overnight. In both routines, the gels subsequently freeze dried (freeze dryer FDB 5503) at -55°C for 24 hours prior to microscopy observation. The preparation of these binary mixtures is illustrated in Figure 2.9.

2.7 METHODS

Small-deformation dynamic-oscillation measurements on shear were made using a controlled strain rheometer (ARG-2) with a 40 mm diameter parallel-plate geometry and 1 mm gap. A thin layer of silicon fluid (50 cP) was used to cover the exposed edge of the sample to prevent loss of moisture in the course of experimentation. This type of mechanical analysis determines the elastic (storage modulus, G') and viscous (loss modulus, G'') components of the network, complex viscosity (η^*) and a measure of the 'phase lag' δ ($\tan \delta = G'' / G'$) of the material.

Experimental sequence for single agarose samples consists of cooling runs from 40 to 5°C at rate of 1°C/min, isothermal step at this temperature for 30 min at a frequency of 1 rad/s, followed by a frequency sweep from 0.1 to 100 rad/s at a strain of 0.1%. Whey-protein rheology involved a temperature sweep from 45 to 80°C at 1°C/min, frequency sweep from 0.1 to 100 rad/s at the end of the heating run, cooling from 80 to 5°C at the same scan rate, isothermal step at the end of the cooling run for 30 min at a frequency of 1 rad/s, followed by a frequency sweep from 0.1 to 100 rad/s at a strain of 1.0%. Binary

mixtures were loaded onto the rheometer at 45°C, driven to 80°C and then to 5°C at rate of 1°C/min to reproduce the experimental protocol for single whey-protein preparations. In a second routine, binary mixtures were loaded onto the rheometer at 45°C and driven to 5°C at rate of 1°C/min to reproduce the experimental protocol for single agarose preparations, which allows whey protein to remain in the native conformation.

Differential scanning calorimetry was performed using MDSC Q2000. The instrument interfaced a refrigerated cooling unit to achieve temperatures down to 0°C and a nitrogen purge cell with a flow rate of 25 mL/min. Heat flow was calibrated using a traceable indium standard and the heat capacity response using a sapphire standard. Typically, about 12 mg of agarose, whey protein and the mixtures thereof would be analysed. Temperature amplitude of modulation was $\pm 0.53^\circ\text{C}$ while the period of modulation was 40 s. Hermetically sealed aluminum pans were used, with the reference being an empty pan. Single systems or binary mixtures were heated from 45 to 90°C, cooled to 0°C and then heated once more to 90°C thus recording various first-order thermodynamic transitions at a scan rate of 1°C/min to match the rheological routine.

Environmental scanning electron microscopy was used to provide tangible evidence of changes in network morphology and topology of binary mixtures as a function of thermal treatment and polymer composition (FEI Quanta 200 ESEM). Whey protein gel cubes of about 10 mm³ in size were prepared by heating and cooling thus triggering the denaturation of protein. Observing the microstructure of these high moisture-content whey protein gels requires exposure to a gaseous secondary electron detector (GSED) at an accelerating voltage of 20 kV and pressure of 5.75 torr with ESEM setting. Observation of agarose gel was done using low vacuum setting at an accelerating voltage of 20 kV and pressure of 5.75 torr. Binary mixtures gel cubes of about 10 mm³ in size were prepared either by heating and cooling thus triggering first the thermal transition of whey protein or by cooling only. The latter routine structures the polysaccharide but

leaves the whey protein unaffected as liquid inclusions in the binary mixture. Observing the microstructure of these high moisture-content gels requires exposure to low vacuum setting at an accelerating voltage of 20 kV and pressure of 5.75 torr.

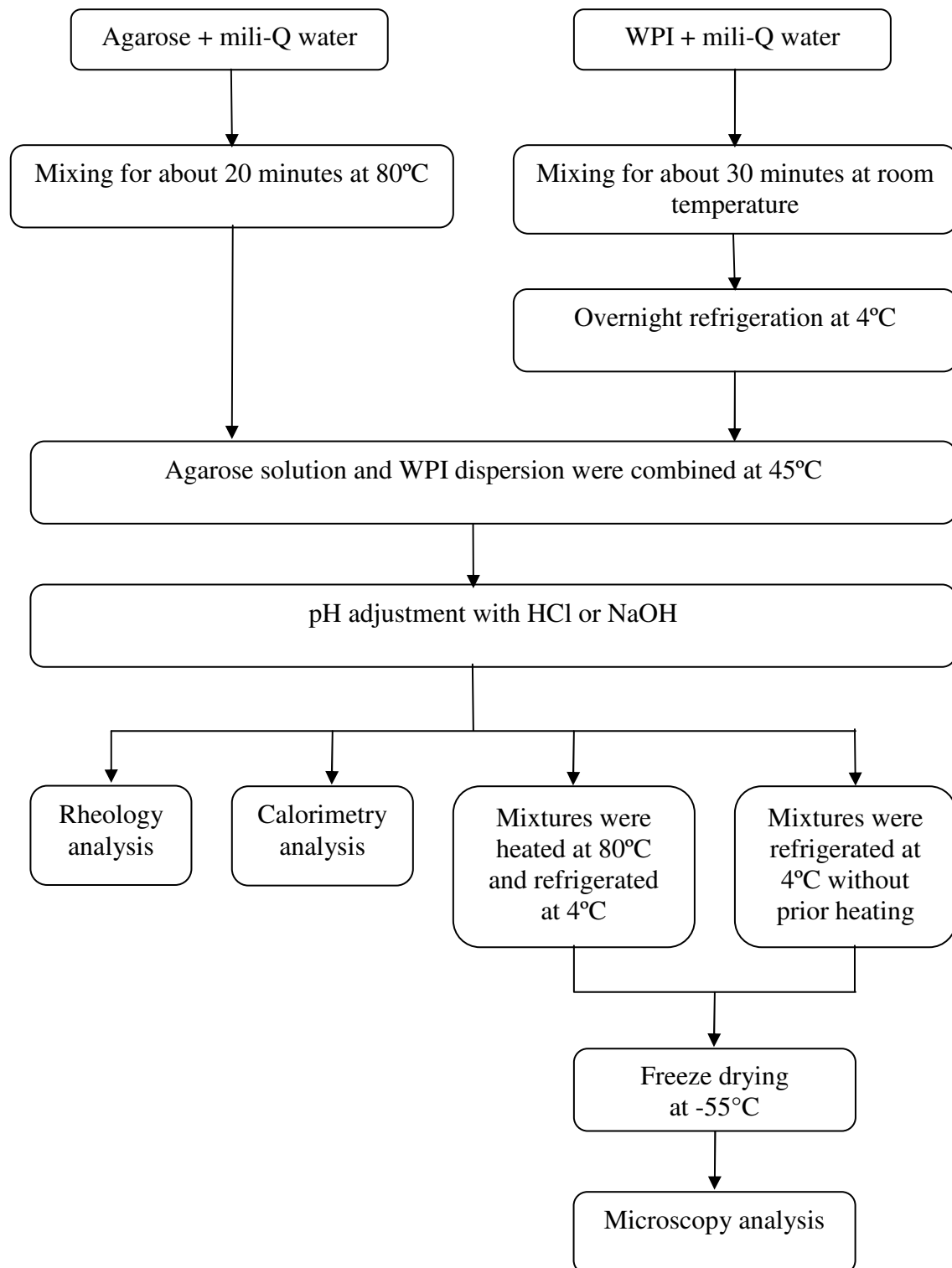


Figure 2.9 Experimental designs of binary mixtures (agarose and whey protein isolate) preparation and analysis.

CHAPTER 3

SEGREGATED PHASE SEPARATION IN AGAROSE/WHEY PROTEIN SYSTEMS INDUCED BY SEQUENCE-DEPENDENT TRAPPING AND CHANGE IN pH

3.1 ABSTRACT

The structural properties and morphology of mixed gels made of aqueous preparations of agarose and whey protein were modified by changing thermal treatment and pH. The conformationally dissimilar polymers phase separated and this process was followed by small-deformation dynamic oscillation in shear, differential scanning calorimetry and environmental scanning electron microscopy. Experimental protocol encourages formation of a range of two-phase systems from continuous agarose matrices perforated by liquid-like whey protein inclusions to phase inverted preparations where a soft protein matrix suspends hard agarose-filler particles. These distinct morphologies have widely different mechanical moduli, which were followed by adapting a theoretical analysis (isostress-isostrain and Lewis-Nielsen blending laws) from the literature in synthetic block polymers and polyblends. Based on this framework of thought, reasonable predictions of the elastic moduli in the composite gels were made that led to patterns of solvent partition between the two polymeric networks. It was shown that proteins, in mixture with polysaccharide, exhibit favorable relative affinity (P -factor) for water molecules at a pH above their isoelectric point. This is an unexpected outcome that adds to the central finding of a single P value for the distribution of solvent between the continuous matrix and discontinuous inclusions of binary gels. It was thus proposed that phase continuity and solvent distribution in agarose/whey protein systems are under kinetic control that can be heavily governed by pH changes in the aqueous environment.

3.2 INTRODUCTION

Agarose is a structural polysaccharide occurring in different species of red seaweed (*Rhodophyceae*). Its primary structure comprises an alternating repeating sequence of 1,3-linked β -D-galactopyranose and 1,4-linked (3 \rightarrow 6)-anhydrogalactopyranose (A and B units, respectively). The 3,6-anhydro units are in the L form, which is reflected in a left-handed helix geometry (Normand, Lootens, Amici, Plucknett, & Aymard, 2000). Furthermore, the anhydride bridge may be absent in a proportion of the 4-linked residues, which changes the geometry of the sugar ring to a form that is sterically incompatible with incorporation in the ordered double helix. The presence of this “kinking” residue is essential for the development of gel networks, as it terminates the ordered junction zone association and allows each chain to participate in more than one intermolecular junction zones (Barrangou, Daubert, & Allen Foegeding, 2006).

Agarose molecules are insoluble in cold water but soluble in hot. Their solutions are heat-stable with essentially constant viscosity at neutral pH and give gels even at concentrations of 0.1% or lower. Agarose gels exhibit thermal hysteresis and the melting temperature is dependent on the concentration used (Fujii, Yano, Kumagai, & Miyawaki, 2000). The gel finds a wide range of industrial applications especially as a moulage material capable of reproducing fine details with great accuracy thus being used in dentistry, plastic surgery, and criminology (Puertolas et al., 2011). In the USA, it is mostly used in microbiology at liquid media concentrations of 0.007 to 0.08%. Even at such low concentrations, agarose is able to prevent the entry of oxygen into liquid media, making the cultivation of anaerobes feasible in air-exposed broths (Yokoyama, Kishida, Uchimura, & Ichinohe, 2006). Agarose is also used in a wide

range of processed food products to improve texture and stability (yoghurts, cream cheeses), as an antitackiness or antistaling ingredient (cookies, cakes, pie fillings, meringues), and in vegetarian and health food products (cereals, meat/fish substitutes) (Barrangou, Drake, Daubert, & Foegeding, 2006).

Traditionally the term “whey protein” has described those milk proteins remaining in the serum after precipitation of the caseins at pH 4.6 at about 20°C. The major families of proteins included in this class are the β -lactoglobulins, α -lactalbumins, serum albumins and immunoglobulins (Fitzsimons, Mulvihill, & Morris, 2007). The primary amino acid sequence of β -lactoglobulin B consists of 162 amino acid residues with a molecular weight of 18,277, with the corresponding primary structure characteristics of the major α -lactalbumin being 123 and 14,174, respectively. In the pH range from 5.2 to 7.5, β -lactoglobulins exist primarily as dimers, which consist of two spheres with radii of 17.9 Å and a distance from centre to centre of 33.5 Å joined as to possess a dyad axis of symmetry. On the acid side of the isoelectric point, especially below pH 3.5, the dimer dissociates into monomers, with the extent of dissociation increasing as the pH is lowered (Chamani et al., 2006). α -Lactalbumin, on the other hand, exists primarily in neutral and alkaline media as a near spherical, compact globular monomer of about 2.2 x 4.4 x 5.7 nm. At pH values below the isoelectric point, α -lactalbumin associates to form dimers and trimers, which lead to a polymeric network formation (Nakamura et al., 2010).

There is only a small amount of β -lactoglobulins and α -lactalbumins in whey (about 0.6%), which is a sidestream product of cheese or casein manufacture. Upon concentration, whey powder is produced with an approximate composition of 76% lactose, 13% protein, 10% ash and 1% fat. To make a 35 or 50% whey protein concentrate (WPC), the dilute solution of whey is concentrated by ultrafiltration (UF)

that physically separates the whey protein and fat from the lactose and minerals. Spray drying concentrates the whey protein solution from about 35 to 95% total solids, and control of the dryer and atomization of the liquid allows low-temperature drying to maintain product solubility (Thomas, Scher, Desobry-Banon, & Desobry, 2004). The manufacture of 80% WPC or whey protein isolate (WPI) is essentially the same as for 35 and 50% WPC products but it includes a diafiltration step to further concentrate the system from about 60 to 80% protein. This enhances the whey protein purity and ingredient functionality as well as controlling the final composition.

Commercial development of the functional product concept saw the use of polysaccharide-protein mixtures as multifunctional agents in material processing (Narchi, Vial, & Djelveh, 2009). Agarose-whey protein preparations are among the basic tools used in achieving the required properties in industrial formulations with superior structural and nutritional functionality. Heating of the whey protein solution disrupts the native conformation and induces aggregation followed by gelation at a high enough temperature. This is distinct from the cold setting behavior of gelatin whose phase morphology in mixture with polysaccharides (dietary fiber or various starches) has been studied frequently in the past (Nickerson et al., 2006).

The present work examines how the differences between the network of associated agarose double helices and the aggregation of thermally unfolded whey-protein molecules effect changes in the phase behavior of their binary mixtures. It uses a protocol of physicochemical analysis to examine the structural properties of the composite gels with emphasis on solvent partition between the two polymeric phases. Besides the sequence-dependent thermal treatment, distinct network structures and steric exclusion patterns are induced by change in pH, which appears to be a necessary parameter to establish the identity of phase separation in these systems.

3.3 EXPERIMENT PROTOCOL

3.3.1 Materials

Agarose (Type 1-B) was purchased from Sigma-Aldrich, Gillingham, UK. The material has an off-white color and high gel strength as recorded for the 1.0% (w/w) preparation in Figure 1a of this investigation ($G' \sim 52$ kPa at 5°C and pH 7.0). Using aqueous size exclusion chromatography, the supplier determined the number average molecular weight of this agarose sample ($M_n \sim 120$ kDa). Moisture, ash and sulfate contents were of less than 5.0%, 0.25% and 0.10% (w/w), respectively. Furthermore, the pH test of 1.5% (w/w) agarose gel was 7.16.

The sample of whey protein was supplied in the form of a creamy white powder by Fonterra, Auckland, New Zealand. It is a protein isolate commercially available as WPI Instantised 894. Kjeldahl analysis produced a protein content ($N \times 6.38$) of 93.0% (w/w; dry basis), which consists of β -lactoglobulin (71.0%; ratio of monomer to dimer is 5:1), α -lactalbumin (18.0%) and 6.0% bovine serum albumin (BSA). Molecular weights of the proteins are 18.6 (monomer), 14.2 and 66.0 kDa, respectively (Mercade-Prieto & Gunasekaran, 2009). The fat, ash and moisture contents are 0.93%, 3.3%, and 4.83% (w/w), respectively, with the pH being around 6.9. The isoelectric pH (pI) ranges from 4.8 for α -La and 5.1 for BSA to 5.3 for β -Lg (Kinsella & Whitehead, 1989). The method of production involves cross flow micro-filtration (MF) and ultra-filtration (UF) through cellulose acetate membranes at ambient temperature, which leaves the final product in the native conformation. This possesses good dispersibility/solubility for the water-holding modelling of the present work.

3.3.2 *Sample Preparation*

Agarose solutions (1.0, 1.25, 1.5 and 2.0% w/w) were prepared by dissolving the powder in mili-Q water at 80°C using vigorous agitation for 20 minutes. For each sample, the pH was then adjusted to specific values (from 4.0 to 8.0 with 0.5 increments) by adding either NaOH (0.01 M) or HCl (0.01 M).

Whey protein solutions were readily prepared by dispersing the powder in mili-Q water at ambient temperature to produce concentrations of 15.0, 20.0, 25.0 and 30.0% (w/w). These were gently stirred for 30 minutes and stored overnight at 4°C to facilitate hydration. The following morning, dispersions were stirred once more for 15 minutes at ambient temperature to further induce homogeneity in the system. Values of pH were adjusted as for agarose to vary between 4.0 and 8.0.

Binary mixtures of agarose and whey protein were made by preparing initially solutions of the individual components, as outlined in the preceding paragraphs. Appropriate amounts of these stock preparations were combined at 45°C, a temperature at which both components remain stable in solution. NaOH or HCl was used to adjust the pH of the mixtures to within the working range.

3.3.3 *Methods*

Small-deformation dynamic-oscillation measurements in shear were made using a controlled strain rheometer (AR-G2 from TA Instruments, New Castle, DE, USA) with a 40 mm diameter parallel-plate geometry and 1 mm gap. A thin layer of silicon fluid (50 cP) was used to cover the exposed edge of the sample to prevent loss of moisture during the course of experimentation. This type of mechanical analysis determines the elastic (storage modulus, G') and viscous (loss modulus, G'') components of the

network, complex viscosity (η^*) and a measure of the 'phase lag' δ ($\tan \delta = G'' / G'$) of the material.

Experimental sequence for single agarose samples consists of cooling runs from 40 to 5°C at rate of 1°C/min, an isothermal step at this temperature for 30 min and a frequency of 1 rad/s, followed by a frequency sweep from 0.1 to 100 rad/s at a strain of 0.1%. Analysis of whey-protein rheology involved a temperature sweep from 45 to 80°C at 1°C/min, frequency sweep from 0.1 to 100 rad/s at the end of the heating run, cooling from 80 to 5°C at the same scan rate, isothermal step at the end of the cooling run for 30 min at a frequency of 1 rad/s, followed by a frequency sweep from 0.1 to 100 rad/s at a strain of 1.0%. Binary mixtures were loaded onto the rheometer at 45°C, driven to 80°C and then to 5°C to reproduce the experimental protocol for single whey-protein preparations previously outlined. In a second routine, binary mixtures were loaded onto the rheometer at 45°C and driven to 5°C to reproduce the experimental protocol for single agarose preparations, which allows whey protein to remain in the native conformation.

Differential scanning calorimetry was performed using MDSC Q2000 (TA Instruments, New Castle, DE, USA). The instrument interfaced a refrigerated cooling unit to achieve temperatures down to 0°C and a nitrogen purge cell with a flow rate of 25 mL/min. Heat flow was calibrated using a traceable indium standard and the heat capacity response using a sapphire standard. Typically, about 12 mg of agarose, whey protein and the mixtures thereof would be analyzed. Temperature amplitude of modulation was $\pm 0.53^\circ\text{C}$ while the period of modulation was 40 s. Hermetically sealed aluminum pans were used, with the reference being an empty pan. Single systems or binary mixtures were heated from 45 to 90°C, cooled to 0°C and then heated once more

to 90°C thus recording various first-order thermodynamic transitions at a scan rate of 1°C/min to match the rheological routine.

Environmental scanning electron microscopy was used to provide tangible evidence of changes in network morphology and topology of binary mixtures as a function of thermal treatment and polymer composition (FEI Quanta 200 ESEM, Hillsboro, Oregon, USA). Gel cubes of about 10 mm³ in size were prepared either by heating followed by cooling thus triggering first the thermal transition of whey protein followed by agarose gelation, or by cooling only. The latter routine structures the polysaccharide but leaves the whey protein unaffected as liquid inclusions in the binary mixture. Observing the microstructure of these high moisture-content gels requires exposure to a gaseous secondary electron detector (GSED) at an accelerating voltage of 20 kV and pressure of 5.75 torr.

3.4 RESULTS AND DISCUSSION

3.4.1 Network Formation in Single Gels of Agarose Polysaccharide and Whey Protein Isolate

Much has been said about the structural and thermal properties of gels made by agarose. Perhaps the best-known aspect of the subject is the formation of cohesive gels even at concentrations as low as 0.1% seen in small-deformation rheometry and the very brittle nature of those gels under large-deformation compression testing (Aymard *et al.*, 2001). The purpose of the present exercise is to provide a series of data for the follow up on phase behavior of agarose/whey protein mixtures.

Figure 3.1a and Figure 3.1b illustrate the dynamic oscillatory properties of agarose preparations with controlled cooling at 1°C/min. The cooling profiles of

agarose at several agarose concentrations are shown in Figure 3.1a whereas Figure 3.1b shows the cooling profiles of agarose at various pH values. Agarose solutions are indistinguishable from water at high temperatures but upon cooling structure formation ensues, which is recorded as a sharp trace at temperature below 35°C. It has previously been suggested that the long and flexible polysaccharide chains in solution participate in the formation of rigid double helices in gels (Normand *et al.*, 2000). This is followed by aggregation, which builds up a three-dimensional structure of considerable opacity and thermal hysteresis in melting and setting temperatures (also observed in this work but not shown presently).

Following a brief sample equilibration and a three-decade frequency sweep at the end of the cooling run, values of the solid-like component of the network were collected and plotted as a function of polymer concentration and adjusted pH in Figure 3.1c. There is a continuous reinforcement in gel rigidity with increasing agarose concentration from 1.0 to 2.0% in preparations, which was also seen in the cooling profiles from 35 to 5°C in Figure 3.1a. In this work, the pH value was also varied from 4.0 to 8.0 at intervals of 0.5 as shown in Figure 3.1b, which has little effect on agarose gelation compared to whey protein gelation (refer to Figure 3.2a). The pH variation did not affect the ability of the agarose to form a three dimensional structure but impacted somewhat on the extent of molecular interactions in the gel. Calibration curves of that nature are a necessary part of the algorithm that will model phase behavior in agarose/whey protein mixtures discussed in the following sections.

It is well known in the literature that besides increasing temperature and ionic strength with added counterions, changes in pH around the isoelectric point ($pI \sim 4.6$) profoundly affect the structural properties of a whey protein gel. This investigation aims to take advantage of changing viscoelasticity in the protein network as a function

of pH variation (from 4.0 to 8.0) in subsequent mixtures with agarose. Figure 3.2a reproduces examples of heating profiles for whey protein systems that were scanned to 80°C at a rate of 1°C/min. Temperatures above 60°C induce unfolding (denaturation) and subsequent association of the unfolded molecules into permanent structures within the experimental constraints, which is recorded as a sharp increase in the values of storage modulus. These are opaque, aggregated structures due to high levels of the material used (15.0%), as compared to transparent, fine stranded gels at low protein concentrations (Chantrapornchai & McClements, 2002). Increasing the pH delays the onset of network formation from about 65°C to 75°C at pH 4.5 and 7.0, respectively.

Subsequent cooling records a monotonic increase in the values of G' in Figure 3.2a without further change in moduli with time at the end of the experimental run (5°C). Cooling of the material reinforces hydrogen bonding in addition to other secondary forces involved in structure formation at the denaturation temperature, i.e. ionic interactions, thiol-disulfide exchange, and non-specific hydrophobic forces (Alting *et al.*, 2003). As for agarose, calibration curves for subsequent modeling of the structural properties in binary mixtures were constructed and shown in Figure 3.2b by plotting storage modulus values obtained at 5°C against whey protein concentration (15.0 to 30.0%). Clearly, changes in pH values from 4.0 to 5.0, which is around the isoelectric point, have a pronounced effect on gel rigidity which increases at least two orders of magnitude, e.g. from about $10^{2.7}$ Pa to 10^5 Pa at pH 4.0 in Figure 3.2b. By contrast, the effect of pH on the agarose gel is less pronounced being confined to a maximum of half-a-decade in modulus values across the concentration range of the polysaccharide in Figure 3.1c.

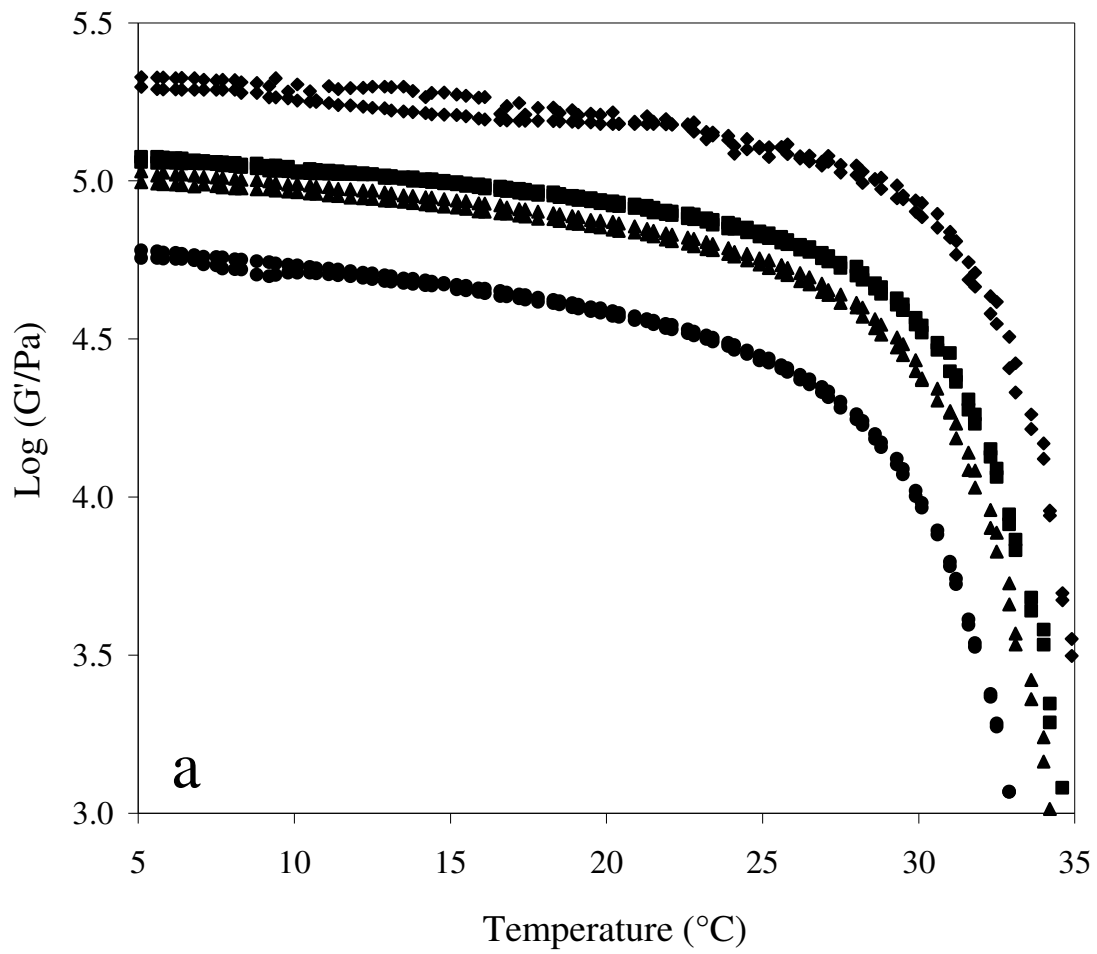


Figure 3.1a Cooling profiles of G' for 1.0 (●), 1.25 (▲), 1.5 (■) and 2.0% (◆) agarose at pH of 4.0 and 7.0 for each polymer concentration (scan rate of 1°C/min).

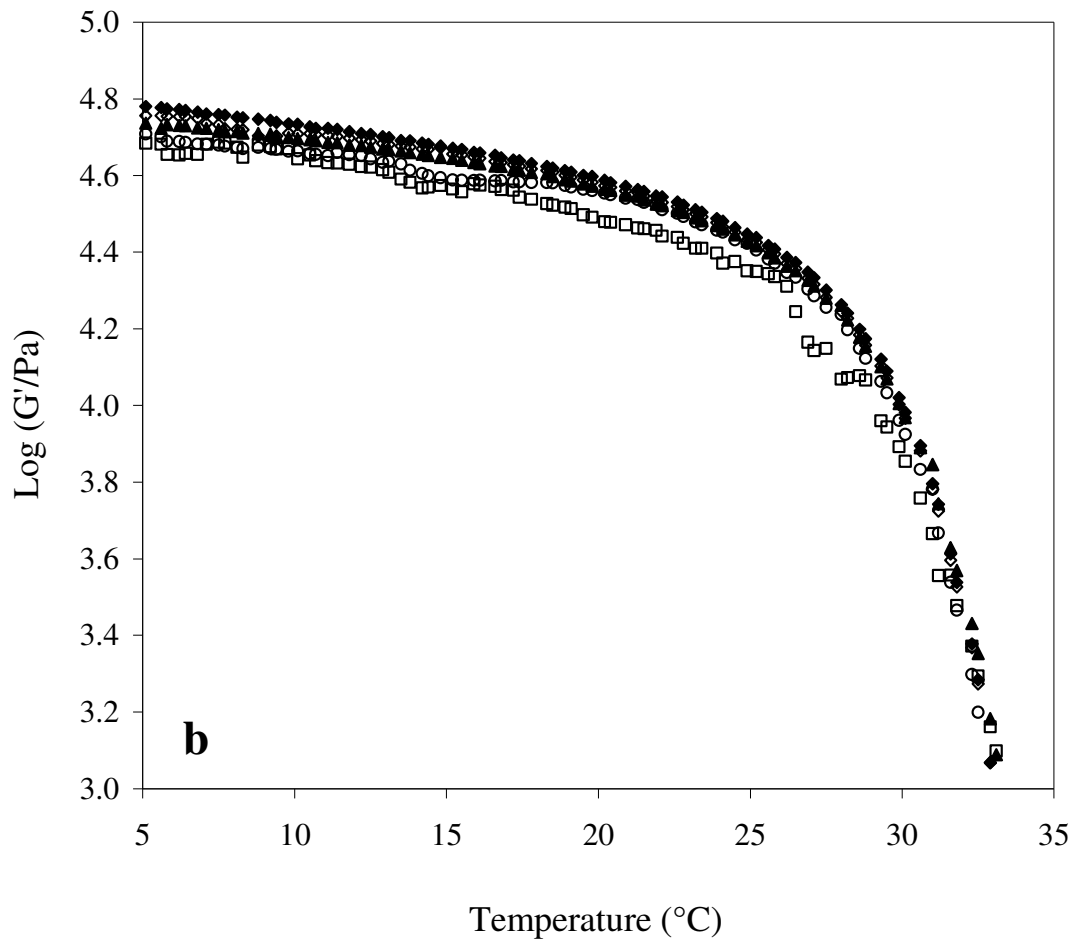


Figure 3.1b Cooling profiles of G' for 1.0% agarose at varying pH values (pH 4 [\blacklozenge], pH 5 [\blacktriangle], pH 6 [\circ], pH 7 [\diamond], and pH 8 [\square]) at a scan rate of $1^\circ\text{C}/\text{min}$).

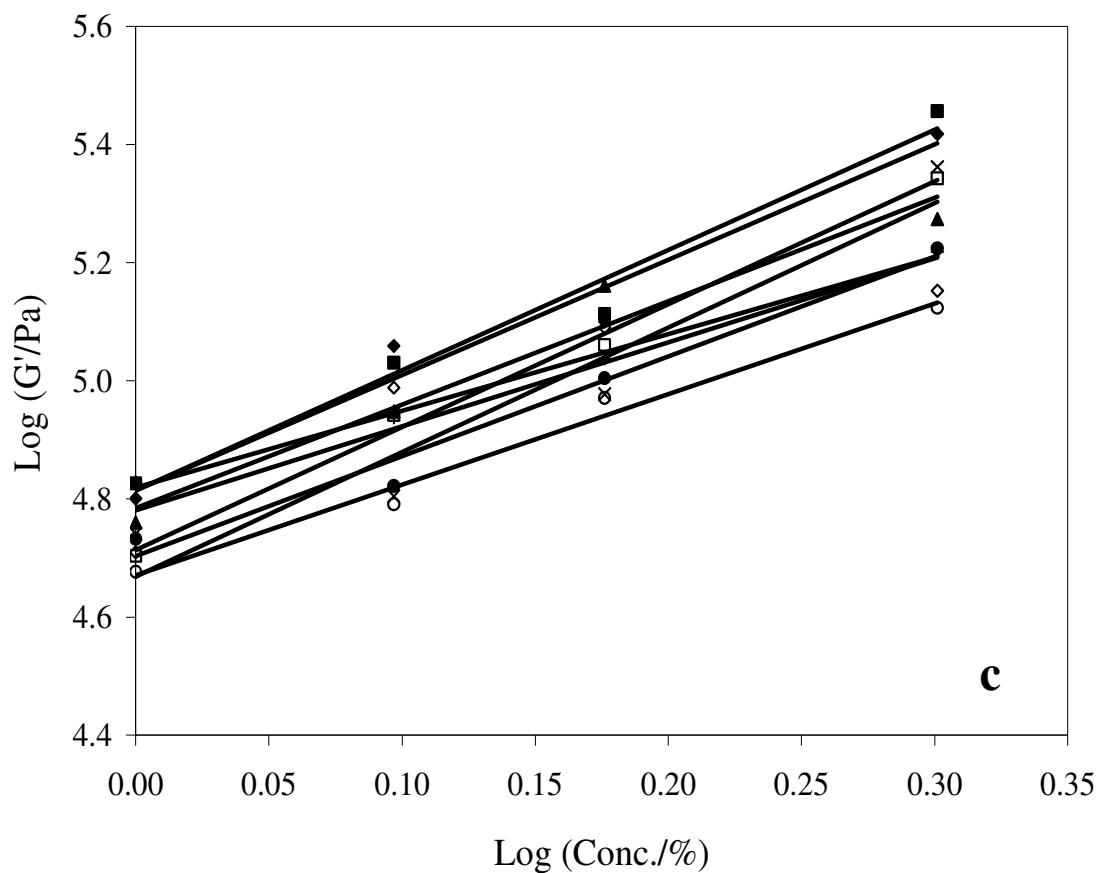


Figure 3.1c Calibration curves of G' at 5°C as a function of agarose concentration at pH values of 4.0 (◆), 4.5 (■), 5.0 (▲), 5.5 (+), 6.0 (○), 6.5 (●), 7.0 (◇), 7.5 (X) and 8.0 (□).

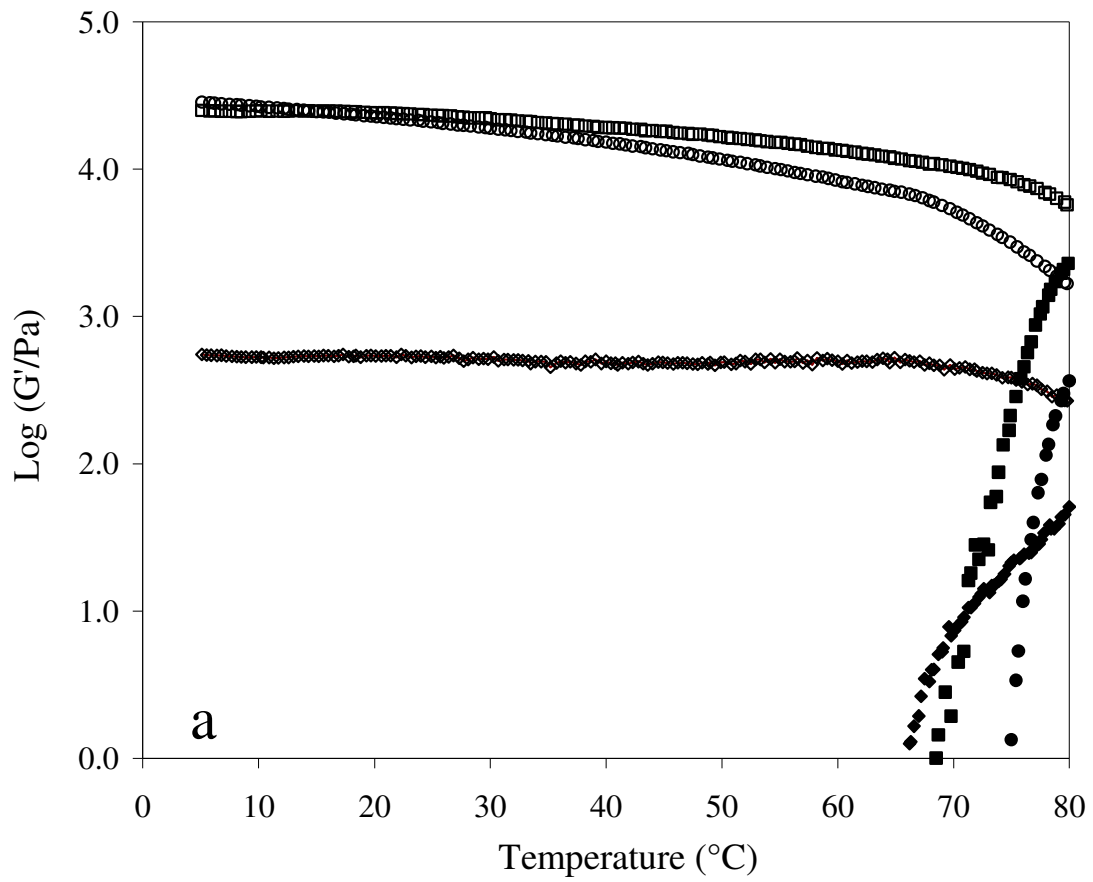


Figure 3.2a G' variation for 15.0% whey protein at pH 4.5 (heating, ◆; cooling, ◇), pH 5.0 (heating, ■; cooling, □) and pH 7.0 (heating, ●; cooling, ○) at a scan rate of $1^{\circ}\text{C}/\text{min}$.

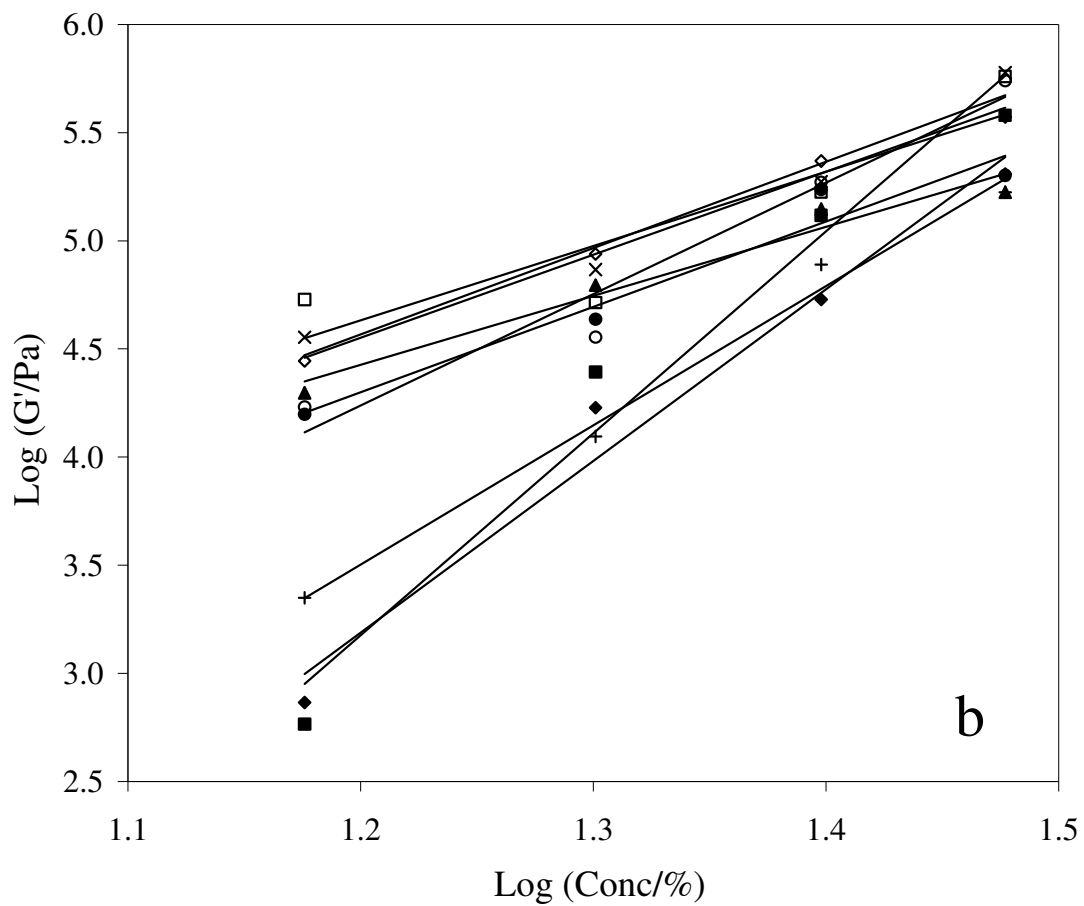


Figure 3.2b Calibration curves of G' at 5°C as a function of whey protein concentration at pH values of 4.0 (◆), 4.5 (■), 5.0 (▲), 5.5 (+), 6.0 (○), 6.5 (●), 7.0 (◇), 7.5 (X) and 8.0 (□).

3.4.2 *Thermomechanical and Microscopy Observations on the Structural Characteristics of Agarose/Whey Protein Mixtures*

Experimental observations reported in the preceding section for single systems will be used to provide a guideline of the phase behavior in aqueous binary mixtures. Following the analysis of single-component gels, a series of binary mixtures was prepared at 45°C keeping the concentration of agarose and whey protein constant at 1.0% and 15.0%, respectively, and altering the pH within the range of 4.0 to 8.0. Two distinct experimental routines were then implemented; the first involved controlled heating of the composite system to 80°C followed by cooling to 5°C, with the second being a cooling run from 45°C to 5°C.

Figure 3.3a and Figure 3.3b illustrate the temperature-dependence of structure formation for selected pH values of the mixture. Figure 3.3a shows rheological properties of binary mixtures that were subjected to both heating and cooling treatment. Heating results in protein denaturation and augmentation of the storage modulus whereas the agarose molecules remain in the disordered conformation. The gelling transition appears earlier and earlier with increasing pH, i.e. as the system moves away from its isoelectric point, an outcome that argues the importance of open globular structures and ionic interactions in the presence of counterions from the batch for incipient gelation. The experimental routine was then reversed reaching at a controlled scan rate a temperature range where agarose can undergo a coil-to-helix transition leading to gelation. Thus the liquid inclusions of the polysaccharide transform into gelled domains in the presence of the protein network, and this is monitored as a rise in G' values along the cooling run at temperatures below 35°C (Figure 3.3a).

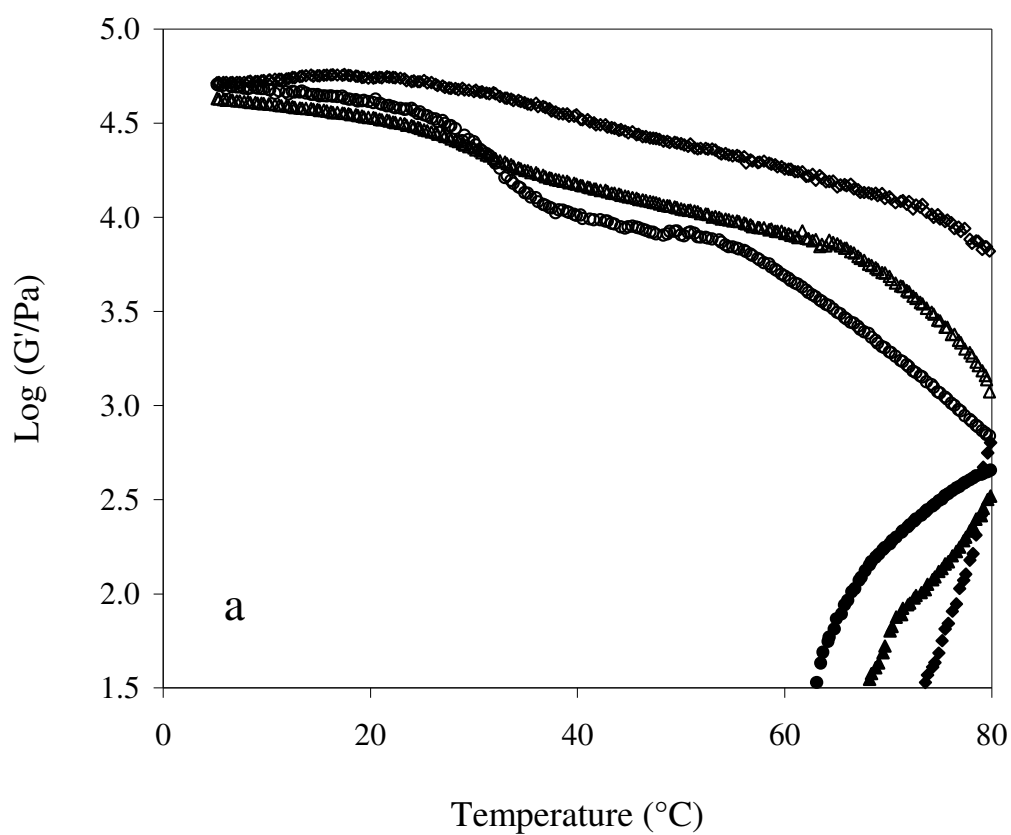


Figure 3.3a Heating (closed symbols) and cooling (open symbols) profiles of G' for mixtures of 1.0% agarose with 15.0% whey protein at pH 5.0 (\blacklozenge, \diamond), pH 7.0 ($\blacktriangle, \triangle$) and pH 8.0 (\bullet, \circ) at a scan rate $1^\circ\text{C}/\text{min}$.

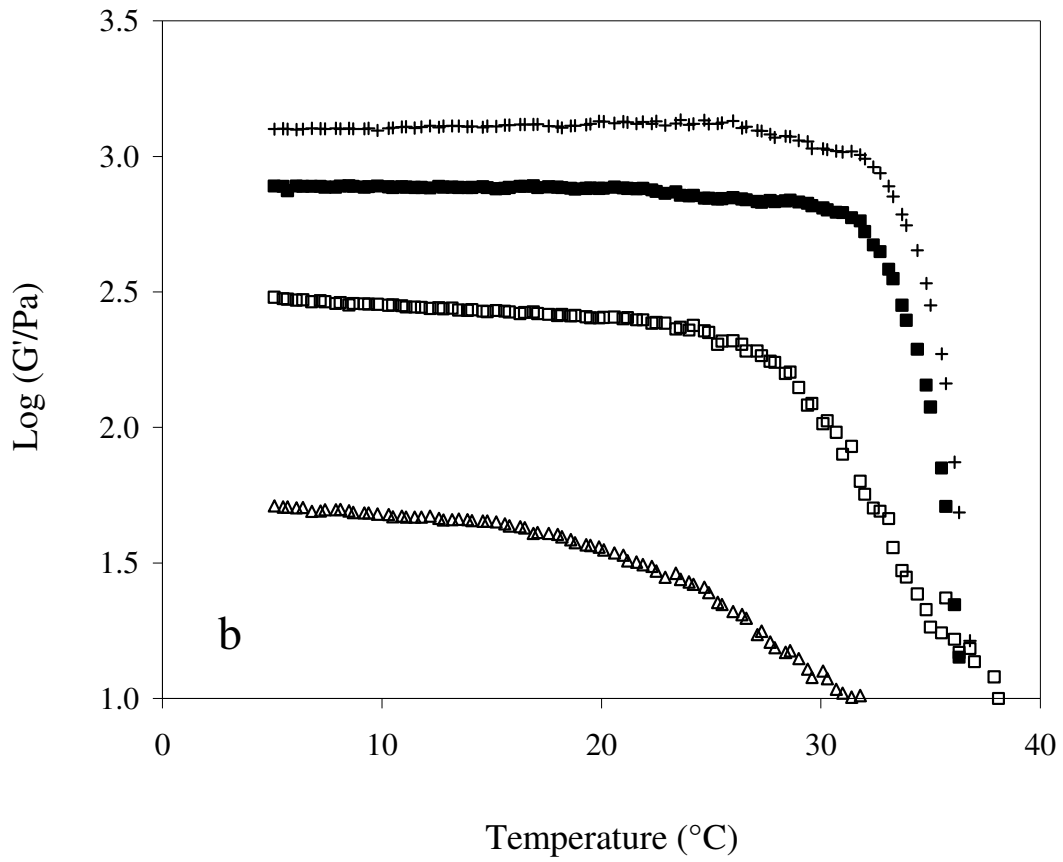


Figure 3.3b Cooling profiles only of G' for mixtures of 1.0% agarose with 15.0% whey protein at pH 4.0 (\square), pH 5.5 (\triangle), pH 7.5 (\blacksquare), and pH 8.0 (+) at a scan rate of $1^{\circ}\text{C}/\text{min}$.

The experimental procedure was concluded by cooling separate blends from 45°C to 5°C at the standard scan rate, and these experimental observations are reproduced in Figure 3.3b. Structure formation is recorded as a sharp conformational transition, which is characteristic of cooperative enthalpic associations in polysaccharide networks (Esquenet et al., 2004). The internal rearrangements and structure of the gels seem to settle within the lower range of the experimental temperatures, as indicated by the modulus traces that asymptotically approach constant values. Overall, structure formation indicates a dominant agarose network supported by similar cooling profiles of single agarose preparations in Figure 3.1a. Shear-modulus variation at the end of the experimental routine is also consistent with data from the calibration curves as a function of adjusted pH in Figure 3.1c. In the absence of heat treatment whey protein remains in the native non-gelling conformation but is capable of holding water in its low-viscosity phase.

Besides mechanical spectroscopy, experimental evidence from differential scanning calorimetry (DSC) can also provide a firm footing on the phase behavior in aqueous preparations of binary mixtures (Mousia et al., 2000). In doing so, fixed amounts of agarose and whey protein were blended at 45°C and these were heated to 90°C at 1°C/min in accordance with the rheological routine. The single system's thermal transition of whey protein and agarose are illustrated in Figure 3.4a and Figure 3.4b respectively. In single whey protein system, pH variation has profound effect on denaturation temperature (refer to Figure 3.4a); the protein denaturation temperature decreases as pH increases. This result is in accordance with an earlier study conducted by Paulsson and his colleagues (1985). On the contrary, pH variation has little effect in gelation temperature of agarose (refer to Figure 3.4b), which supports the rheological result shown in Figure 3.1b.

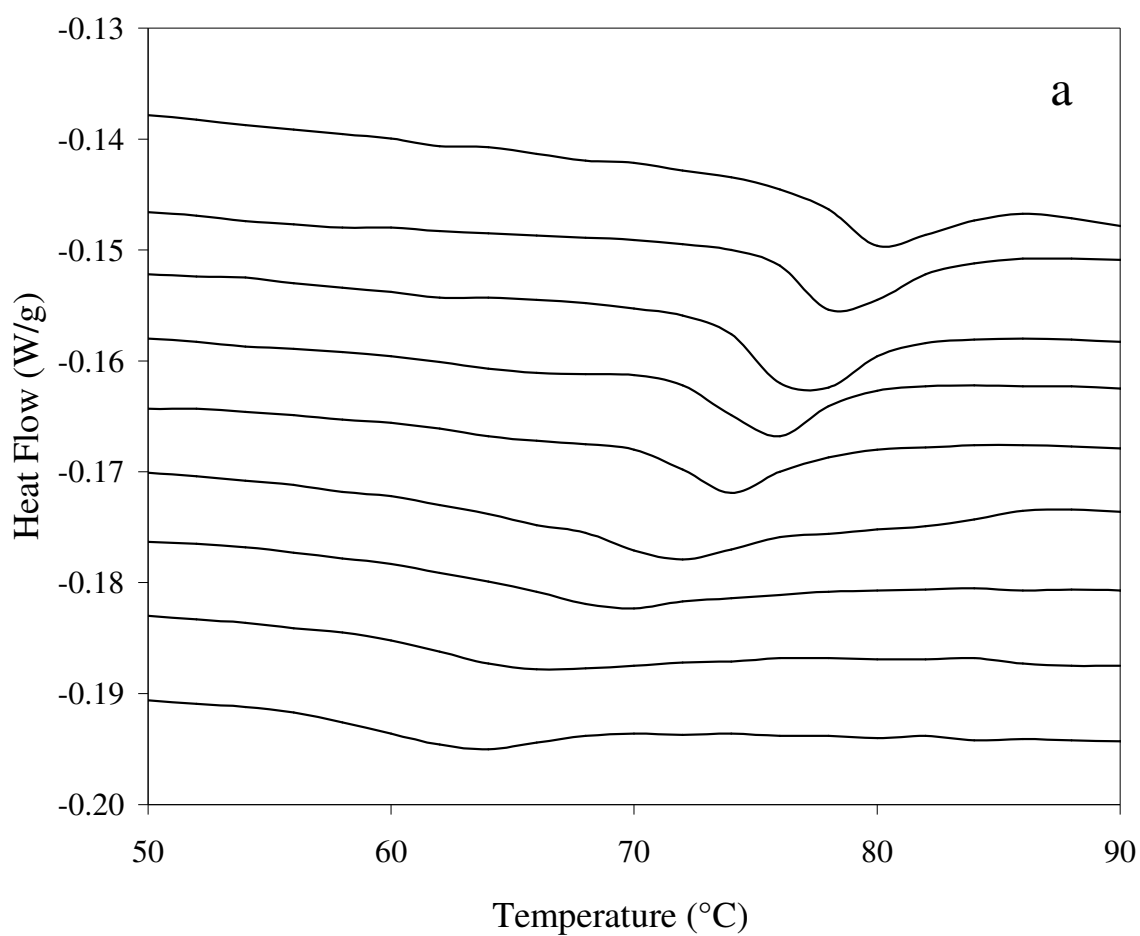


Figure 3.4a DSC endotherms for the heating profiles of 15.0% whey protein at pH of 4.0, 4.5, 5.0, 5.5, 6.0, 6.5, 7.0, 7.5 and 8.0 shown in the graph from top to bottom.

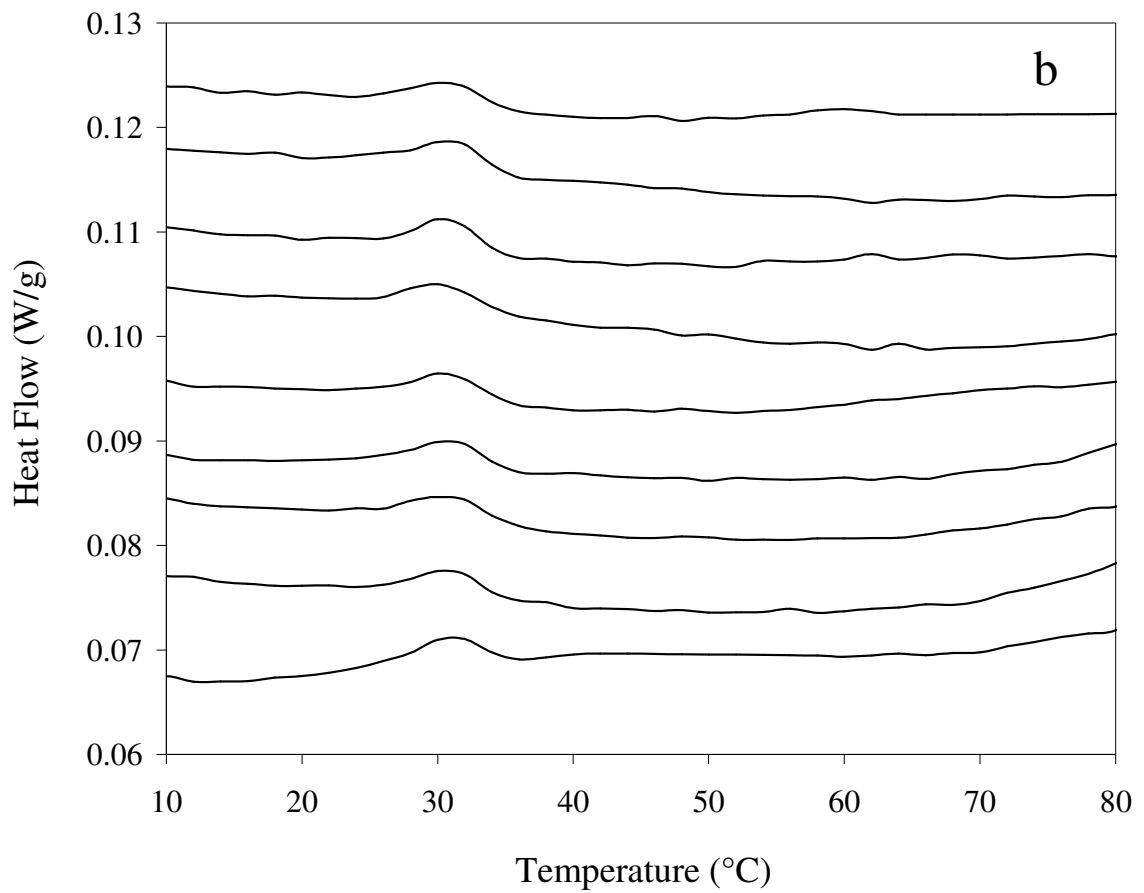


Figure 3.4b DSC exotherms for the cooling profiles of 2.0% agarose at pH of 4.0, 4.5, 5.0, 5.5, 6.0, 6.5, 7.0, 7.5 and 8.0 shown in the graph from top to bottom.

Figure 3.4c illustrates typical endothermic peaks as a function of reduced acidity in mixtures (top to bottom spectra). A relatively sharp peak with a maximum heat flow temperature (T_{max}) of 79°C denotes the cooperative conformational transition of the protein molecules upon heating at pH 4.0. By comparison, the process of thermal denaturation becomes increasingly gradual at higher values of pH as the protein exhibits a net negative charge. In addition, heat flow maxima culminate at lower temperatures, e.g. at 64°C at pH 8.0, an outcome that is consistent with the early onset of gelation with increasing pH in heat treated samples of Figure 3.3a.

Subsequent cooling of the mixtures at the same scan rate produces well-formed exothermic peaks throughout the experimental pH range (Figure 3.4d). Maximum heat flow temperature for all samples remains unaffected by pH and culminates at about 32°C. This is the cooperative process of coil-to-helix transition in agarose networks being congruent to the onset temperature of gelation recorded in cooled only samples in Figure 3.3b. Identical thermal events in terms of temperature sequence and overall peak form for each transition were recorded for the denaturation or gelation of single whey protein or agarose preparations (Figure 3.4a and Figure 3.4b), which argues that both components form gel networks in the mixture as in the individual preparations. Results also suggest that there are no specific interactions between agarose and whey protein (i.e. no formation of heterotypic junctions), which could distort the peaks of the individual gels and generate a new thermal event in the DSC spectrum (Nitta, Kim & Nishinari, 2003).

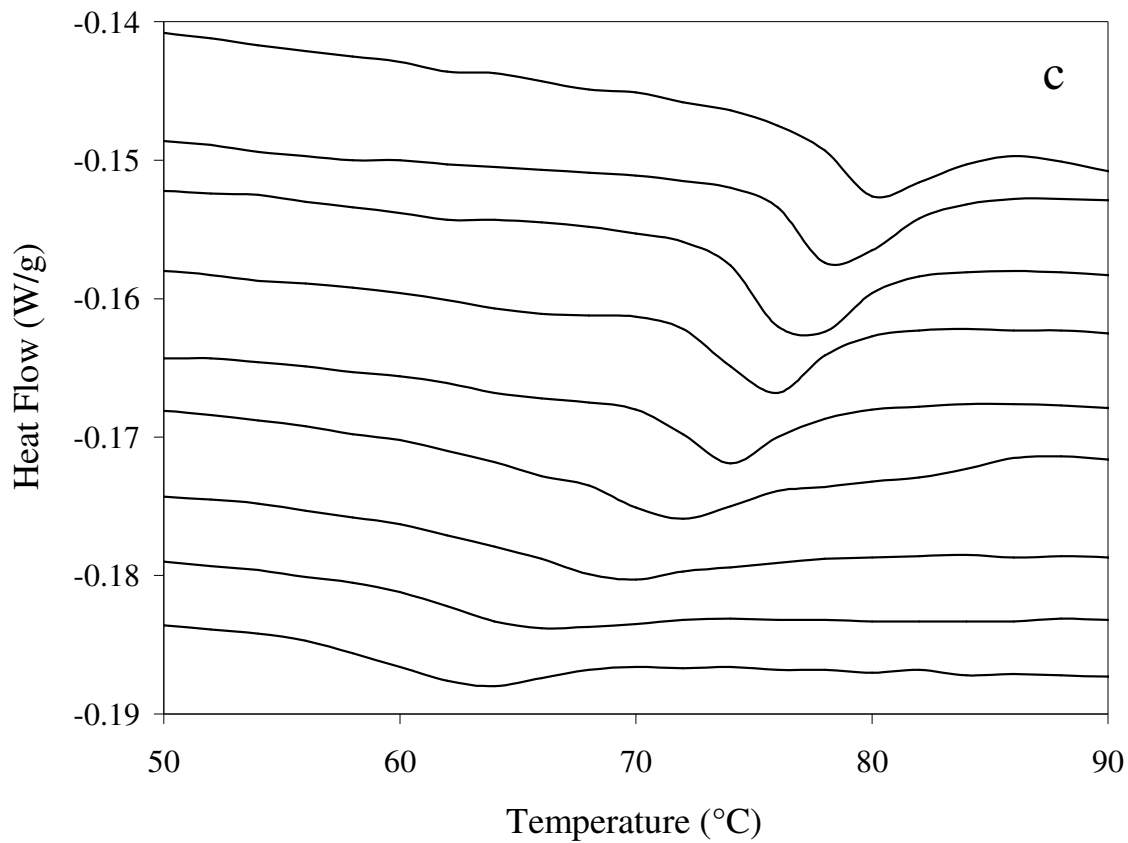


Figure 3.4c DSC endotherms for the heating profiles of 2.0% agarose with 15.0% whey protein mixture at pH of 4.0, 4.5, 5.0, 5.5, 6.0, 6.5, 7.0, 7.5 and 8.0 shown in the graph from top to bottom.

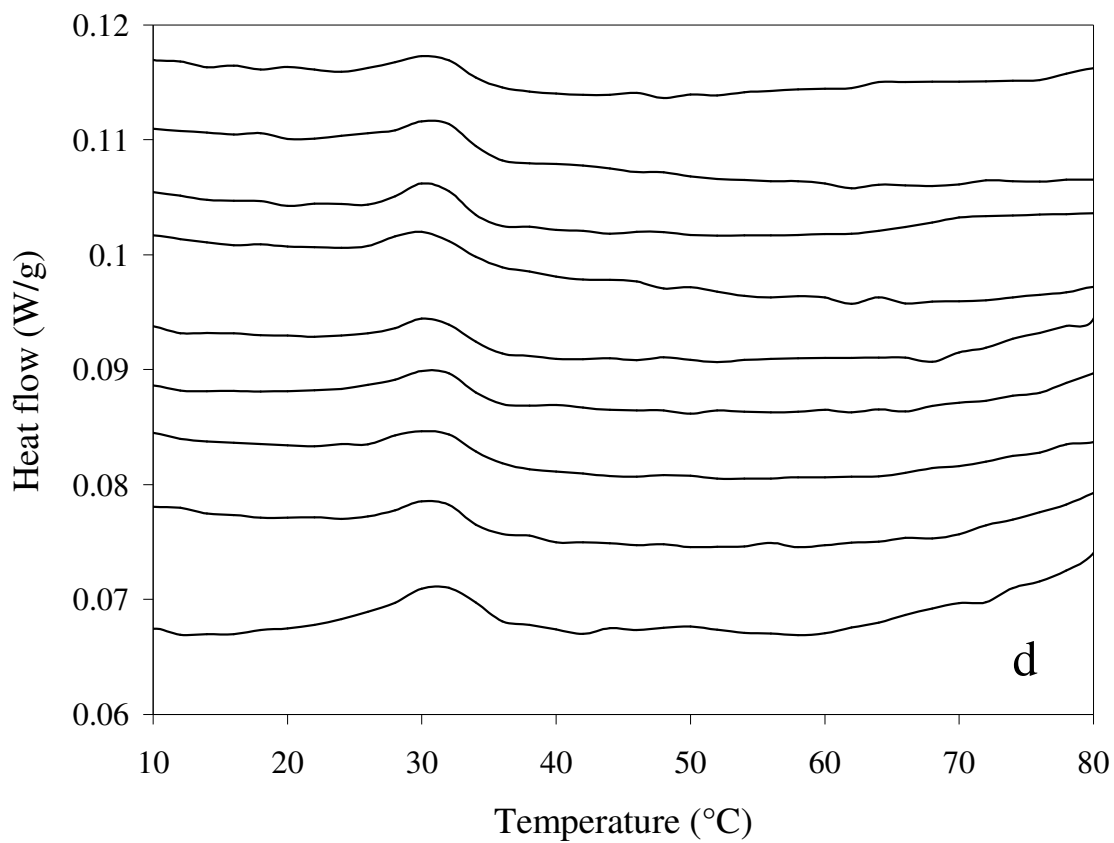


Figure 3.4d DSC exotherms for the cooling profiles of 2.0% agarose with 15.0% whey protein mixtures at pH of 4.0, 4.5, 5.0, 5.5, 6.0, 6.5, 7.0, 7.5 and 8.0 shown in the graph from top to bottom (scan rate in all of these cases is 1°C/min).

Finally, images from environmental scanning electron microscopy were taken to provide tangible evidence of changes in network morphology and phase topology in agarose/whey protein mixtures as a function of external stimuli. Figure 3.5 shows whey protein gels at varying pH values. As whey protein system moving away from its isoelectric point (Figure 3.5b), the size of aggregates increases (Figure 3.5a, Figure 3.5c, and Figure 3.5d). The size of aggregates is larger in an alkaline environment compared with an acid environment as shown in Figure 3.5d and Figure 3.5a respectively. This result is in agreement with a study conducted by Damodaran (2008) that suggested a higher degree of protein unfolding at extreme alkaline pH values compared with extreme acidic pH values.

Figure 3.6a illustrates the globular structures of a whey protein network at pH 4.0 having been heated to 80°C. Structural knots in the acidic environment are rather fine, in the order of 5 μm , as compared to the protein spheroids at pH 7.0 (in the order of 20 or 30 μm) that appear to form a partially fused network (Figure 3.6b). Cooling of the denatured protein structure in the presence of agarose stimulates further gelation hence yielding two component networks with contrasting refractive indices in Figure 3.6c. At acidic pH, optically dense protein particles appear to form a continuous phase, which is interrupted by elongated polysaccharide chains. Phase separated patterns between a smooth polysaccharide phase and coarse protein spheroids are also evident in the mixture sampled at neutral pH (Figure 3.6d).

This work focused primarily on thermally treated preparations, since it is understood that cooling experiments yield dendritic polymer networks of agarose supporting liquid inclusions of whey protein. The micrographs of these types of networks at two pH values (pH 4.0 and pH 7.5) are illustrated in Figure 3.7 in which

the agarose is the continuous phase. The whey protein inclusions are not distinctly visible due to absence of thermal treatment to induce denaturation and aggregation.

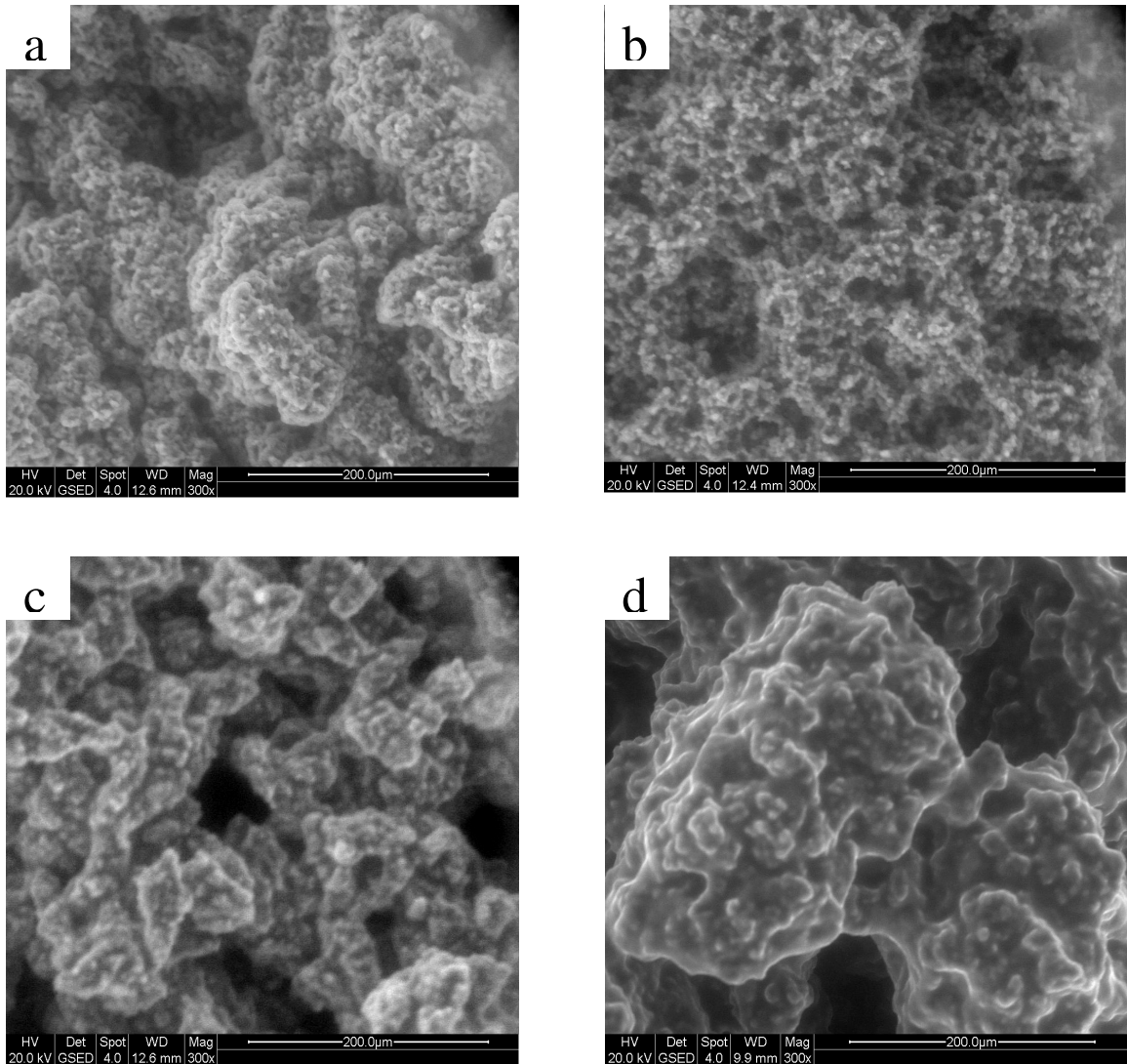


Figure 3.5 ESEM images of 15.0% whey protein (a) at pH 4.0, (b) at pH 5.0, (c) at pH 6.0 and (d) at pH 7.5, with all samples being thermally treated (heating followed by cooling); magnification is 200 µm.

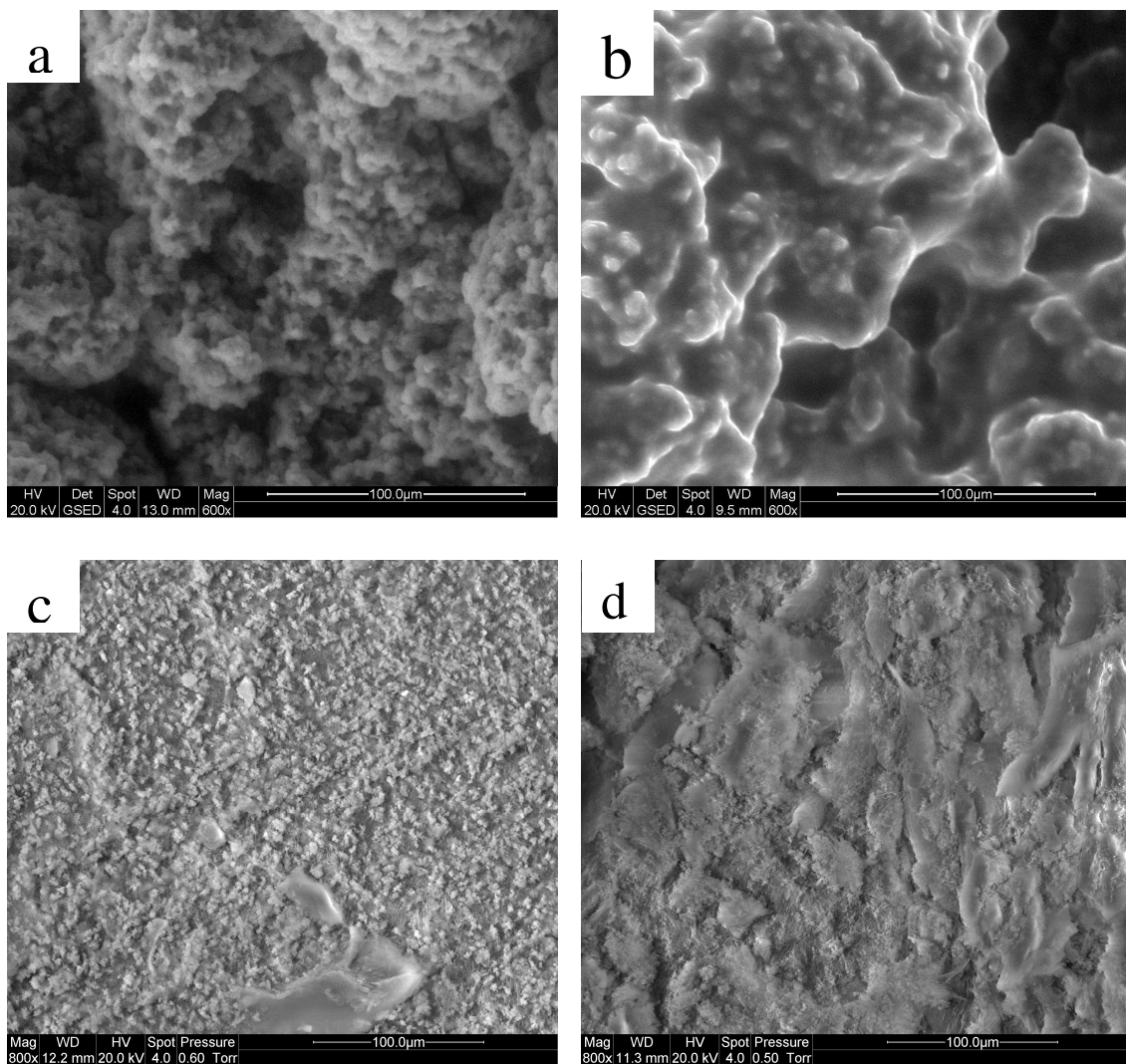


Figure 3.6 ESEM images of (a) 15.0% whey protein at pH 4.0, (b) 15.0% whey protein at pH 7.0, (c) 2.0% agarose with 15.0% whey protein at pH 4.0 and (d) 2.0% agarose with 15.0% protein at pH 7.0, with all samples being thermally treated (heating followed by cooling); magnification is 100 µm.

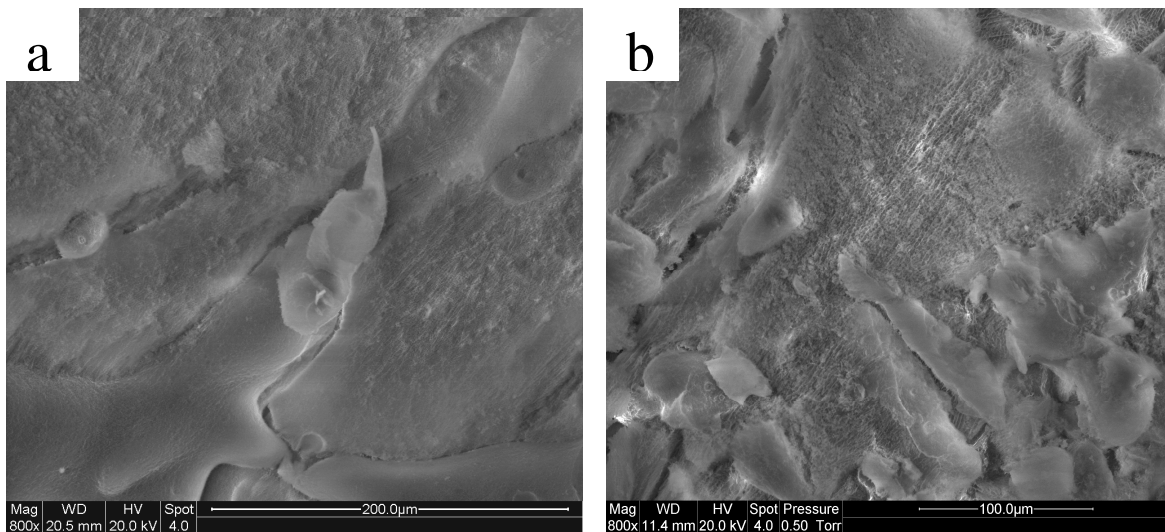


Figure 3.7 SEM images of 2.0% agarose with 15% whey protein (a) at pH 4.0 and (b) at pH 7.5, without thermal treatment (cooling only).

3.4.3 *Theoretical Modeling of the Phase Behavior in Agarose/Whey protein Mixtures*

Qualitative analysis in the preceding sections provided insights into network characteristics and the phase behavior of our binary mixtures in relation to thermal treatment and change in pH. Further explorations can be made by relating mechanical properties of the two components to the overall behavior of the composite gel so that the nature of phase continuity and the solvent partition between polymeric phases is reasonably understood. The approach that found considerable utility in the quantitative description of the structural properties of biopolymer composite gels relates the overall storage modulus on shear to those of the two polymeric phases by applying the so-

called “blending laws” (Gilsenan, Richardson & Morris, 2003). A mathematical expression is thus developed that relates the mechanical properties of the composite and bulk components as follows:

$$G'_c = \phi_x G'_x + \phi_y G'_y \quad [3.1]$$

and

$$G'_c = (\phi_x / G'_x + \phi_y / G'_y)^{-1} \quad [3.2]$$

where G'_c , G'_x and G'_y are the storage moduli on shear of the composite, X-phase polymer and Y-phase polymer, respectively, with ϕ_x and ϕ_y ($\phi_x + \phi_y = 1$) being the phase volumes of the two polymeric components X and Y.

Figure 3.8a and Figure 3.8b reproduce examples at pH of 4.5 and 7.5 respectively of the computerized output designed to check the applicability of blending laws to the mixed systems that have been taken through the full thermal treatment, i.e. loading at 45°C, heating to 80°C and then cooling to 5°C. Following this treatment, the two components form gelled networks, and an expedient way to predict the distribution of solvent between the two phases is to calculate the values of storage modulus for all possible distributions in order to find which one matches the experimental value of the mixture (Morris, 2009). In the present illustration, the solvent content of the whey-protein phase (S_{wp}) is plotted on the x axis. At very low values of S_{wp} , where most of the water is with the agarose phase, the protein is extremely concentrated hence $G'_{wp} \gg G'_{ag}$. Conversely, at very high values of S_{wp} , $G'_{wp} \ll G'_{ag}$.

At one critical value of solvent partition, the moduli of the two phases cross over and under these conditions it becomes apparent from equations [3.1] and [3.2] that the isostrain and isostress blending laws also yield this common value ($G'_{wp} = G'_{ag} = G'_U = G'_L$). Up to this point, the upper bound value (G'_U) corresponds to a whey protein continuous system, and the lower bound value (G'_L) to agarose continuous. At higher

values of solvent partition, $G'_{U(ag)}$ relates to an agarose continuous phase and $G'_{L(wp)}$ to whey protein continuous. As a result, whey protein continuous curves run from the top left to the bottom right, whereas agarose continuous curves extend from the bottom left to the top right of the graph. Experimental moduli of the composite recorded at 5°C appear to intersect a lower bound arrangement in blending-law modeling yielding an S_{wp} values of 0.71 (at pH 4.5) and 0.97 (at pH 7.5). These outcomes are consistent with whey protein being denatured upon heating to create the continuous phase in the mixture and agarose forming hard filler particles upon subsequent cooling.

Thermal denaturation triggers drastic changes in the viscoelasticity of whey protein whose phase behavior in mixture with agarose was examined using the blending laws. To further ascertain the effect of conformational changes on solvent partition between polymeric phases, agarose/whey protein mixtures were cooled from 45°C to 5°C to alter the rigidity of the polysaccharide phase only. Using these experimental settings, quantitative analysis of the mechanical properties for the binary system of this investigation was carried out and the examples of pH 4.5 and pH 7.5 are depicted in Figure 3.9a and Figure 3.9b accordingly. Clearly, the basic blending laws cannot follow the change in structural properties once the discontinuous phase is in the form of liquid whey protein droplets, with the experimental value of the composite system falling well below their predictions. The data argue that the modulus of the solid-like phase of agarose divided by the modulus of the liquid-like phase of whey protein ($G'_{wp} \ll 1.0$ Pa at 5°C) yields values in the order of thousands.

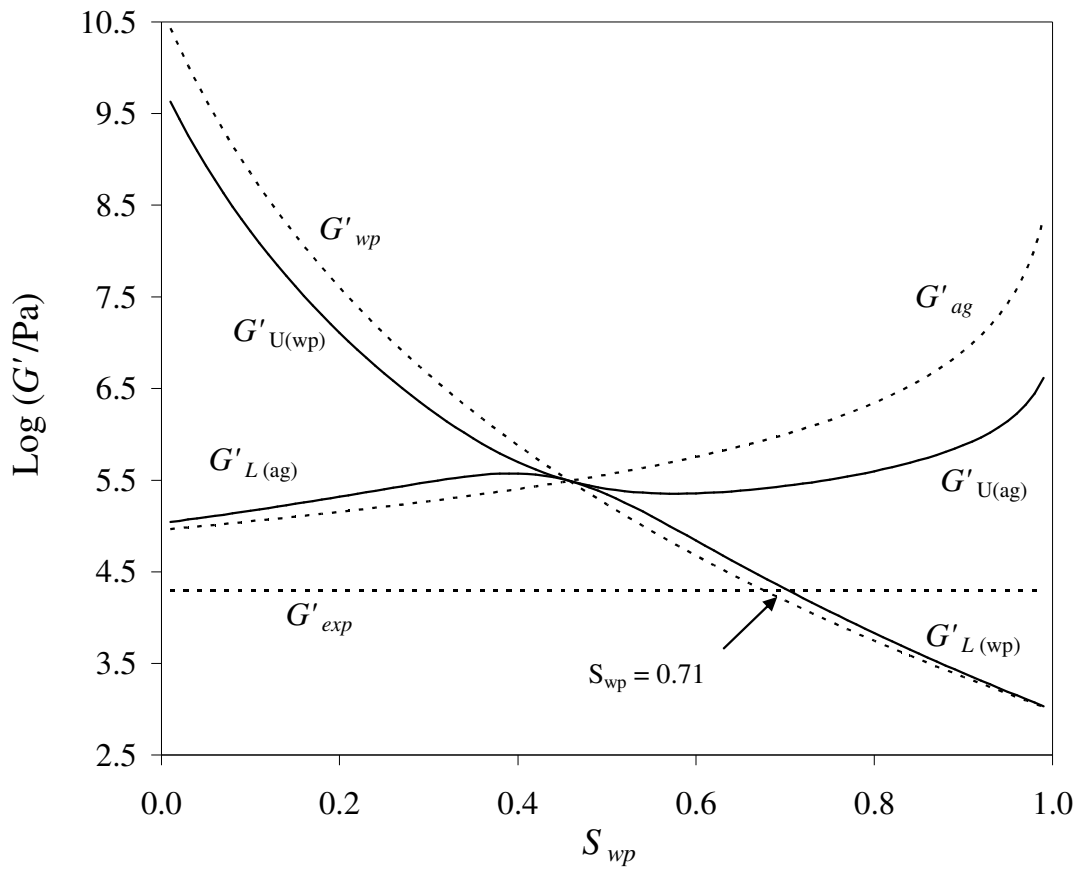


Figure 3.8a Computerized modeling of the phase topology of 1.0% agarose with 15.0% whey protein mixture, which was exposed to heating and cooling, at pH 4.5 using the isostrain and isostress blending laws. Storage modulus values of agarose (G'_{ag}) and whey protein (G'_{wp}) are represented by dashed lines while the upper ($G'_{U(ag)}$; $G'_{U(wp)}$) and lower ($G'_{L(ag)}$; $G'_{L(wp)}$) bounds are illustrated as solid lines. Experimental composite modulus (G'_{exp}) taken at 5°C is also shown to intersect the calculated lower bound at a specific value of S_{wp} .

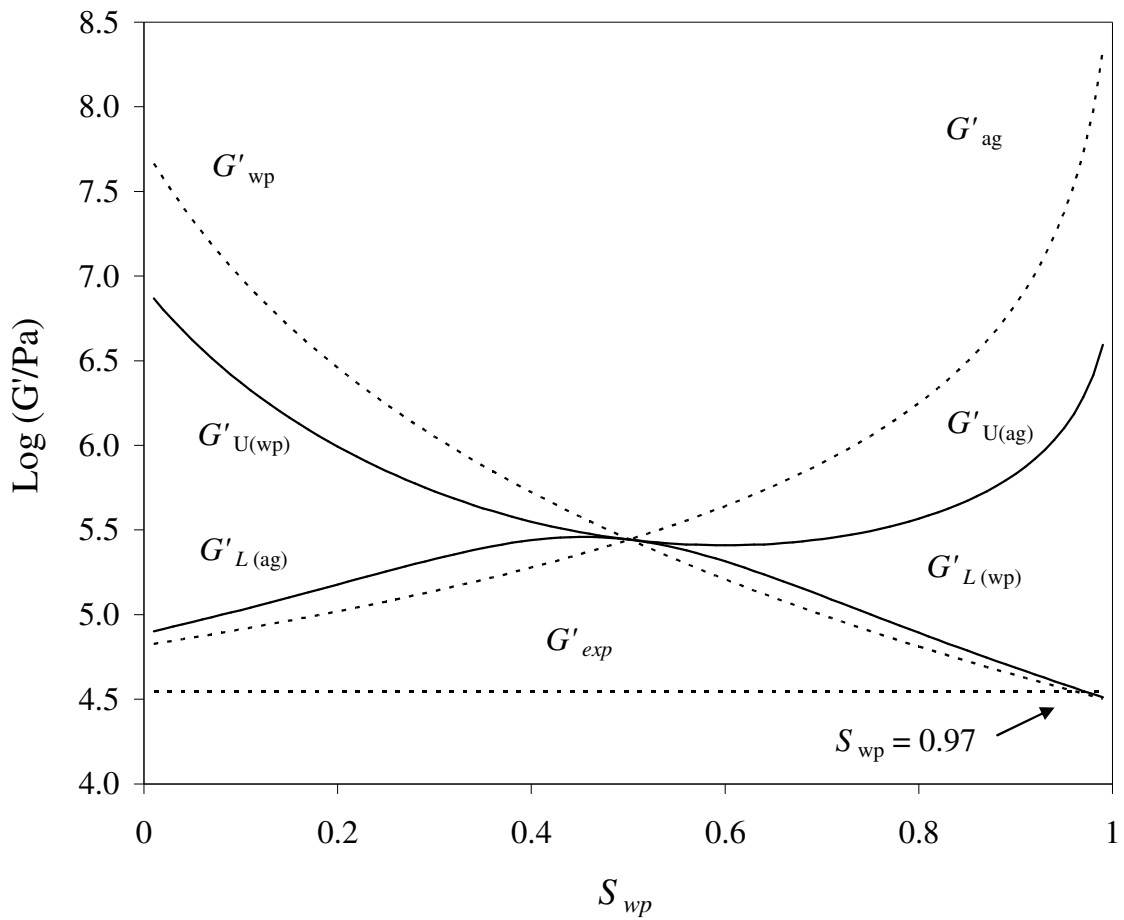


Figure 3.8b Computerized modeling of the phase topology of 1.0% agarose with 15.0% whey protein mixture, which was exposed to heating and cooling, at pH 7.5 using the isostrain and isostress blending laws. Storage modulus values of agarose (G'_{ag}) and whey protein (G'_{wp}) are represented by dashed lines while the upper ($G'_{U(ag)}$; $G'_{U(wp)}$) and lower ($G'_{L(ag)}$; $G'_{L(wp)}$) bounds are illustrated as solid lines. Experimental composite modulus (G'_{exp}) taken at 5°C is also shown to intersect the calculated lower bound at a specific value of S_{wp} .

This modulus ratio is roughly the correct indicator for synthetic polyblends and block polymers whose viscoelastic characteristics can be rationalized with the theoretical advance achieved by Lewis and Nielsen. The analytical expression of this framework of thought is given as follows (Petersson & Oksman, 2006; Shrinivas, Kasapis & Tongdang, 2009):

$$G'_1 / G'_c = (1 + A_i B_i \phi_2) / (1 - B_i \psi \phi_2) \quad [3.3]$$

$$B_i = [(G'_1 / G'_2) - 1] / [(G'_1 / G'_2) + A_i] \quad [3.4]$$

$$\psi = 1 + [(1 - \phi_m) / \phi_m^2] \phi_2 \quad [3.5]$$

where in equations [3.3] to [3.5], G'_c , G'_1 and G'_2 are the shear moduli of the composite, continuous rigid phase of agarose and soft filler of whey protein, and ϕ_2 is the phase volume of the said filler. The framework takes into account the shape of the filler *via* an inverted Einstein coefficient ($A_i = 1/A$), which is very sensitive to the morphology of the composite. A further level of refinement was achieved by considering the concept of maximum packing fraction (ϕ_m) of the filler phase.

Figure 3.9a and Figure 3.9b show the standard of agreement obtained using equations [3.3] to [3.5] for the experimental shear modulus of the cooled only agarose/whey protein mixture at pH 4.5 and pH 7.5 respectively. For the purpose of modeling, the Einstein coefficient was held constant at the theoretical value for dispersed spheres, $A = 1.5$ (Nielsen, 1974), hence the only adjustable parameter of the fit is the maximum packing fraction of the dispersed phase. The latter is a rather difficult parameter to obtain experimentally but, for each pH value of the aqueous mixture, experimental moduli of the composite at 5°C intersect convincingly the part of the Lewis-Nielsen prediction that falls dramatically with S_{wp} at an ϕ_m value of 0.601. This estimate corresponds to loose packing of spheroidal inclusions (Torquato, Truskett

& Debenedetti, 2000), which is the expected outcome for the reduction of interfacial tension between two phase-separated polymeric domains.

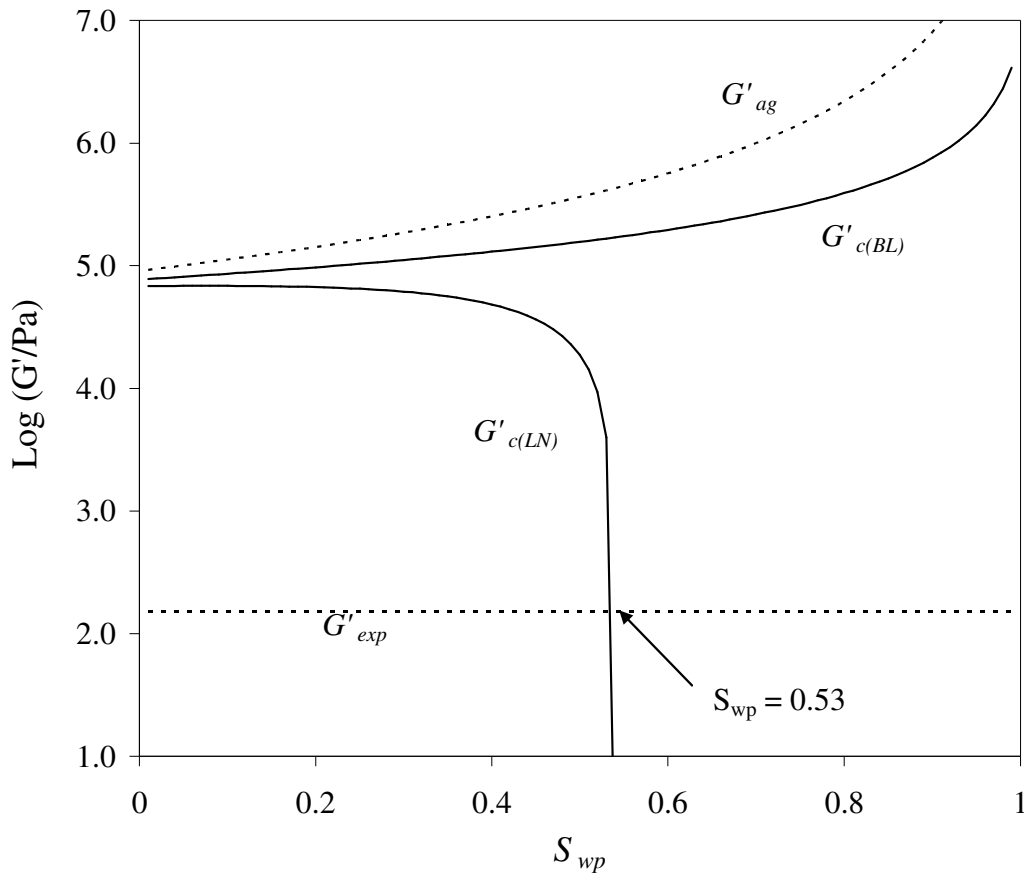


Figure 3.9a Computerized modeling of the phase topology of 1.0% agarose plus 15.0% whey protein, which was exposed to a cooling routine only, at pH 4.5 using the Lewis-Nielsen and isostrain blending laws. Storage modulus values of agarose (G'_{ag}) are represented by a dashed line while the calculated composite moduli according to Lewis-Nielsen ($G'_{c(LN)}$) and blending ($G'_{c(BL)}$) laws are illustrated as solid lines. Experimental composite modulus (G'_{exp}) taken at 5°C is also shown to intersect the Lewis-Nielsen predictions at a specific value of S_{wp} .

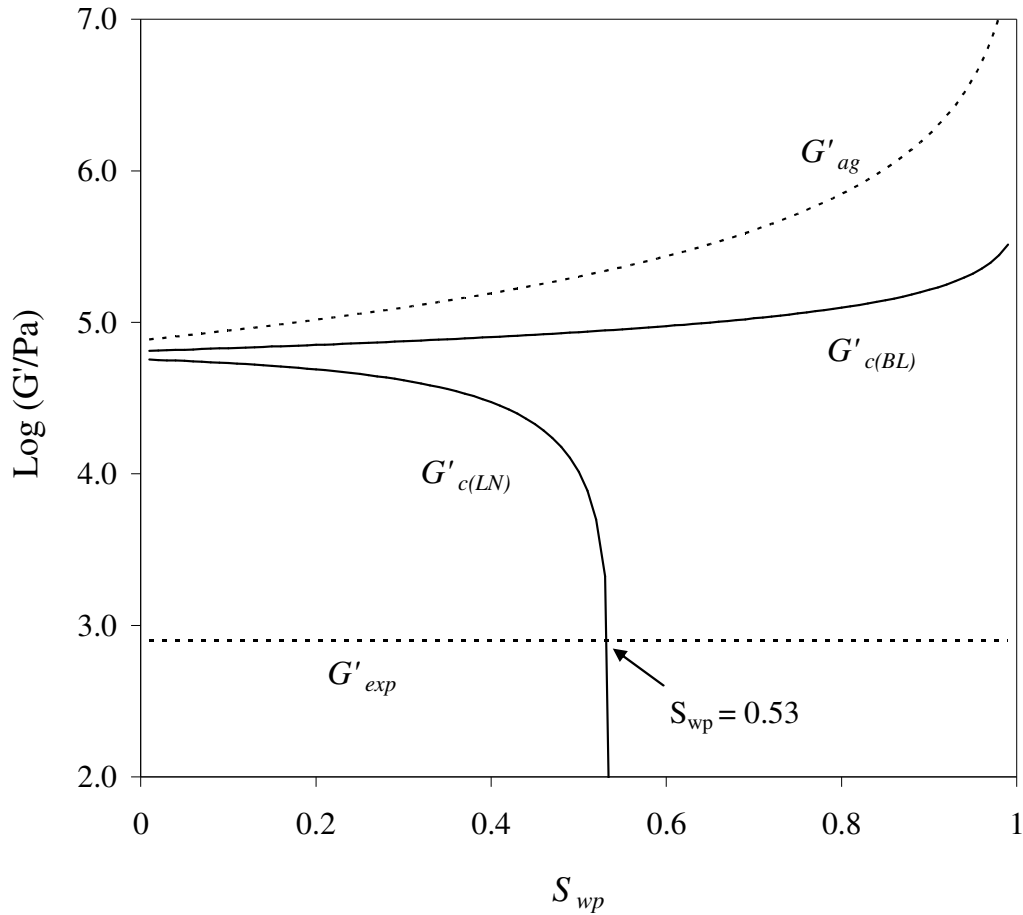


Figure 3.9b Computerized modeling of the phase topology of 1.0% agarose plus 15.0% whey protein, which was exposed to a cooling routine only, at pH 7.5 using the Lewis-Nielsen and isostrain blending laws. Storage modulus values of agarose (G'_{ag}) are represented by a dashed line while the calculated composite moduli according to Lewis-Nielsen ($G'_{c(LN)}$) and blending ($G'_{c(BL)}$) laws are illustrated as solid lines. Experimental composite modulus (G'_{exp}) taken at 5°C is also shown to intersect the Lewis-Nielsen predictions at a specific value of S_{wp} .

Solvent contents for whey protein in its native conformation in Figure 3.9a and Figure 3.9b ($S_{wp} = 0.53$) are considerably lower than the denatured counterpart in Figure 3.8a ($S_{wp} = 0.71$) and Figure 3.8b ($S_{wp} = 0.97$) consequently. Based on Figure 3.9a and Figure 3.9b, S_{wp} values at pH 4.5 and pH 7.5 are similar which indicate that pH variation has very little influence on the cooled only agarose/whey protein mixture.

The composition of Figures 3.8a and Figure 3.9a is thorough but there is too much detail. To clearly show the distribution of solvent between the two phases and to allow for meaningful comparisons in agarose/whey protein systems where the pH values have been adjusted systematically, the “solvent avidity” factor, P , is utilized (Clark *et al.*, 1983):

$$P = (S_{wp}/C_{wp})/(S_{ag}/C_{ag}) \quad [3.6]$$

In equation [3.6], C_{ag} and C_{wp} are the nominal (original) concentrations of the two macromolecules in preparations. Clearly, values of P -factor contrast the level of solvent found within phases per unit of the initial concentration of the corresponding polymer.

In Figure 3.10, the outcome of composite bounds analysis, experimental storage moduli and solvent partition between phases shown in Figures 3.8a and Figure 3.9a have been reproduced by plotting against the P -factor derived from equation [3.6]. Clearly, considerable changes are predicted in the distribution of solvent in the system as a function of thermal treatment and pH change to create three families of points. There is no systematic variation in P estimates, within the group of data for the cooling routine, remaining well below 0.10. It appears that the liquid-like whey protein phase allows diffusion of water molecules in the gelled agarose phase, which holds as the continuous matrix ten times more solvent than the protein per unit concentration. Reversing the experimental routine to heating followed by cooling creates a composite gel with whey protein as the supporting matrix that changes the pattern of water

partition between the constituent phases. At acidic pH, constant values for the distribution of solvent in the system are obtained ($P = 0.25 \pm 0.10$), with agarose remaining the “hydrophilic network”. At alkaline pH, however, the P -factor increases sharply reaching values of about 2.20 in favor of the continuous whey-protein phase.

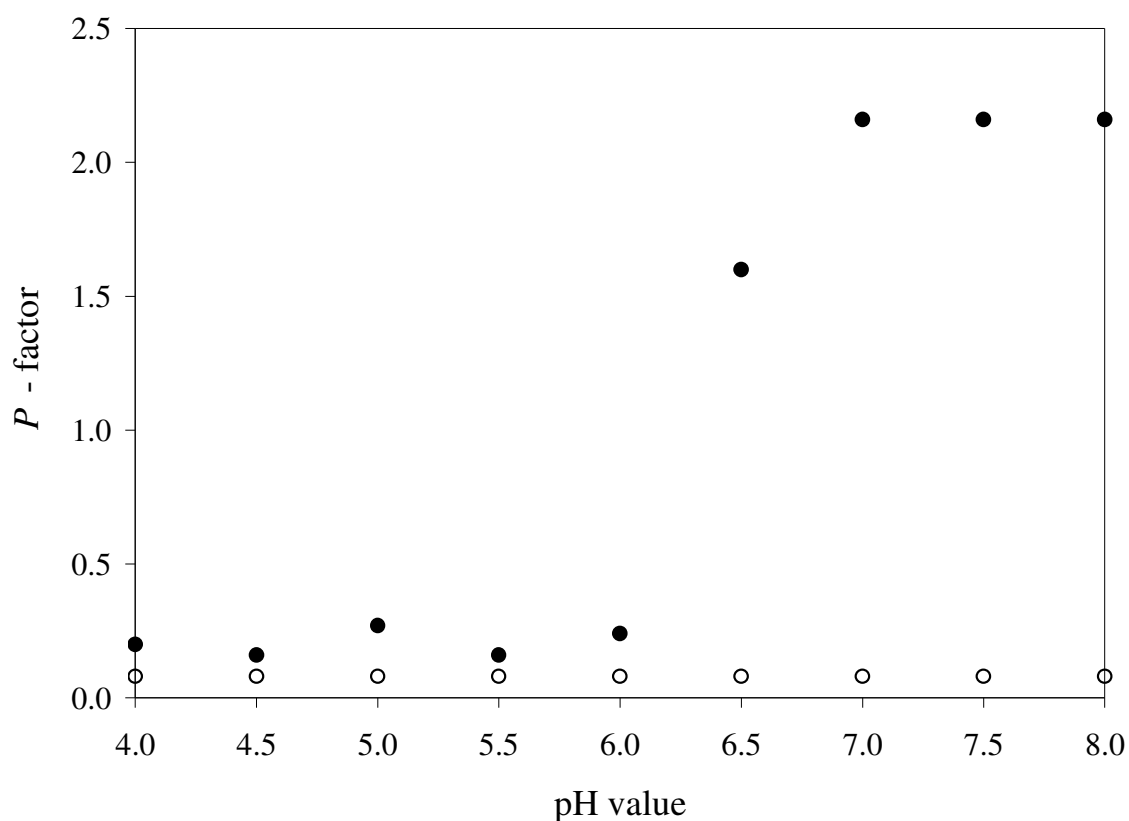


Figure 3.10 Data for the relative solvent partition (P -factor) plotted against adjusted pH for the mixed systems of 1.0% agarose plus 15.0% whey protein, which were subjected to both heating and cooling (●) or a cooling only treatment (○).

3.5 CONCLUSIONS

The present chapter is part of an effort to better understand segregative phase separation in aqueous biopolymer mixtures. Results demonstrate that the combination of complementary physical techniques such as mechanical spectroscopy, differential scanning calorimetry and electron microscopy can characterize the micromolecular organization of binary systems as a function of thermal treatment and change in pH. In terms of solvent partition between two polymeric phases, a helpful picture of the importance of conformational changes with experimental temperature or acidity in the phase behavior of a mixed system is given. Rheological data were modeled using theoretical frameworks adapted from the synthetic polymer research.

Variation in the values of the P -factor for agarose/whey protein samples at a fixed polymer concentration is distinct from previous estimates reported in the literature for composite gels, e.g., gelatin/hydrolyzed starch, gelatin/low methoxy pectin and sodium caseinate/ β -glucan. The latter group of binary systems exhibited isostrain or isostress phase behavior according to the blending-law equations [3.1] and [3.2] and classic phase inversion from one continuous matrix to another with increasing concentration of the second polymeric component (Gilsenan et al., 2003a; Kasapis et al., 1993; Kontogiorgos et al., 2006).

It was found that phase inversion in binary mixtures, due to increasing concentration of the second (Y) component, resulted in two distinct clusters of P predictions, one for the X-continuous composite and the other for the Y-continuous composite following phase inversion. The lack of systematic variation in these predictions with polymer concentration before or after phase inversion and the magnitude of P values in each cluster of points, which always favors the continuous-phase forming polymer, reflects fundamental

differences in the interplay between the kinetics of ordering/gelation and microscopic phase separation in those materials.

In addition, designing experimental conditions that encourage formation of a bicontinuous mixture, where both polymers form a continuous network, allows increasing concentrations of a given component to exhibit favorable relative affinity for solvent in the system. This type of behavior has been reported, for example, in gelatin/agarose gels where the presence of two continuous phases allowed the slower-gelling component (gelatin) to exhibit enhanced water holding capacity leading to a monotonic change in P values with increasing concentrations of the protein in the system (Shrinivas, Kasapis, & Tongdang, 2009). This outcome for bicontinuous mixtures is distinct from the central finding of a single value of the P -factor observed in the distribution of solvent between the continuous matrix of polymer X and the discontinuous inclusions of polymer Y mentioned for several composite gels in the preceding paragraph (Gilsenan et al., 2003a; Kasapis et al., 1993; Kontogiorgos et al., 2006).

This work complements research findings in the literature by presenting an unexplored aspect of segregative phase separation by adjusting the pH values in mixtures of the two conformationally dissimilar macromolecules of agarose and whey protein. Modeling of the rearrangement of water molecules between the two constituents has demonstrated that the P values are profoundly affected by pH in the aqueous system. Thus, the proportion of solvent associated with the protein phase increases rapidly at slightly acidic and alkaline pH where the protein exhibits a higher degree of unfolding than below the isoelectric point (see also micrographs in Figure 3.6). This is due to ionization of partially buried carboxyl, phenolic and sulfhydryl groups that cause certain unraveling of the polypeptide chains as they attempt to expose themselves to the aqueous environment (Monahan, German, & Kinsella, 1995).

Water diffuses in the anisotropic medium of the two polymers seeking osmotic equilibrium, but the decline in the amount of solvent kept in the agarose phase with increasing pH argues for mixed gels that are kinetically trapped in the local medium. Variation in solvent-partition data from this work, and earlier reports in the literature, suggest that P values derived under a particular thermal regime, kinetic rate of gelation, polymer composition of mixtures and pH variation in preparations should not be related to the Flory-Huggins interaction parameter (χ). This describes the energy of interaction between the two biopolymers and solvent in solution (segment-segment and solvent-segment pair interactions) (Csaki, Nagy, & Csemesz, 2005), hence the molecular forces that govern their phase diagram in solution. It appears, however, that aggregation followed by gelation in whey protein or agarose phases arrest the composite system at intermediate conditions away from thermodynamic equilibrium.

CHAPTER 4

EPILOGUE AND FUTURE RESEARCH

The overall aim of this Thesis is to continue the debate on the formulation of a scientific basis for an optimal choice of constituents and composition in low-solid materials comprising binary mixtures of biopolymer with industrial relevance. Low-solid biomaterials with industrial applications increasingly include a number of non-starchy polysaccharides, i.e. various types of dietary fiber, and dairy proteins to deliver a range of properties such as structure, storage stability, processability, etc. Broadly speaking, these include systems with less than 40% solids, as opposed to high-solid materials with more than 70% solids in preparations. Thus the ingredients of this investigation, i.e. agarose and whey proteins in an environment of alkaline or acidic pH are found to have a wide range of low-solid industrial applications.

The market value of these products is increasingly significant. This is to a good extent in response to governmental key recommendations to develop novel food products that utilize whey proteins and dietary fiber in formulations, for example:

- i) as a substitute for fat in yellow-fat spreads and processed (soft cheeses)
and
- ii) as a functional ingredient in starch based materials for the development of breakfast cereals, snacks and energy bars.

Such formulations will offer real benefit by respecting the concerns of the consumer around the world for a low-calorie and low glycemic-index diet. In the case of whey protein, further benefits include the introduction of bioactive-compounds (found in

whey protein) like colon-tumor preventing sulfur amino acids and immune-system enhancing antioxidants and antimicrobials such as lactoferrins and lactoperoxidases, to name but a few. Thus, understanding the structure-function relationships of natural whey powders in relation to other ingredients like agarose and processing parameters (e.g. change in pH) should yield product formulations of improved nutritional value and consumer acceptability.

Work of this Thesis has tried to address a common observation among artisans in the field that by and large, manufacturing of low-solid materials containing two (or more) biopolymers as structuring ingredients is regarded as being craft based. In the case of whey protein and dietary fiber, agarose in this case, there have been no systematic studies on the kinetics of structure development of products as a function of changing pH from the alkaline to acidic environment. The lack of fundamental understanding and control of such properties has the potential to hamper the ability of the industry to match the kinetics of structure formation to the timescale of manufacturing processes and storage in order to improve the consumer acceptance of many polymer-composite based products. For example, the difficulty of studying the distribution of solvent (water molecules in processed foods) in phase-separated mixtures in relation to the gelled state, as opposed to the thermodynamic equilibrium in solution yielding a bimodal in the phase diagram, is acknowledged in the literature.

To address the issue of solvent distribution between the two phases, work has been carried out in several laboratories on how biphasic gels behave in terms of phase continuity and phase inversion as a function of external stimuli. The milestone of this approach is based on the assumption that either bulk phase separation to equilibrium takes place first with gelation then occurring subsequently and independently in each phase or the fastest gelling component does so prior to the establishment of a true

thermodynamic equilibrium with subsequent gelation of the second, slower gelling component. As described in this Thesis, a number of theoretical treatments from the realm of synthetic polymer research were developed for use in biomaterials including the blending laws and the equations of Lewis-Nielsen.

The conclusions drawn from the theoretical postulates were put to the test by acquiring independent evidence about the structural and mechanical properties of mixed gels using mainly mechanical spectroscopy, differential scanning calorimetry and electron/optical microscopy. Studies were done using mixtures of several biopolymers, e.g. hydrolyzed starch, gelatin, low methoxy pectin, deacylated gellan, κ -carrageenan, in an attempt to identify a general pattern of behavior in the phase separation of biphasic gels.

The present investigation adds to that by providing valuable information on the phase behavior of whey proteins and agarose as a function of changing pH. It documents the increasing capacity of the protein to hold solvent in its phase at pH above its isoelectric point where a higher degree of unfolding is exhibited. Overall, the analysis (theoretical model and experimental techniques) was extremely encouraging and the lack of direct (instrumental) determination of phase-composition makes it a most appropriate tool of attack for future research on biopolymer composite gels. This type of research should then be able to educate technology by improving manufacturing processes and create competitive advantage for the food industry in contributing to the development of a variety of added value materials in the market.

Regarding suggestions for future research on the subject, the following key issues have so far received little attention and should be addressed by applying the techniques and concepts of materials science approach in biomaterial structure-function relationships:

- i) To start with, advances in imaging technology should allow direct determination of the composition of individual phases in biphasic composite-gels of whey protein and soluble dietary fiber, using Z-stack confocal laser microscopy, augmented by Fourier transform infrared spectroscopy.
- ii) Effect of homogenization on the size of the dispersed phase of whey protein microgels and its influence on the structure and functionality of dietary-fiber containing composite materials.
- iii) Orientation of bio-fibers (e.g., cellulose whiskers from grains) in gelled matrices of whey protein, using modified constitutive equations taking into account the effect of shear history, and the size, shape and phase volume of the filler particles, to model small-deformation mechanical properties.
- iv) Effect of preprocessing of the whey powders and processing variables (thermal stress, mechanical stress, etc.) on the state of thermodynamic compatibility and failure (breakdown) properties of composite gels with dietary fiber, which are likely to be of greater practical significance than the non-destructive (small-deformation) measurements used in most previous research.

REFERENCES

- Aguilera, J. M. (1995). Gelation of whey proteins. *Food Technology*(October), 83-89.
- Alting, A. C., Hamer, R. J., de Kruif, C. G., Paques, M., & Visschers, R. W. (2003). Number of thiol groups rather than the size of the aggregates determines the hardness of cold set whey protein gels. *Food Hydrocolloids*, 17(4), 469-479.
- Araki, C. (1937). Fractionation of agar-agar. *J. Chem. Soc. Japan*, 58(1338).
- Arnott, S., Fulmer, A., Scott, W. E., Dea, I. C. M., Moorhouse, R., & Rees, D. A. (1974). The agarose double helix and its function in agarose gel structure. *Journal of Molecular Biology*, 90(2), 269-284.
- Aymard, P., Martin, D. R., Plucknett, K., Foster, T. J., Clark, A. H., & Norton, I. T. (2001). Influence of thermal history on the structural and mechanical properties of agarose gels. *Biopolymers*, 59(3), 131-144.
- Barrangou, L. M., Daubert, C. R., & Foegeding, E. A. (2006). Textural properties of agarose gels. I. Rheological and fracture properties. *Food Hydrocolloids*, 20(2-3), 184-195.
- Barrangou, L. M., Drake, M., Daubert, C. R., & Foegeding, E. A. (2006). Textural properties of agarose gels. II. Relationships between rheological properties and sensory texture. *Food Hydrocolloids*, 20(2-3), 196-203.
- Bernal, V., & Jelen, P. (1985). Thermal stability of whey proteins - a calorimetric study. *J. Dairy Sci.*, 68, 2847.
- Borwankar, R. P. (1992). Food Texture and Rheology - A Tutorial Review. *Journal of Food Engineering*, 16(1-2), 1-16.
- Bourne, M. C. (2002). *Food Texture and Viscosity: Concept and Measurement* (2nd ed.). San Diego: Academic Press.

- Bourne, M. C., & Rao, M. A. (1990). Viscosity measurements of foods. In D. Y. C. Fung & R. F. Mathews (Eds.), *Instrumental Methods for Quality Assurance of Food* (pp. 211-229). New York: Marcel Dekker.
- Braudo, E. E., Muratalieva, I. R., Plaschina, I. G., & Tolstoguzov, V. B. (1991). Correlation between the temperatures of formation/breakdown of the gel network and conformational transitions of agarose macromolecules. *Carbohydrate Polymers*, 15(317).
- Braudo, E. E., Muratalieva, I. R., Plaschina, I. G., Tolstoguzov, V. B., & Markovich, I. S. (1991). Studies on the mechanisms of gelation of k-carrageenan and agarose. *Colloid Polym. Sci.*, 269(1148).
- Cayot, P., & Lorient, D. (1997). Structure-function relationships of whey proteins. In S. Damodaran & A. Paraf (Eds.), *Food Proteins and their Applications* (pp. 225-256). New York: Marcel Dekker.
- Chamani, J., Moosavi-Movahedi, A. A., Rajabi, O., Gharanfoli, M., Momen-Heravi, M., Hakimelahi, G. H., . . . Varasteh, A. R. (2006). Cooperative α -helix formation of β -lactoglobulin induced by sodium n-alkyl sulfates. *Journal of Colloid and Interface Science*, 293(1), 52-60.
- Chantrapornchai, W., & McClements, D. J. (2002). Influence of NaCl on optical properties, large-strain rheology and water holding capacity of heat-induced whey protein isolate gels. *Food Hydrocolloids*, 16(5), 467-476.
- Chiti, F., & Dobson, C. M. (2006). Protein misfolding, functional amyloid, and human disease. *Annual Reviews of Biochemistry*, 75, 333-366.
- Clark, A. H. (1987). The application of network theory to food systems. In J. M. V. Blanshard & P. Lillford (Eds.), *Food Structure and Behaviour* (pp. 13-34). London: Academic Press.

- Clark, A. H., Richardson, R. K., Rossmurphy, S. B., & Stubbs, J. M. (1983). Structural and mechanical properties of agar/gelatin co-gels - small deformation studies. *Macromolecules*, *16*(8), 1367-1374.
- Clark, A. H., & Ross-Murphy, S. B. (2009). Biopolymer network assembly: Measurement and theory. In S. Kasapis, I. T. Norton & J. B. Ubbink (Eds.), *Modern Biopolymer Science: Bridging the Divide between Fundamental Treatise and Industrial Application* (pp. 1-27). San Diego: Elsevier.
- Csaki, K. F., Nagy, M., & Csemesz, F. (2005). Influence of the chain composition on the thermodynamic properties of binary and ternary polymer solutions. *Langmuir*, *21*, 761-766.
- Damodaran, S. (2008). Amino acids, Peptides, and Proteins. In S. Damodaran, K. L. Parkin & O. R. Fennema (Eds.), *Fennema's Food Chemistry* (4 ed., pp. 217-329). Boca Raton: CRC Press.
- Damodaran, S., & Kinsella, J. E. (1981). The effect of neutral salts on the stability of macromolecules. *J. Biol. Chem.*, *256*, 3394.
- Dang, H. V., Loisel, C., Desrumaux, A., & Doublier, J. L. (2009). Rheology and microstructure of cross-linked waxy maize starch/whey protein suspensions. *Food Hydrocolloids*, *23*(7), 1678-1686.
- Davies, W. E. A. (1971). The theory of elastic composite materials. *J. Phys. D: Appl. Phys.*, *4*, 1325-1339.
- Dea, I. C. M., McKinnon, A. A., & Rees, D. A. (1972). Tertiary and quaternary structure in aqueous polysaccharide systems which model cell wall cohesion: Reversible changes in conformation and association of agarose, carrageenan and galactomannans. *Journal of Molecular Biology*, *68*(1), 153-172.

- deWit, J. N. (1981). Structure and functional behavior of whey proteins. *Neth. Milk Dairy J.*, 35, 47.
- deWit, J. N., & Klarenbeek, G. (1984). Effects of various heat treatments on structure and solubility of whey proteins. *Journal of Dairy Science*, 67(11), 2701-2710.
- Duckworth, M., Hong, K. C., & Yaphe, W. (1970). The agar polysaccharides of *Gracilaria* species. *Carbohydrate Research*, 18, 1-9.
- Esquenet, C., Terech, P., Boue, F., & Buhler, E. (2004). Structural and rheological properties of hydrophobically modified polysaccharide associative networks. *Langmuir*, 20(9), 3583-3592.
- Ewbank, J. J., & Creighton, T. E. (1993a). Pathway of disulfide-coupled unfolding and refolding of bovine α -lactalbumin. *Biochemistry (Easton)*, 32(3677).
- Ewbank, J. J., & Creighton, T. E. (1993b). Structural characterization of the disulfide folding intermediates of bovine α -lactalbumin. *Biochemistry (Easton)*, 32(3677).
- FEI. (2008). Electron microscopy [Booklet].
- FEI. (2009). Quanta™ Scanning Electron Microscope Retrieved 11 March 2011, from <http://www.fei.com/products/scanning-electron-microscopes/quanta.aspx>
- Fitzsimons, S. M., Mulvihill, D. M., & Morris, E. R. (2007). Denaturation and aggregation processes in thermal gelation of whey proteins resolved by differential scanning calorimetry. *Food Hydrocolloids*, 21(4), 638-644.
- Flory, P. J. (1974). Introduction. *Faraday Discussion of the Chemical Society*, 57, 7-18.
- Fonkwe, L. G., Narsimhan, G., & Cha, A. S. (2003). Characterization of gelation time and texture of gelatin and gelatin-polysaccharide mixed gels. *Food Hydrocolloids*, 17(6), 871-883.

- Fox, P. F., & Mulvihill, D. M. (1982). Milk proteins: Molecular, colloidal, and functional properties. *J. Dairy Res.*, *49*, 679.
- Fujii, T., Yano, T., Kumagai, H., & Miyawaki, O. (2000). Scaling analysis on elasticity of agarose gel near the sol-gel transition temperature. *Food Hydrocolloids*, *14*(4), 359-363.
- Gill, P. S., Sauerbrunn, S. R., & Reading, M. (1993). Modulated differential scanning calorimetry. *Journal of Thermal Analysis*, *40*(3), 931-939.
- Gilsenan, P. M., Richardson, R. K., & Morris, E. R. (2003a). Associative and segregative interactions between gelatin and low-methoxy pectin. Part 3 - Quantitative analysis of co-gel moduli. *Food Hydrocolloids*, *17*(6), 751-761.
- Gilsenan, P. M., Richardson, R. K., & Morris, E. R. (2003b). Associative and segregative interactions between gelatin and low-methoxy pectin: Part 2 - Co-gelation in the presence of Ca²⁺. *Food Hydrocolloids*, *17*(6), 739-749.
- Goldstein, J. I., Newbury, D. E., Echlin, P., Joy, D. C., Lyman, C. E., Lifshin, E., . . . Michael, J. R. (2003). *Scanning Electron Microscopy and X-Ray Microanalysis* (3rd ed.). New York: Springer.
- Grinberg, V. Y., & Tolstoguzov, V. B. (1972). Thermodynamic compatibility of gelatin with some -glucans in aqueous media. *Carbohydrate Research*, *25*(2), 313-321.
- Grinberg, V. Y., & Tolstoguzov, V. B. (1997). Thermodynamic incompatibility of proteins and polysaccharides in solutions. *Food Hydrocolloids*, *11*(2), 145-158.
- Harwalkar, V. R. (1986). Kinetic study of thermal denaturation of proteins in whey. *Milchwissenschaft*, *41*(4), 206-209.
- Hiraoka, Y., & Sugai, S. (1984). Thermodynamics of thermal unfolding of bovine apo- α -lactalbumin. *International Journal of Peptide and Protein Research*, *23*(5), 535-542.

- Kasapis, S. (2009). Unified application of the materials-science approach to the structural properties of biopolymer co-gels throughout the industrially relevant level of solids. In S. Kasapis, I. T. Norton & J. B. Ubbink (Eds.), *Modern Biopolymer Science: Bridging the Divide between Fundamental Treatise and Industrial Application*. San Diego: Elsevier.
- Kasapis, S., Morris, E. R., Norton, I. T., & Clark, A. H. (1993). Phase equilibria and gelation in gelatin/maltodextrin systems -- Part IV: composition-dependence of mixed-gel moduli. *Carbohydrate Polymers*, 21(4), 269-276.
- Kimseng, K., & Meissel, M. (2001). Short overview about the ESEM, from www.calce.umd.edu/general/Facilities/ESEM.pdf
- Kinsella, J. E., & Whitehead, D. M. (1989). Proteins in Whey: Chemical, Physical, and Functional Properties. In J. E. Kinsella (Ed.), *Advances in Food and Nutrition Research* (Vol. 33, pp. 343-438). San Diego: Academic Press, Inc.
- Kontogiorgos, V., Ritzoulis, C., Biliaderis, C. G., & Kasapis, S. (2006). Effect of barley β -glucan concentration on the microstructural and mechanical behaviour of acid-set sodium caseinate gels. *Food Hydrocolloids*, 20(5), 749-756.
- Langton, M., & Hermansson, A.-M. (1992). Fine-stranded and particulate gels of β -lactoglobulin and whey protein at varying pH. *Food Hydrocolloids*, 5(6), 523-539.
- Manoj, P., Kasapis, S., & Hember, M. W. N. (1997). Sequence-dependent kinetic trapping of biphasic structures in maltodextrin-whey protein gels. *Carbohydrate Polymers*, 32(2), 141-153.
- Mercade-Prieto, R., & Gunasekaran, S. (2009). Alkali cold gelation of whey proteins. Part II: Protein concentration. *Langmuir*, 25, 5793-5801.

- Miranda, G., Haxe, G., Scanff, P., & Pelissier, J. P. (1989). Hydrolysis of α -lactalbumin by chymosin and pepsin. *Lait*, 69(451).
- Mohammed, Z. H., Hember, M. W. N., Richardson, R. K., & Morris, E. R. (1998). Application of polymer blending laws to composite gels of agarose and crosslinked waxy maize starch. *Carbohydrate Polymers*, 36(1), 27-36.
- Monahan, F. J., German, J. B., & Kinsella, J. E. (1995). Effect of pH and temperature on protein unfolding and thiol-disulfide interchange reactions during heat-induced gelation of whey-proteins. *Journal of Agricultural and Food Chemistry*, 43(1), 46-52.
- Morris, E. R. (1992). The effect of solvent partition on the mechanical properties of biphasic biopolymer gels: an approximate theoretical treatment. *Carbohydrate Polymers*, 17(1), 65-70.
- Morris, E. R. (2009). Functional interactions in gelling biopolymer mixtures. In S. Kasapis, I. T. Norton & J. B. Ubbink (Eds.), *Modern Biopolymer Science: Bridging the Divide between Fundamental Treatise and Industrial Application* (pp. 167-198). San Diego: Elsevier.
- Mousia, Z., Farhat, I. A., Blachot, J. F., & Mitchell, J. R. (2000). Effect of water partitioning on the glass-transition behaviour of phase separated amylopectin-gelatin mixtures. *Polymer*, 41(5), 1841-1848.
- Nakamura, T., Makabe, K., Tomoyori, K., Maki, K., Mukaiyama, A., & Kuwajima, K. (2010). Different Folding Pathways Taken by Highly Homologous Proteins, Goat [α]-Lactalbumin and Canine Milk Lysozyme. *Journal of Molecular Biology*, 396(5), 1361-1378.

- Narchi, I., Vial, C., & Djelveh, G. (2009). Effect of protein-polysaccharide mixtures on the continuous manufacturing of foamed food products. *Food Hydrocolloids*, 23(1), 188-201.
- Nickerson, M. T., Farnworth, R., Wagar, E., Hodge, S. M., Rousseau, D., & Paulson, A. T. (2006). Some physical and microstructural properties of genipin-crosslinked gelatin-maltodextrin hydrogels. *International Journal of Biological Macromolecules*, 38, 40-44.
- Nielsen, L. E. (1974a). *Mechanical properties of polymers and composites* (Vol. 2). New York: Marcel Dekker.
- Nielsen, L. E. (1974b). Morphology and the elastic modulus of block polymers and polyblends. *Rheologica Acta*, 13, 86-92.
- Nitta, Y., Kim, B. S., & Nishinari, K. (2003). Synergistic gel formation of xyloglucan/gellan mixtures as studied by rheology, DSC, and circular dichroism. *Biomacromolecules*, 4(6), 1654-1660.
- Normand, V., Aymard, P., Lootens, D. L., Amici, E., Plucknett, K. P., & Frith, W. J. (2003). Effect of sucrose on agarose gels mechanical behaviour. *Carbohydrate Polymers*, 54(1), 83-95.
- Normand, V., Lootens, D. L., Amici, E., Plucknett, K. P., & Aymard, P. (2000). New insight into agarose gel mechanical properties. *Biomacromolecules*, 1(4), 730-738.
- Oakenfull, D., Pearce, J., & Burley, R. W. (1997). Protein gelation. In S. Damodaran & A. Paraf (Eds.), *Food Proteins and their Applications* (pp. 111-142). New York: Marcel Dekker.
- Padua, G. W. (1993). Microwave heating of agar gels containing sucrose. *J. Food Sci.*, 58(1426).

- Papiz, M. Z., Sawyer, L., Eliopoulos, E. E., North, A. C. T., Findlay, J. B. C., Sivaprasadarao, R., . . . Kraulis, P. J. (1986). The structure of β -lactoglobulin and its similarity to plasma retinol-binding protein. *Nature*, *324*, 383-385.
- Paulsson, M., Hegg, P. O., & Castberg, H. B. (1985). Thermal stability of whey proteins studied by differential scanning calorimetry. *Thermochimica Acta*, *95*(2), 435-440.
- Petersson, L., & Oksman, K. (2006). Biopolymer based nanocomposites: Comparing layered silicates and microcrystalline cellulose as nanoreinforcement. *Composites Science and Technology*, *66*(13), 2187-2196.
- Piculell, L., Nilsson, S., & Muhrbeck, P. (1992). Effects of small amounts of kappa-carrageenan on the rheology of aqueous iota-carrageenan. *Carbohydrate Polymers*, *18*(3), 199-208.
- Puertolas, J. A., Vadillo, J. L., Sanchez-Salcedo, S., Nieto, A., Gomez-Barrena, E., & Vallet-Regi, M. (2011). Compression behaviour of biphasic calcium phosphate and biphasic calcium phosphate-agarose scaffolds for bone regeneration. *Acta Biomaterialia*, *7*(2), 841-847.
- Rahman, M. S., Machado-Velasco, K. M., Sosa-Morales, M. E., & Velez-Ruiz, J. F. (2009). Freezing Point: Measurement, Data, and Prediction. In M. S. Rahman (Ed.), *Food Properties Handbook* (2nd ed., pp. 153-192). Boca Raton: CRC Press.
- Rao, M. A. (2007). *Rheology of fluid and semisolid foods: Principles and applications* (2nd ed.). New York: Springer.
- Reiner, M. (1964). The Deborah number. *Physics Today*(January 1964), p. 62.
- Ross-Murphy, S. B., & Shatwell, K. P. (1993). Polysaccharide strong and weak gels. *Biorheology*, *30*(217).

- Schorsch, C., Jones, M. G., & Norton, I. T. (1999). Thermodynamic incompatibility and microstructure of milk protein/locust bean gum/sucrose systems. *Food Hydrocolloids*, 13, 89-99.
- Shrinivas, P., Kasapis, S., & Tongdang, T. (2009). Morphology and mechanical properties of bicontinuous gels of agarose and gelatin and the effect of added lipid phase. *Langmuir*, 25(15), 8763-8773.
- Smith, D. M., & Culbertson, J. D. (2000). Proteins: Functional Properties. In G. L. Christen & J. S. Smith (Eds.), *Food Chemistry: Principles and Applications* (pp. 131-148). West Sacramento: Science Technology System.
- Stanley, N. (2006). Agars. In A. M. Stephen, G. O. Phillips & P. A. Williams (Eds.), *Food Polysaccharides and Their Applications* (2nd ed., pp. 217-238). Boca Raton: CRC Press.
- Swaigood, H. E. (1982). Chemistry of milk protein. In P. F. Fox (Ed.), *Developments in Dairy Chemistry - I* (Vol. 1). London: Applied Sci.
- Syrbe, A., Fernandes, P. B., Dannenberg, F., Bauer, W., & Klostermeyer, H. (1995). Whey protein and polysaccharide mixtures: polymer incompatibility and its applications. In E. Dickinson & D. Lorient (Eds.), *Food Colloids and Macromolecules* (pp. 328-339). Cambridge, UK: The Royal Society of Chemistry.
- TA Instruments. (n.d.-a). Differential Scanning Calorimeters Retrieved 9 March 2011, from <http://www.tainstruments.com/product.aspx?id=10&n=1&siteid=11>
- TA Instruments. (n.d.-b). Rheometers Retrieved 11 March 2011, from <http://www.tainstruments.com/product.aspx?id=43&n=1&siteid=11>
- TA Instruments. (n.d.-c). Thermal Analysis Review: Modulated DSC Theory (Technical Report TA-211B) Retrieved 21 February 2011, from

http://www.chemshow.cn/UploadFile/datum/1000/tainst_2008211819799648.p

[df](#)

- Thomas, L. C. (2005). Modulated DSC® Paper #2, Modulated DSC® Basics, Calculation and Calibration of MDSC® Signals (Technical Report TP 007). New Castle: TA Instruments.
- Thomas, M. E. C., Scher, J., Desobry-Banon, S., & Desobry, S. (2004). Milk powders ageing: Effect on physical and functional properties. *Critical Reviews in Food Science and Nutrition*, 44(5), 297-322.
- Tolstoguzov, V. B. (1993). Thermodynamic aspect of food protein functionality. In K. Nishinari & E. Doi (Eds.), *Food Hydrocolloids - Structures, Properties, and Functions* (pp. 327-340). New York: Plenum Press Div Plenum Publishing Corp.
- Tolstoguzov, V. B. (1995). Some physico-chemical aspects of protein processing in foods. Multicomponent gels. *Food Hydrocolloids*, 9(4), 317-332.
- Tolstoguzov, V. B. (1997). Protein-polysaccharide interactions. In S. Damodaran & A. Paraf (Eds.), *Food Proteins and their Applications* (pp. 171-198). New York: Marcel Dekker.
- Torquato, S., Truskett, T. M., & Debenedetti, P. G. (2000). Is random close packing of spheres well defined? *Physical Review Letters*, 84(10), 2064-2067.
- van der Linden, E., & Foegeding, E. A. (2009). Gelation: Principles, Models, and Applications to Proteins. In S. Kasapis, I. T. Norton & J. B. Ubbink (Eds.), *Modern Biopolymer Science: Bridging the Divide between Fundamental Treatise and Industrial Application* (pp. 29-91). San Diego: Elsevier.
- Yokoyama, E., Kishida, K., Uchimura, M., & Ichinohe, S. (2006). Comparison between agarose gel electrophoresis and capillary electrophoresis for variable

numbers of tandem repeat typing of *Mycobacterium tuberculosis*. *Journal of Microbiological Methods*, 65(3), 425-431.

Zeman, L., & Patterson, D. (1972). Effect of the solvent on polymer incompatibility in solution. *Macromolecules*, 5(4), 513-516.



COA ID: 8944-500-02

Certificate of Analysis

COA Number: 81571201-2

Product Description: **WHEY PROTEIN ISOLATE
INSTANTISED 894**
Customer: **FONTERRA AUSTRALIA PTY LTD**
Buyer Order: **M401731**

Factory: **2539**
Batch/Cypher: **GT20**
Manufacture Date: **20 February 2009**

Parameter	Units of Measure	Test Method	Mean Result
Protein (6.38 x N) as is	% m/m	Kjeldahl	88.71
Fat	% m/m	SBR	0.93
Moisture	% m/m	Gravimetric	4.83
Ash	%m/m	TGA 600	3.3
pH	pH units	5% TS 20°C	6.9
Lactose Monohydrate	% m/m	Phenol Sulphuric	0.8
Bulk Density	g/ml	Niro 35 tap	0.33
Flavour DFC		Sensory Evaluation	Typical
Aerobic Plate Count	cfu/g	IDF 100B	1200
Coliforms	cfu/g	Count IDF73B	<1
Escherichia coli	/g	Detection IDF170A/LST-MUG	Not Detected
Yeasts and Moulds	cfu/g	IDF 94B	<1
Coag Positive Staphylococci	/g	Detection IDF60C	Not Detected
Salmonella	/750g	Detection FDA	Not Detected
Listeria	/125g	Detection ISO	Not Detected

LF Number: 0681571301

Page 1 of 2



COA ID: 8944-500-02

Certificate of Analysis

COA Number: 81571201-2

Fonterra hereby certifies that the product supplied against this certificate was manufactured in New Zealand and samples have been examined and subjected to laboratory analysis. Such products are manufactured and tested in premises registered under sanitary requirements by the New Zealand Food Safety Authority. All premises are subject to regular audit to ensure compliance with the terms of, and conditions, of registration.

Signatory: Stan Bunting

Title: Quality and Compliance Manager

Date: 10 June 2009

customer.service@fonterra.com

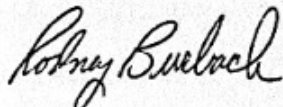
Should you have any further queries please contact your Customer Service Representative or Account Manager

Certificate of Analysis

SIGMA-ALDRICH

Product Name Agarose,
Type I-B, low EEO
Product Number A0576
Product Brand SIAL
CAS Number 9012-36-6

TEST	SPECIFICATION	LOT 112K1630 RESULTS
APPEARANCE	WHITE TO OFF-WHITE POWDER	OFF-WHITE POWDER
SOLUBILITY	CLEAR COLORLESS TO VERY SLIGHTLY HAZY VERY FAINT YELLOW AT 1.5 GM PLUS 100 MLS OF WATER	CLEAR VERY FAINT YELLOW SOLUTION AT 1.5 GM PLUS 100 ML OF WATER
MOISTURE CONTENT	< OR = 6.0%	2.94%
PH TEST (1.5% GEL)	6.16 TO 7.36	6.78
RESIDUE ON IGNITION	< OR = 0.25	0.10%
SULFATE	< OR = 0.10	0.060%
GEL STRENGTH (1.5% GEL)	2800 TO 4300 G/CM2	3500 G/CM2
GEL POINT (1.5% GEL)	35.4 DEG C TO 37.1 DEG C	36.5 DEG C
MELTING TEMPERATURE	87.0 DEG C TO 90.0 DEG C	89.3 DEG C
TURBIDITY (1.5% GEL)	10 TO 28 NP COLEMAN	19 NP COLEMAN
ELECTROENDOSMOSIS (-MR)	< OR = 0.15	0.11
RECOMMENDED RETEST	3 YEARS	DECEMBER 2005
QC RELEASE DATE		DECEMBER 2002



Rodney Burbach, Manager
Quality Control
St Louis, Missouri USA



Specification

<http://certificates.merck.de>

Date of print: 04.01.2011

1.06482.5000 Sodium hydroxide pellets suitable for use as excipient
EMPROVE® exp Ph Eur, BP, FCC, JP, NF, E 524

	Spec. Values	
Assay		
acidimetric, NaOH	≥ 98.0	%
total alkalinity calc. as NaOH	98.0 - 100.5	%
Identity	passes test	
Appearance of solution	passes test	
Insoluble substances and organic matter	passes test	
Carbonate (as Na ₂ CO ₃)	≤ 0.5	%
Chloride (Cl)	≤ 0.005	%
Phosphate (PO ₄)	≤ 0.002	%
Silicate (SiO ₂)	≤ 0.01	%
Sulphate (SO ₄)	≤ 0.003	%
Total nitrogen (N)	≤ 0.0005	%
Heavy metals (as Pb)	≤ 0.0005	%
Al (Aluminium)	≤ 0.001	%
As (Arsenic)	≤ 0.0003	%
Cu (Copper)	≤ 0.0005	%
Fe (Iron)	≤ 0.001	%
Hg (Mercury)	≤ 0.00001	%
K (Potassium)	≤ 0.1	%
Pb (Lead)	≤ 0.00005	%
Zn (Zinc)	≤ 0.0025	%
Residual solvents (Ph. Eur./USP/ICH)	excluded by manufacturing process	

Conforms to the purity criteria on food additives according to the European Commission directive 96/77/EC. Residues of metal catalysts or metal reagents acc. to EMEA/CHMP/SWP/4446/2000 are not likely to be present.

Specification

1.06482.5000 Sodium hydroxide pellets suitable for use as excipient
EMPROVE® exp Ph Eur,BP,FCC,JP,NF,E 524

Dr. Andreas Lang

responsible laboratory manager quality control

This document has been produced electronically and is valid without a signature

Certificate of Analysis

SIGMA-ALDRICH

Product Name Hydrochloric acid,
reagent grade, 37%
Product Number 435570
Product Brand SIAL
CAS Number 7647-01-0
Molecular Formula HCl
Molecular Weight 36.46

TEST	SPECIFICATION	LOT 00659BH RESULTS
APPEARANCE	COLORLESS LIQUID	COLORLESS LIQUID
TITRATION	36.5% - 38.0% (WITH NaOH)	37.1% (WITH NaOH) *
COLOR TEST	20 APHA (MAXIMUM)	3 APHA *
QUALITY CONTROL	APPROVED JANUARY 24, 1997 JSB	* SUPPLIER DATA
ACCEPTANCE DATE		JUNE 2007



Barbara Rajzer, Supervisor
Quality Control
Milwaukee, Wisconsin USA